Report FH-11-7612

DEPLOYABLE HEAD RESTRAINTS

John W. Melvin
James H. McElhaney

Highway Safety Research Institute
The University of Michigan
Ann Arbor, Michigan 48105

June 30, 1971

Final Report for Period 1 July 1970-30 June 1971

Prepared for:

National Highway Traffic Safety Administration
U.S. Department of Transportation
Federal Highway Administration
Nassif Building
7th and E Streets, S.W.
Washington, D.C. 20591

1. Report No.	2. Government Accession No.	3. Recipient's Catalog No.
HSRI-71-103		

4. Title and Subtitle	5. Report Date
Deployable Head Restraints	30 June 1971
	6. Performing Organization Code

7. Author(s)	8. Performing Organization Report No.
J. W. Melvin and J. H. McElhaney	

9. Performing Organization Name and Address	10. Work Unit No.
Highway Safety Research Institute The University of Michigan Huron Parkway and Baxter Road Ann Arbor, Michigan 48105	11. Contract or Grant No. FH-11-7612
12. Sponsoring Agency Name and Address National Highway Traffic Safety Administration U.S. Department of Transportation Nassif Building, 7th and E Streets, S.W. Washington, D.C. 20591	13. Type of Report and Period Covered Final Report 1 July 1970-30 June 1971
	14. Sponsoring Agency Code

15. Supplementary Notes

16. Abstract

The object of this research program was to develop and demonstrate deployable head restraint systems that automatically deploy to prevent crash injury without significantly compromising driver vision during normal vehicle operations. This work involved defining deployable head restraint system requirements, evaluating crash sensors and deployable head restraint configurations, selecting and designing systems and then performing a testing, development and demonstration program on prototype systems.

Two basic types of systems were designed and built; one was an inflatable system and the other was a rigid sliding device. Both systems were subjected to a series of impact sled tests utilizing anthropometric dummies. The results of this program demonstrate that deployable head restraints are technically feasible and that they can provide a general level of performance better than conventional fixed head restraints.

Recommendations were made regarding general performance requirements for deployable head restraints and associated seat back structures.

17. Key Words	18. Distribution Statement

19. Security Classif.(of this report)	20. Security Classif.(of this page)	21. No. of Pages	22. Price

Form DOT F 1700.7 (8-69)

TABLE OF CONTENTS

TABLE OF CONTENTS (Continued)

FIGURES

FIGURES (Continued)

FIGURES (Continued)

TABLES

ACKNOWLEDGEMENTS

This research program was carried out by the staff members of the Biosciences Division of the Highway Safety Research Institute, The University of Michigan. The program was under the direction of Drs. J. W. Melvin and J. H. McElhaney. The participation and assistance in the program of N. Alem, J. Brindamour, D. Currin, M. Dunlap, C. Dunn, S. Fisher, E. Gulash, A. Henke, G. Person, R. Pontius, D. Raney, S. Stewart, P. VanLuven, B. Vicars and J. Warden is appreciated. The participation of Drs. V. L. Roberts, R. G. Snyder and H. D. Portnoy, M.D. in the evaluation of head restraint deisngs is also appreciated.

1. INTRODUCTION

Rear-end collisions are the most frequently occurring type of motor vehicle collision. During the year of 1968 there were 14.6 million accidents involving motor vehicles in the United States. Of that total, 49% or 7.04 million were same direction or rear-end type accidents (U.S. Bureau of Public Roads, 1970). The total number of fatal accidents during this same period was 46,800, with rear-end type accidents accounting for 9% or 4500 accidents. Thus, although the rear-end collision is a common type of accident, the fatality rate associated with it is low, particularly for the occupants of the vehicle being struck from the rear. The generally low severity of most rear-end collisions is indicated by the results of a statistical analysis of the accident report data of the combined files of The University of Michigan and UCLA for 1968-69 which produced the frequency distribution of crash closing velocities at impact shown in Figure 1. The mean closing velocity was 26 mph or approximately a 13 mph barrier crash equivalent. The characteristic types of injuries sustained by occupants of the struck vehicle in non-fatal accidents are the so-called "whiplash" or hyperextension injuries. These injuries range from minor temporary neck and back aches to severe injuries involving dislocated and fractured cervical vertebrae and spinal damage. Quite frequently the soft tissues and ligaments of the neck are torn or strained.

A study of 207 cases of hyperextension-hyperflexion injuries was made recently by Gurdjian, Cheng, and Thomas (Gurdjian, 1970) in which 137 of the cases were caused by rear-end collisions. Gurdjian's list of the potential for injury in these cases includes injury to the bones of the neck, spinal nerves extending out of the cervical spine, and the sympathetic nerves along the lateral aspect of the spine, as well as injuries to the muscles and ligaments of the neck. Blood vessel injury, spinal cord injury and, in some cases, even brain injury (subdural hematomas) can occur from hyperextension (Ommaya, 1969). In the less severe forms of whiplash injury the mechanisms of injury are not readily diagnosed even though definite symptoms exist. In many cases the symptoms do not show up until some later time.

In order to better understand the mechanics of whiplash, Mertz and Patrick, 1967, performed rear-end collision simulations with dummies, cadavers and a volunteer. They concluded that neck torque is the limiting injury factor in both hyperextension and hyperflexion environments, and that for the

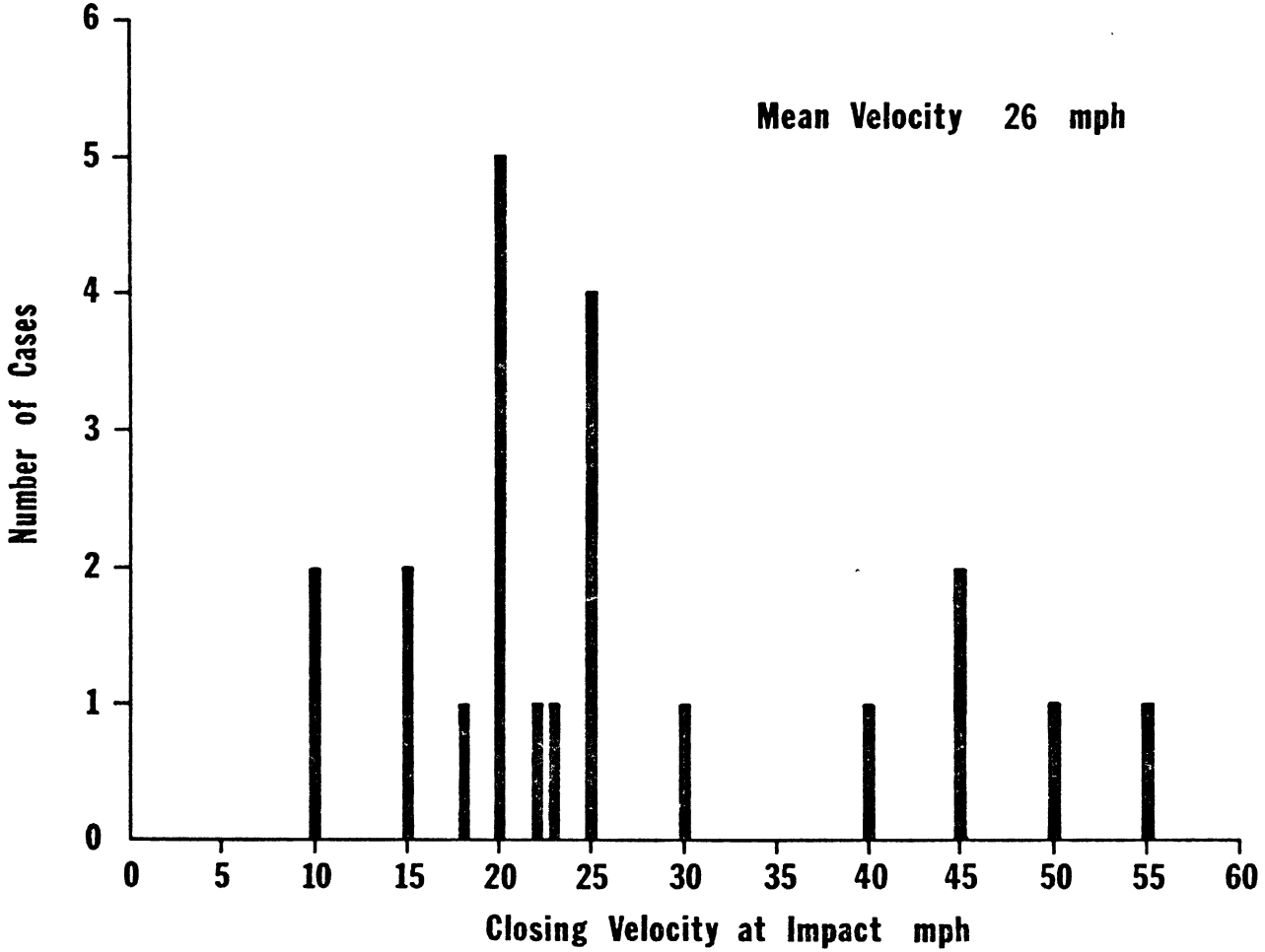

FIGURE 1. REAR END COLLISION DATA, UNIVERSITY of MICHIGAN AND U.C.L.A. COMBINED FILES, 1968-69

elimination of hyperextension injury the extension angle must be kept under 80 degrees and preferably under 60 degrees. A more recent study utilizing live baboons (Portnoy, 1970) concluded that head restraint design should minimize head to restraint distances for maximum effectiveness in severe crash environments.

In spite of the non-lethal nature of many whiplash injuries, the high frequency of occurrence of rear-end collisions and the resulting number of injuries produced by such accidents can create serious public health problems in terms of disability and medical expense.

Since January 1, 1969, all new automobiles manufactured for sale in the United States have been required to include head restraint protection for occupants at each outboard front seating position. The two most common forms of head restraint presently in use in automobiles are either fixed extensions of the seat back or a separate head cushion, which is adjustable for height, attached to the seat back. The FMVSS Standard 202 pertaining to head restraints requires that during a half-sine acceleration pulse of 8 to 9.6 G amplitude and 80 to 96 msec duration, the rearward rotation of the head relative to the torso shall be limited to 45 degrees by the action of the head restraint.

Current head restraint systems can provide protection for vehicle occupants during crashes. However, they too often do not because of improper adjustment. In addition, they restrict rearward visibility for many drivers and are therefore a design compromise hopefully providing adequate protection while sacrificing not too much in rearward visibility. The concept of a deployable head restraint offers a promising solution to this problem. Since it would remain out of sight in the seat back until required, it would not compromise rearward visibility or comfort, and the size, shape and location of the deployed head restraint can be optimized with regard to biomechanical factors involved in preventing injury. Similarly, consideration can be directed toward providing protection from oblique impacts in addition to rear-end impacts and rebounds.

The program to develop prototype deployable head restraint systems was carried out in the form of a series of interrelated tasks which culminated in the design, construction and testing of the prototype systems. The three preliminary tasks were:

Task 1. Define Deployable Head Restraint System Requirements

Task 2. Evaluate Crash Sensors

Task 3. Evaluate Deployable Head Restraint Configurations

Task 1 involves definition of the safety requirements of a deployable headrest while Task 3 involves the evaluation of various concepts from the safety viewpoint as well as reliability, cost, tolerance to environmental conditions, etc. These two tasks were initiated simultaneously at the beginning of the project. A set of performance requirements was developed based on analytical studies simulating the motions experienced by an automobile occupant in a collision while actual hardware as proposed by such manufacturers as Eaton, Yale and Towne, Inc., Ensign Bickford Co. and Olin Corp., among others, was studied to determine the state of the art which has been reached by possible volume producers of deployable head restraint systems. Task 2 provided the necessary information on crash sensor characteristics to define system deployment times.

Following completion of the above tasks and construction of the prototype systems, a thorough test, development and demonstration program was carried out to study the effectiveness of the deployable head restraint concept. The following sections of this report discuss in detail the various phases of the overall project.

2. CONCLUSIONS AND RECOMMENDATIONS

The results of this study indicate that deployable head restraints are technically feasible and that they can provide a general level of performance better than conventional fixed head restraints. The deployable head restraint can be packaged in such a manner as to allow the short driver to see over it for rearward vision and still be highly effective in providing head restraint for the tall driver. By virtue of the fact that the head restraint is in place only when needed in an accident situation it can be placed much further forward than a fixed head restraint resulting in greatly reduced motion of the occupant's head during a crash. The necessary forward placement of the head restraint is such that it would not impair the driver's ability to control the car following the crash and thus it can remain in place to guard against subsequent multiple collisions.

Of the two basic types of deployable head restraint designs studied in this program, the inflatable systems seem to offer many advantages over rigid systems. Some of these advantages are:

1. Compact packaging
2. Low inertia during deployment
3. Great latitude in final deployed shape
4. Ability to expand fore and aft while deploying vertically

These advantages are modified somewhat by the necessity for achieving adequate fore and aft stiffness in the inflatable systems. At this point in their development, bag type inflatable head restraints were found to require a rigid rotating flap to provide the necessary stiffness. The possibility of utilizing self-stiffening inflatable structures, such as dropweave fabric, offers a means of overcoming this drawback.

The inflatable deployable head restraint developed during this program (See Figures 28, 29, 30 and 31) proved to be extremely effective for both large and small occupants in crash simulations equivalent to car-to-car rear-end crash velocities of 20 mph, 60 mph and 80 mph. The system was evaluated using criteria based on the following concepts:

1. Minimization of both linear and rotational rearward head displacement.
2. Minimization of head linear and angular accelerations.
3. Minimization of differential motions of the head relative to the torso.

4. Minimization of occupant ramping up the seat back.

5. Minimization of occupant rebound.

The overall effectiveness of the head restraint system depends greatly upon the effectiveness of the seat back structure it is mounted on and upon the extent to which their overall responses are matched. The excellent results obtained in this program for the inflatable head restraint-seat combination demonstrate the value of well matched components in producing uniform occupant motions and the value of minimizing elastic energy storage by utilizing a basically rigid load carrying seat structure. As an example of the performance of the total system, the input sled pulse of Test A-373 (an 80 mph car-to-car equivalent velocity crash simulation with a peak acceleration of 40 G's) produced in the 95th percentile male dummy a peak head A-P acceleration of 42 G's, a peak head angular acceleration of 916 rad/sec^2 with a corresponding angular velocity peak of 16.8 rad/sec with no head-neck extension. Comparison of these results with estimated human concussive tolerance values given by Ommaya (1970) for head rotational motion of 1800 rad/sec^2 at 50 rad/sec indicate levels below those believed to be tolerable.

In contrast to the excellent performance of the head restraint system, sensing of rear-end crashes poses problems in some cases. For crashes involving significant collapse of conventional car rear-end structures existing, inertial type crash sensors appear to be adequate. However, there are many low speed collisions requiring head restraint where the acceleration levels overlap into the possible road noise range thereby rendering the inertial type crash sensor ineffective in discriminating a crash from a road shock. In addition, the response of present inertial sensors may not be rapid enough for future square wave type crush structures. Incorporation of a sensor system into the design of rear energy-absorbing bumpers may offer a possible solution to rear-end crash sensing difficulties. Head restraints are effective in frontal crashes when occupant rebound occurs and therefore a deployable head restraint should also be activated during frontal crashes.

This program has demonstrated the basic feasibility of deployable head restraints; however, many areas of the subject are in need of further study. It is recommended that future studies on deployable head restraint concentrate on the following items:

1. Development of totally inflating systems with self-contained fore and aft stiffness.

2. Development of optimum inflatable head restraint shapes for oblique as well as direct rear-end impacts.

3. Development of new crash sensor concepts for sensing rear-end collisions.

4. Development of optimized inflation devices with characteristics that produce minimal effect on malpositioned occupants and minimal noise.

3. TASK 1. DEFINITION OF DEPLOYABLE HEAD RESTRAINT SYSTEM REQUIREMENTS

The goals of this task were to determine:

1. The crash conditions in which a protective headrest is required;
2. Occupant motions in these cases;
3. The point in time and location of the occupant when a deployable head restraint would be useful in preventing occupant injury; and,
4. The response characteristics of a deployable device necessary to prevent potential injuries to the vehicle occupants.

The basic tool used in this task was the HSRI two-dimensional crash victim computer model. The model was exercised in both frontal and rear impact simulations using experimentally determined crash profiles and idealized crash profiles.

3.1 FRONT-END COLLISIONS - NO HEAD RESTRAINT

The three frontal crash deceleration profiles which were chosen for use in this phase of the study were an average 40 mph frontal barrier impact based on information from DOT, an idealized 40 mph 30 G trapezoidal pulse, and an idealized 20 mph 15 G trapezoidal pulse. These pulses are shown in Figure 2. The occupant sizes simulated were 5th percentile female and 95th percentile male in order to bracket the range of occupant sitting heights. Both 21-inch and 25-inch seatback heights were used. The front seat occupants were restrained with either seat belt, airbag or seat belt plus shoulder harness arrangements. For rear seat occupants, the same conditions were used except that they were either unrestrained or restrained by seat belt only. Contact surfaces representing the back and top of the front seat were included in the rear seat occupant simulations. The computer simulation matrix for the frontal collisions is given as part of Table 1.

3.2 REAR-END COLLISIONS - NO HEAD RESTRAINT

The rear-end crash deceleration profiles which were chosen for this study were all based on car to car simulations as opposed to car to barrier. They were: 30 mph - 1966 Chevrolet (Severy 1968), 55 mph - 1967 Ford (Severy 1968), 5 mph - 1962 Rambler (HSRI),an idealized 30 mph-10 G trapezoidal pulse, and an idealized 80 mph-40 G trapezoidal pulse. These crash profiles are shown

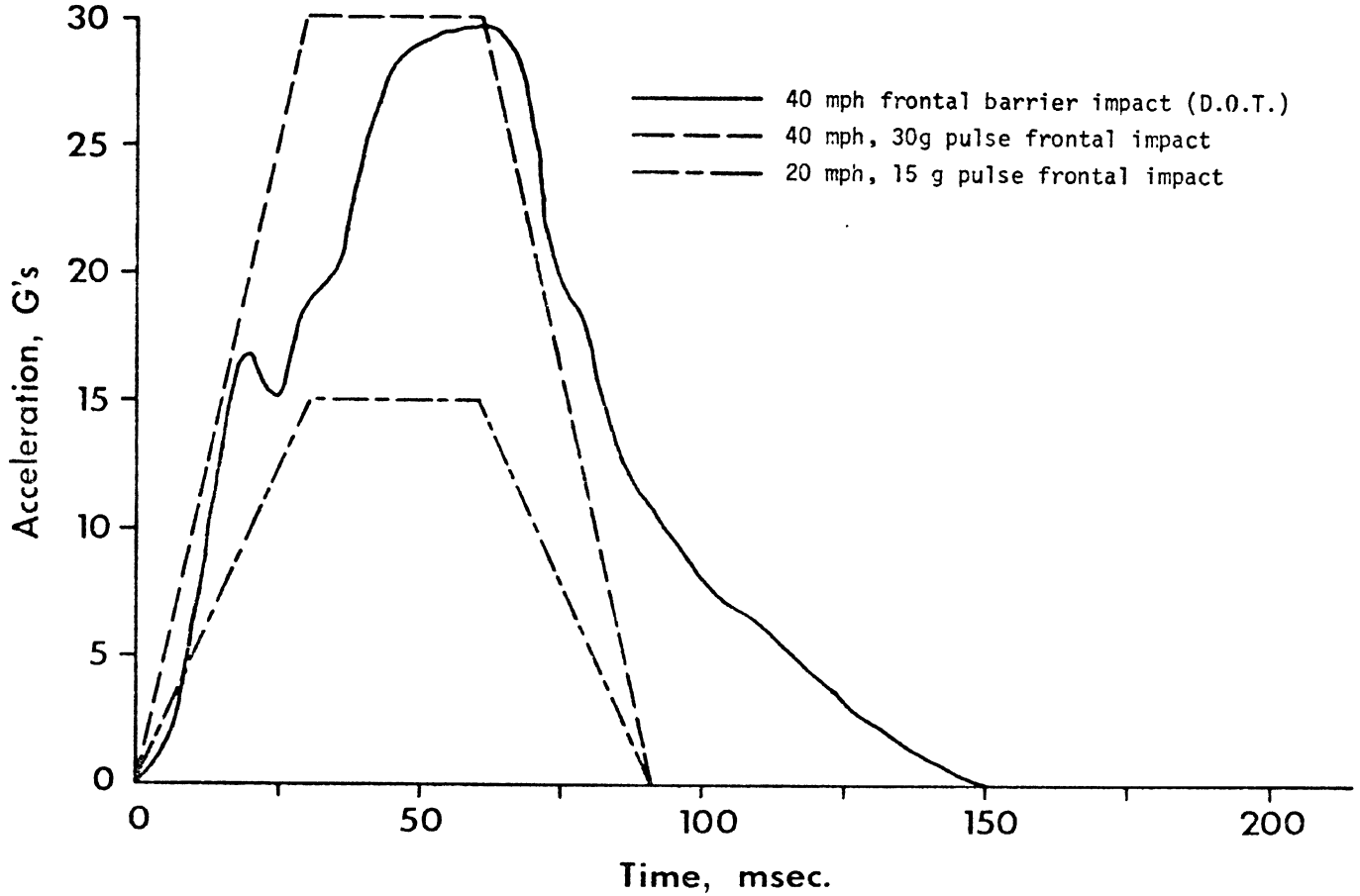

FIGURE 2. FRONTAL CRASH PROFILES USED IN COMPUTER SIMULATIONS

TABLE 1. COMPUTER SIMULATION MATRIX - NO HEAD RESTRAINT

Front Seat Occupant - Front Collision

40 mph DOT Pulse			40 mph, 30 G Pulse			20 mph, 15 G Pulse		
SBH	%	Rest	SBH	%	Rest	SBH	%	Rest
21	95	SB	21	95	SB	21	95	SB
21	95	SB&H	21	95	SB&H	21	95	SB&H
21	95	Bag	21	95	Bag	21	95	Bag
21	5	SB	21	5	SB	21	5	SB
21	5	SB&H	21	5	SB&H	21	5	SB&H
21	5	Bag	21	5	Bag	21	5	Bag
25	95	SB	25	95	SB	25	95	SB
25	95	SB&H	25	95	SB&H	25	95	SB&W
25	95	Bag	25	95	Bag	25	95	Bag
25	5	SB	25	5	SB	25	5	SB
25	5	SB&H	25	5	SB&H	25	5	SB&W
25	5	Bag	25	5	Bag	25	5	Bag

Rear Seat Occupant - Front Collision

40 mph, DOT Pulse			40 mph, 30 G Pulse			20 mph, 15 G Pulse		
SBH	%	Rest	SBH	%	Rest	SBH	%	Rest
21	95	SB	21	95	SB	21	95	SB
21	95	U	21	95	U	21	95	U
21	5	SB	21	5	SB	21	5	SB
21	5	U	21	5	U	21	5	U
25	95	SB	25	95	SB	25	95	SB
25	95	U	25	95	U	25	95	U
25	5	SB	25	5	SB	25	5	SB
25	5	U	25	5	U	25	5	U

Front Seat Occupant - Rear Collision

30 mph, Severy			55 mph Severy			30 mph, 10 G Pulse		
SBH	%	Rest	SBH	%	Rest	SBH	%	Rest
21	95	SB	21	95	SB	21	95	SB
21	95	U	21	95	U	21	95	U
21	5	SB	21	5	SB	21	5	SB
21	5	U	21	5	U	21	5	U
25	95	SB	25	95	SB	25	95	SB
25	95	U	25	95	U	25	95	U
25	5	SB	25	5	SB	25	5	SB
25	5	U	25	5	U	25	5	U

LEGEND: SBH = Seat Back Height % = Dummy Size (5% Female or 95% Male)
Rest = Restraint System (SB - seat belt; SB&H - seat belt and harness; U - unrestrained; Bag - airbag).

in Figure 3. The occupant sizes simulated were 5th percentile female and 95th percentile male and both 21-inch and 25-inch seat-back heights were used. The occupants were either unrestrained or restrained by a lap belt only. The computer simulation matrix for the rear-end collisions is given as part of Table 1 (with the exception of the one run which was made with the 80 mph-40 G crush structure pulse).

3.3 RESULTS OF COMPUTER SIMULATION FOR OCCUPANTS WITH NO HEAD RESTRAINT

The computer simulations for both frontal and rear-end crashes indictated the need for head restraint either to prevent severe hyperextension of the neck and/or to prevent occupant interaction when rear seat passengers were involved in frontal crashes. The crash profiles chosen for the study were in many cases quite severe and thus provide practical minimum limits on points in time and practical maximum limits on occupant motions.

3.4 FRONTAL CRASH - FRONT SEAT OCCUPANTS

For this case rebound from a seat belt-shoulder harness combination produced occupant configurations requiring head restraint in the shortest time after crash initiation. The results were:

95th percentile male - 160 msec.

5th percentile female - 150 msec

3.5 FRONTAL CRASH - REAR SEAT OCCUPANTS

For this case both lap belt restraint and no restraint gave similar results with both 95th percentile male and 5th percentile female simulations. The occupant's head approached the configuration where a deployable head restraint would prevent occupant interaction at approximately 90 msec.

3.6 REAR-END CRASH - FRONT SEAT OCCUPANTS

In all the simulations carried out, severe hyperextension occurred. This is shown in Figures 4 and 5 by the schematic representations of the computer results for both 95th percentile male and the 5th percentile female. Choosing a time for critical occupant configuration to minimize injury depends on the tolerance criteria employed for evaluation (i.e. angular acceleration, neck torque, extension angle, etc.). The criteria employed in this study is discussed under the section on Task 3.

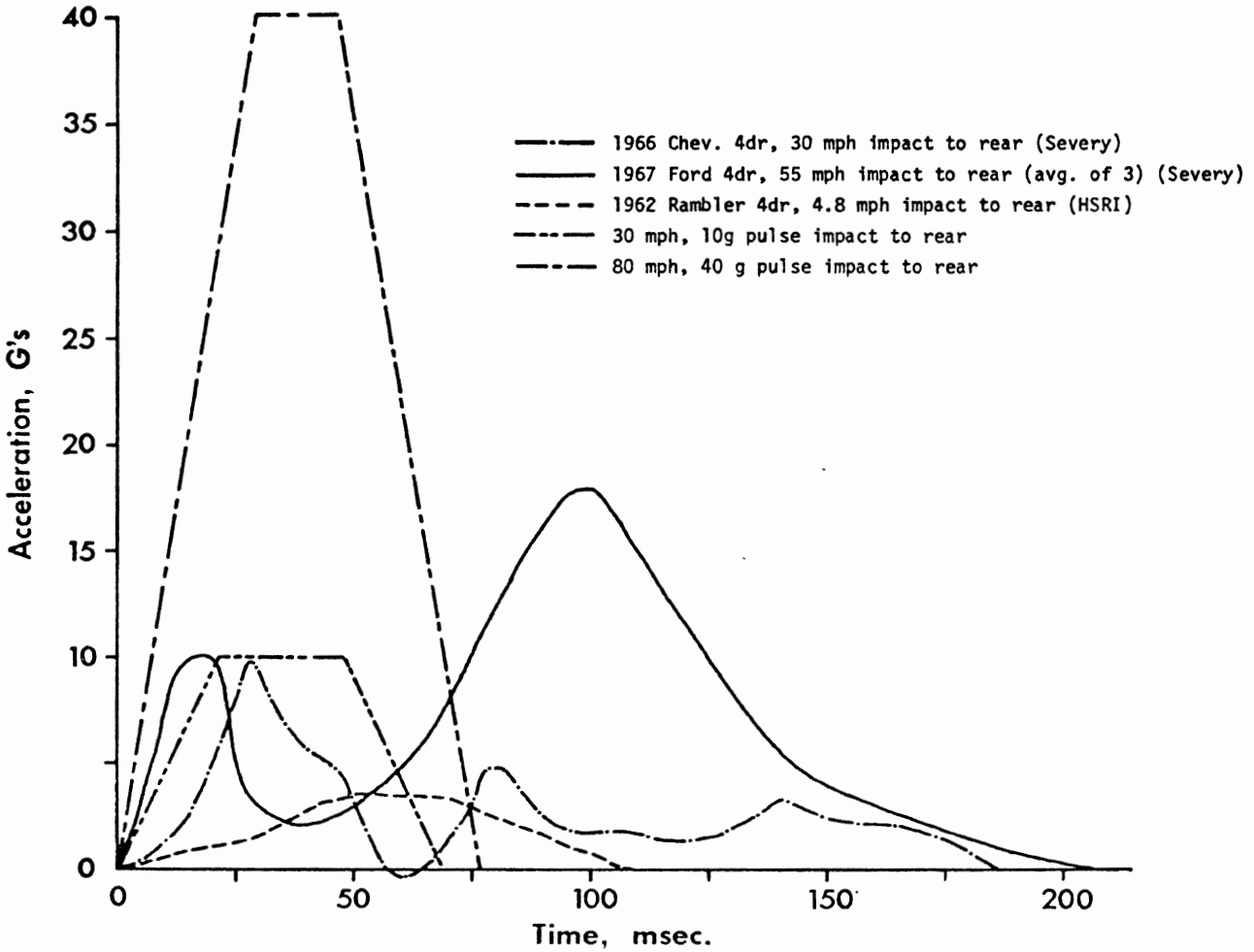

FIGURE 3. REAR END CRASH PROFILES USED IN COMPUTER SIMULATIONS

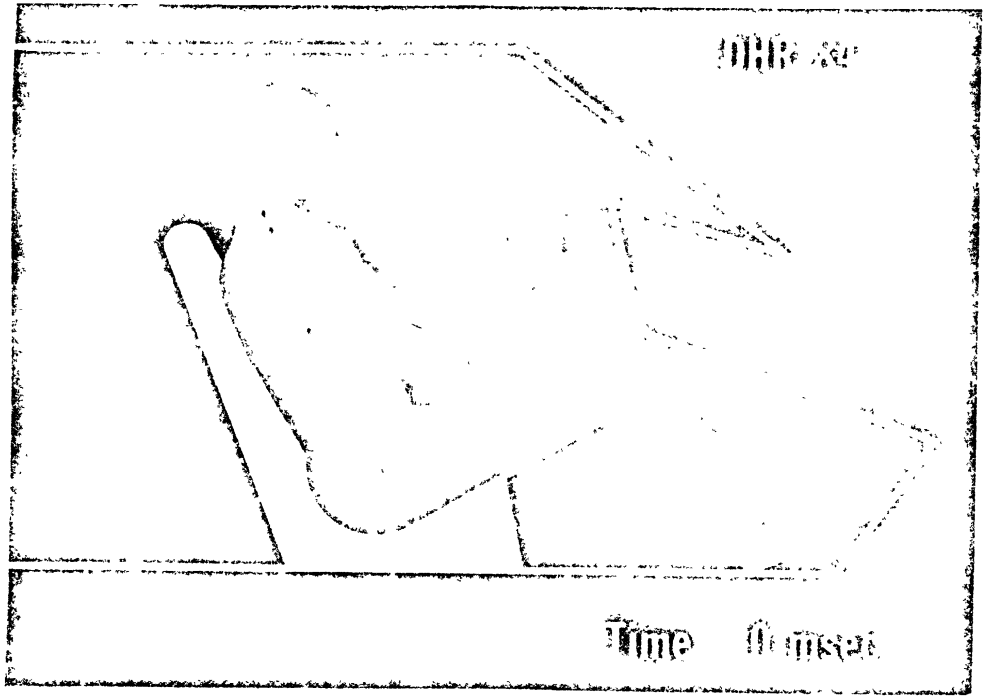

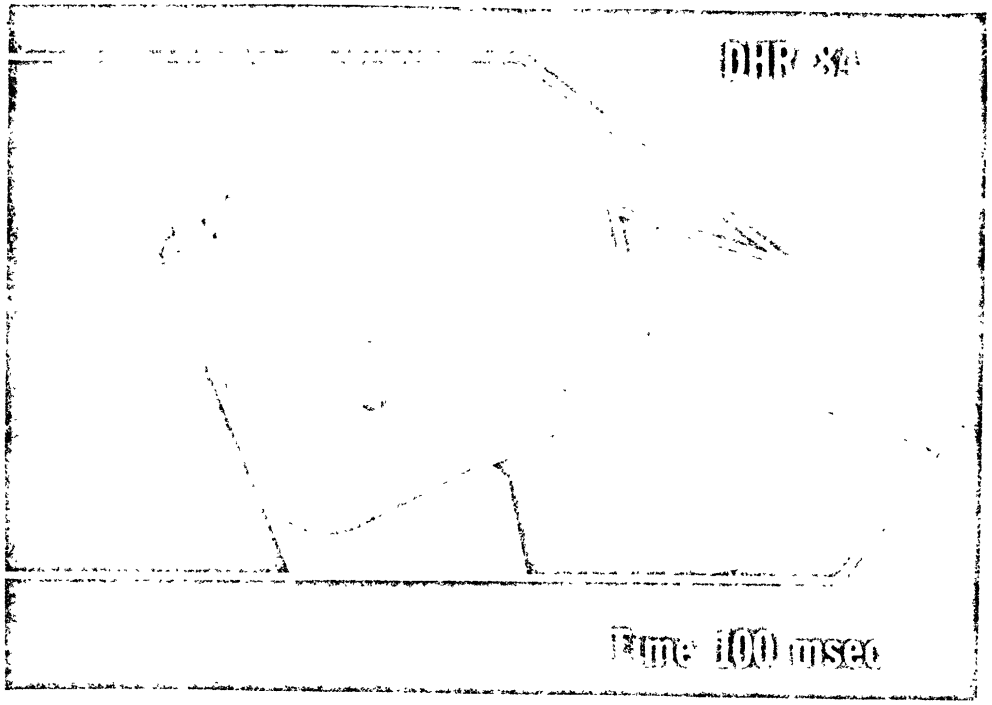

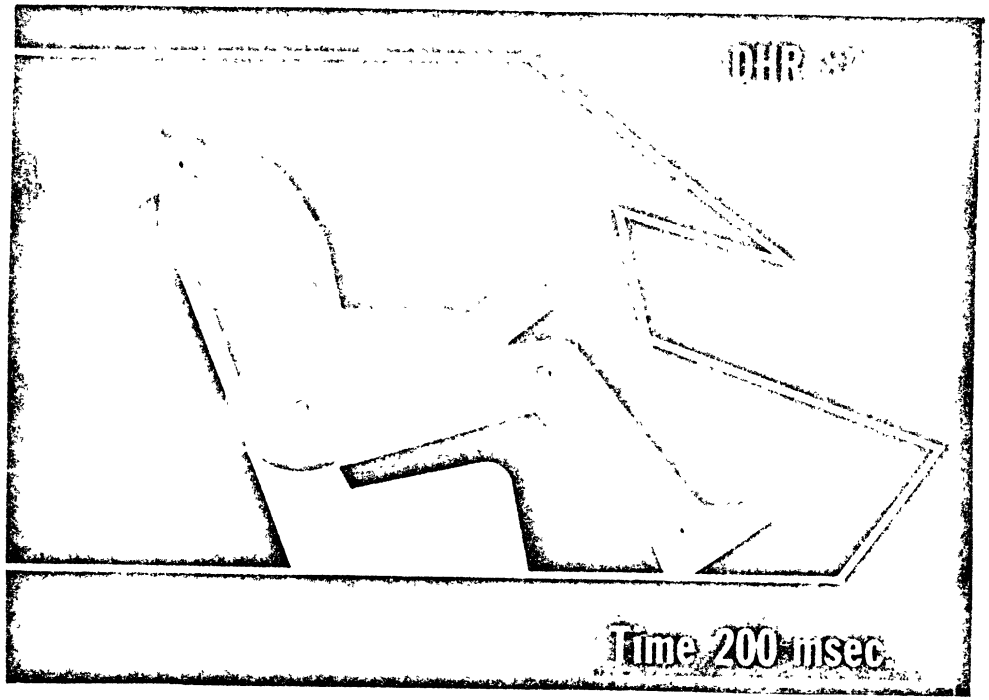

95th Percentile Male - no belts
25 inch seat back height
Crash Pulse - 30 mph, Severy - Figure 3.
NOTE: In this simple graphic display the seat back remains in its original position, this was not the case in the actual computer simulation.

Figure 4. Computer Simulation Run DHR 84

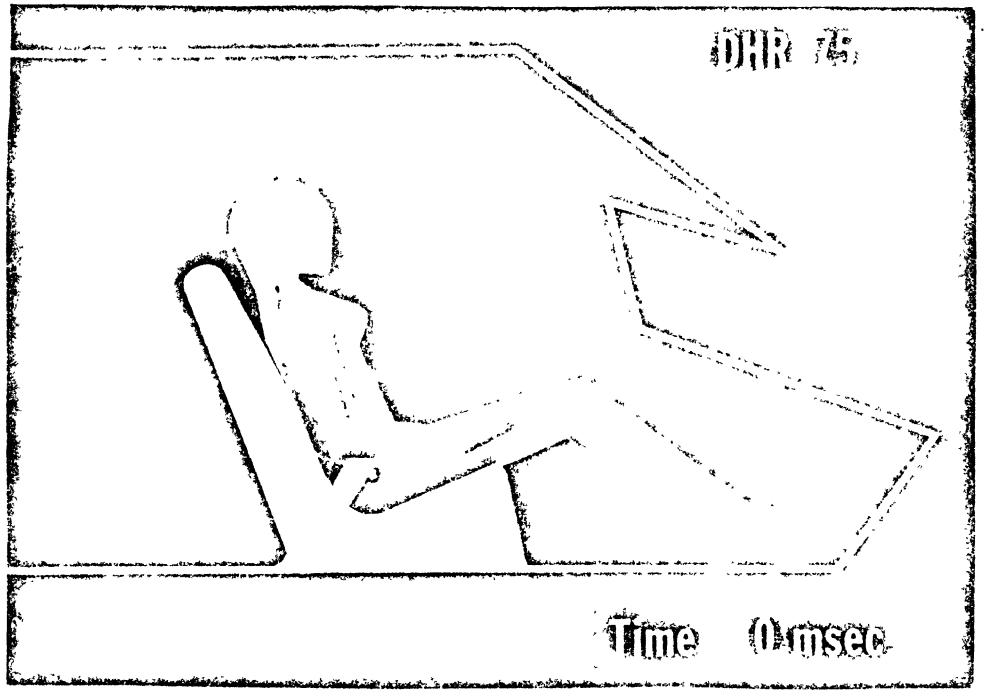

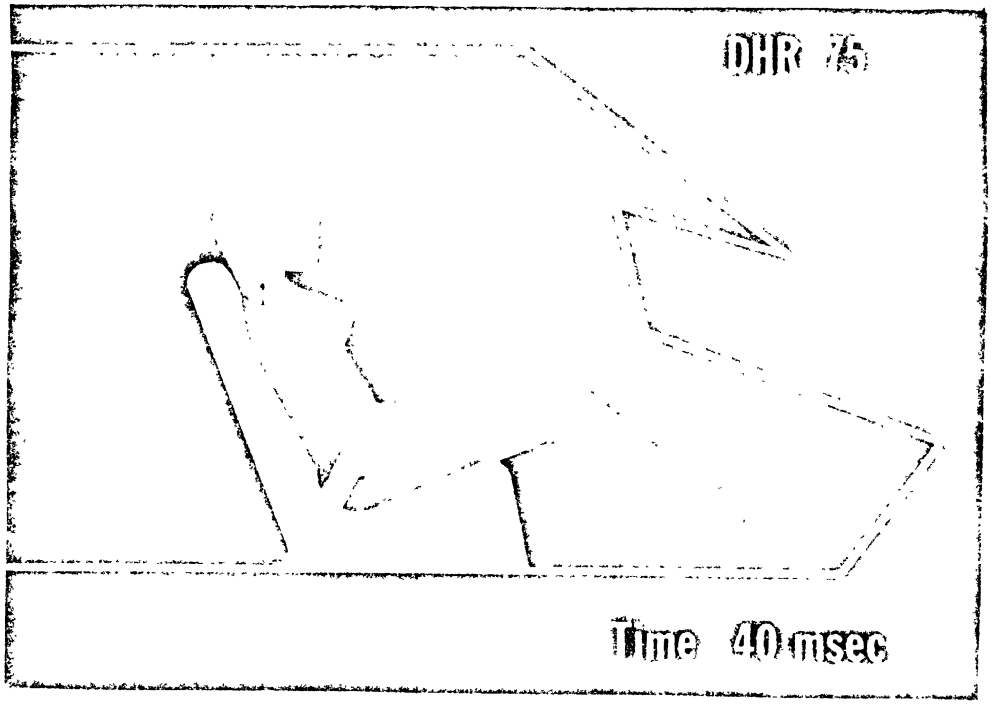

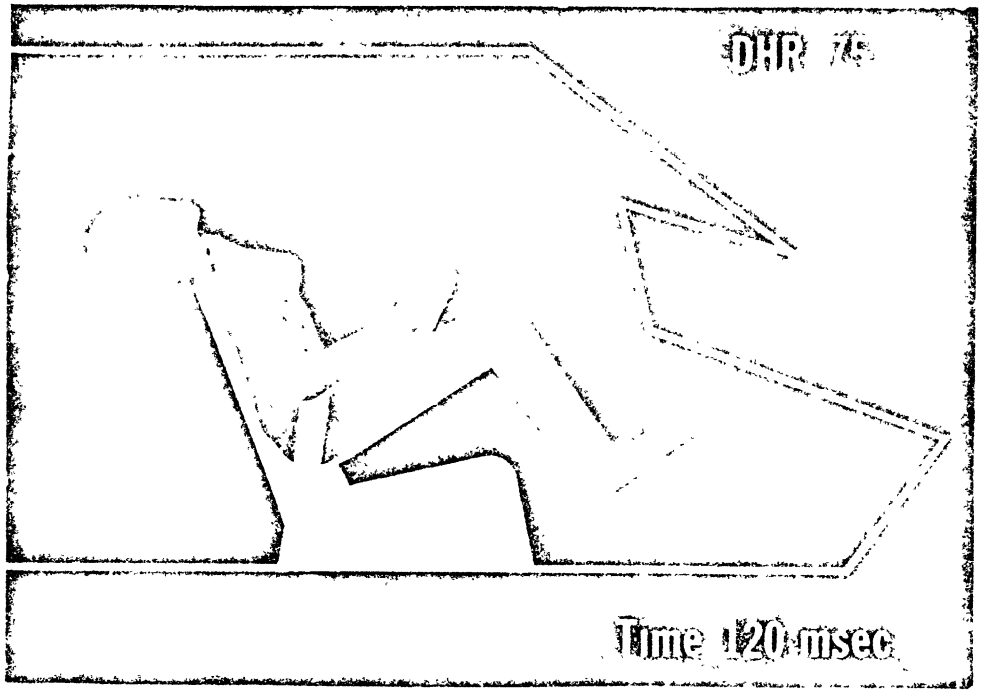

5th Percentile Female - lap belt
21 inch seat back height
Crash Pulse - 55 mph, Severy - Figure 3.
NOTE: In this simple graphic display the seat back remains in its original position, this was not the case in the actual computer simulation.

Figure 5. Computer Simulation Run DHR 75

3.7 COMPUTER SIMULATION OF DEPLOYABLE HEAD RESTRAINT PERFORMANCE

The HSRI two-dimensional crash victim computer model was modified by the addition of an upper seat back structure that produced a plane surface which satisfied the condition, discussed in the section on Task 3, that the occupant's head (either 95th percentile male or 5th percentile female) would begin to contact the surface at 40 msec after the initiation of the most severe conventional rear-end crash profile (55 mph, Severy, shown in Figure 3). The upper structure was initially given the same load-deflection properties as those of the seat back. The modified computer model was then exercised using the rear-end crash profiles shown in Figure 3. The computer simulation matrix for this study is shown in Table 2.

In general, the results of the simulations indicated excellent performance of the chosen head restraint configuration. The relative angle between the head and the torso, which starts at a positive 15°, did not even approach zero until the second half of the crash pulse with typical maximum negative angles in the range of 20° during the rearward motion into the seat. Rebound of the occupants out of the seat produced larger negative or extension angles due to the torso rebounding more rapidly than the head. In the case of the 95th percentile male simulations, interactions of the occupant's head with the roof of the car produced serious head loading but the extension angles did not exceed 45°. This interaction was due in part to the occupant ramping up the seat back into the roof and occurred even with seat belt restraint. Figures 6 and 7 show typical schematic representations of two of the computer simulations showing the performance characteristics of head restraint and the head-roof interaction problem.

In order to study the effect of head restraint load-deflection characteristics on occupant motions, simulations were performed with a head restraint one half as stiff and a head restraint twice as stiff as the system simulated initially. Compared to the initial simulation, both the stiffer and the less stiff systems tended to produce slightly higher head decelerations. The stiffer system did not allow as high head rotations as occurred initially, but produced higher rotations when there was head-roof contact. The less stiff system allowed larger initial head rotations than the other two systems.

It is quite apparent from the computer simulations of the head restraint system that the load-deflection characteristics of the restraint must be carefully selected with respect to the seat-back characteristics to minimize head

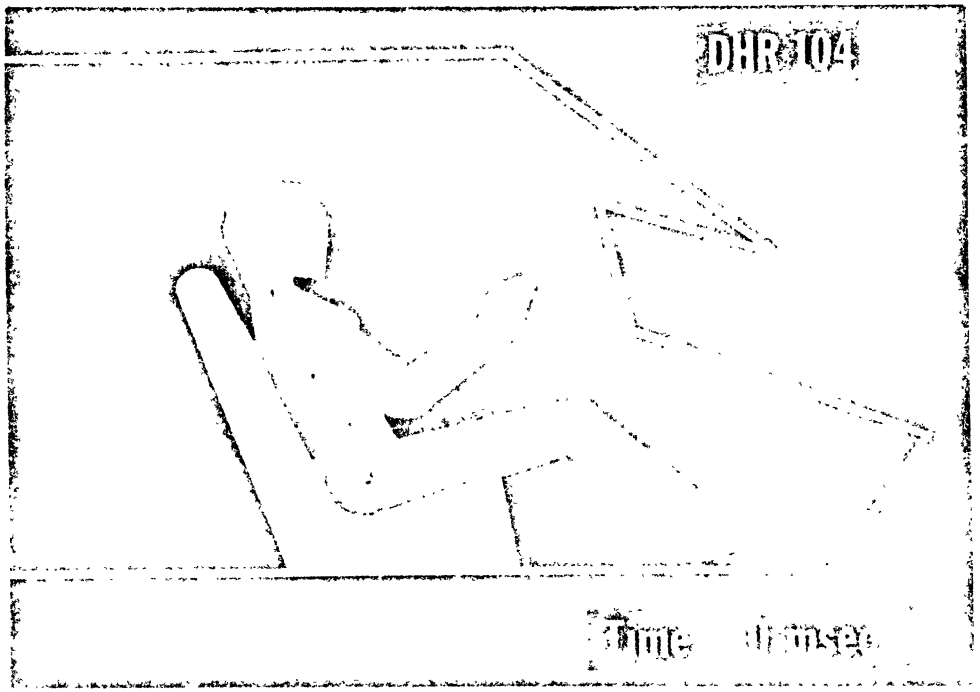

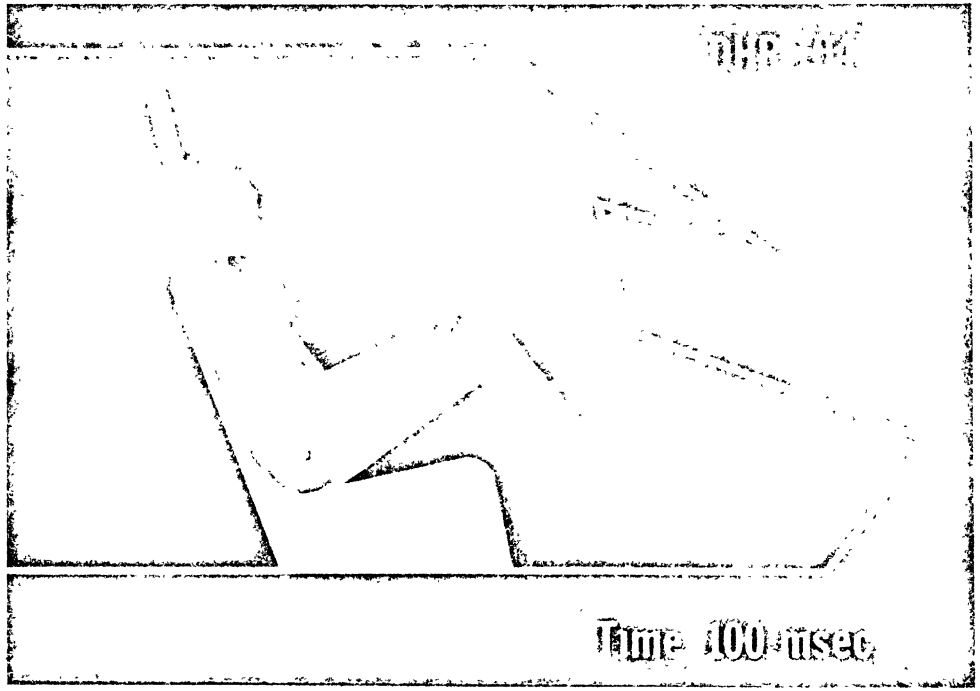

5th Percentile Female - no belts
Deployable Head Restraint Seat
Crash Pulse - 55 mph, Severy - Figure 3.
NOTE: In this simple graphic display the seat back remains in its original position, this was not the case in the actual computer simulation.

Figure 6. Computer Simulation Run DHR 104

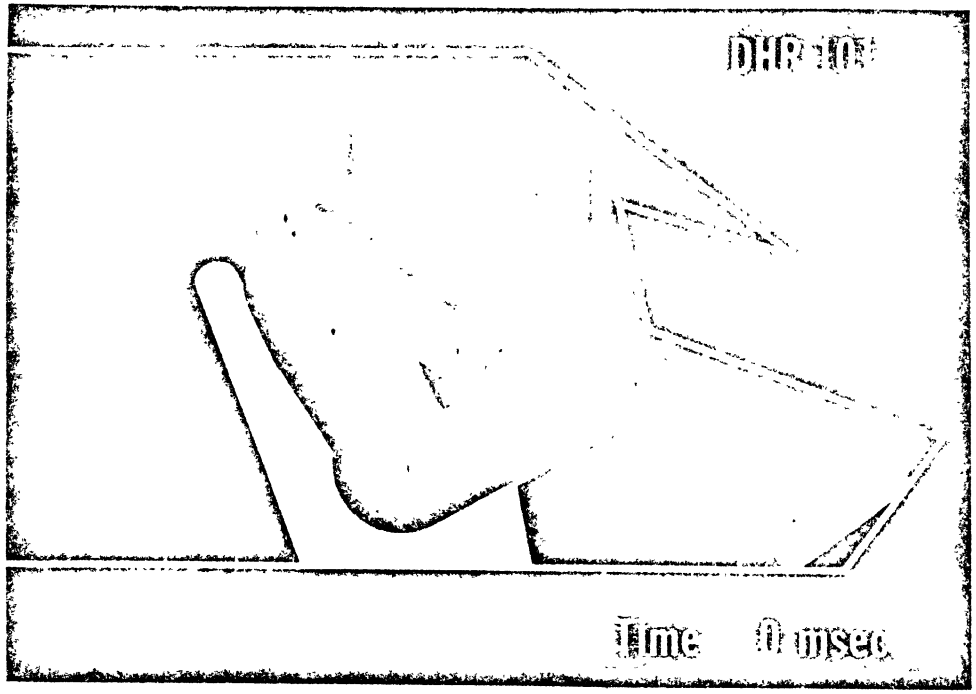

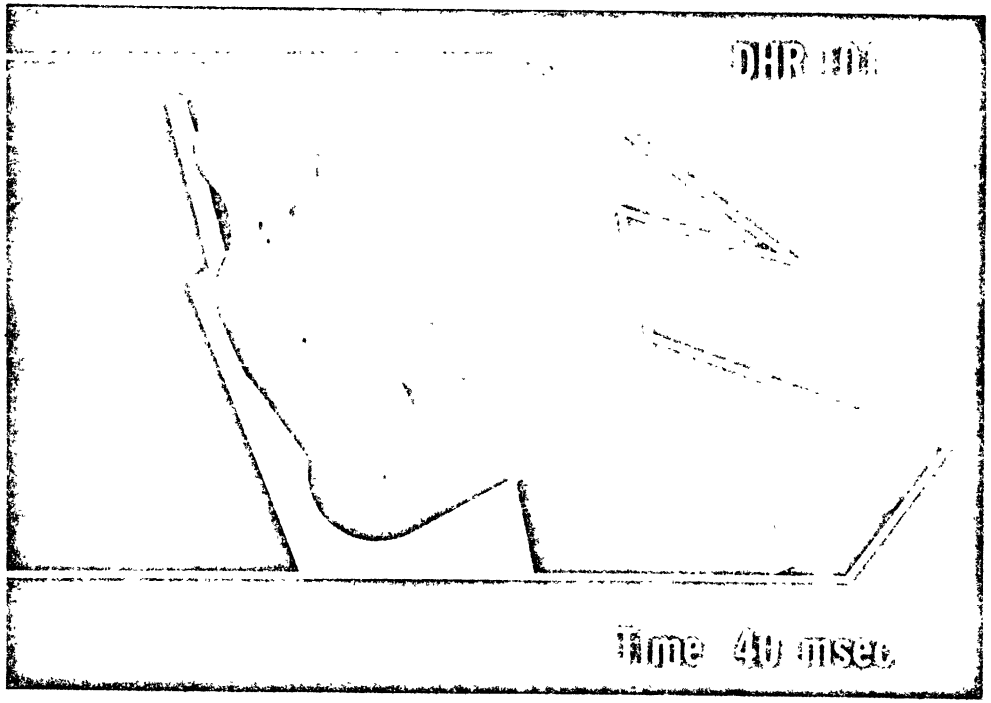

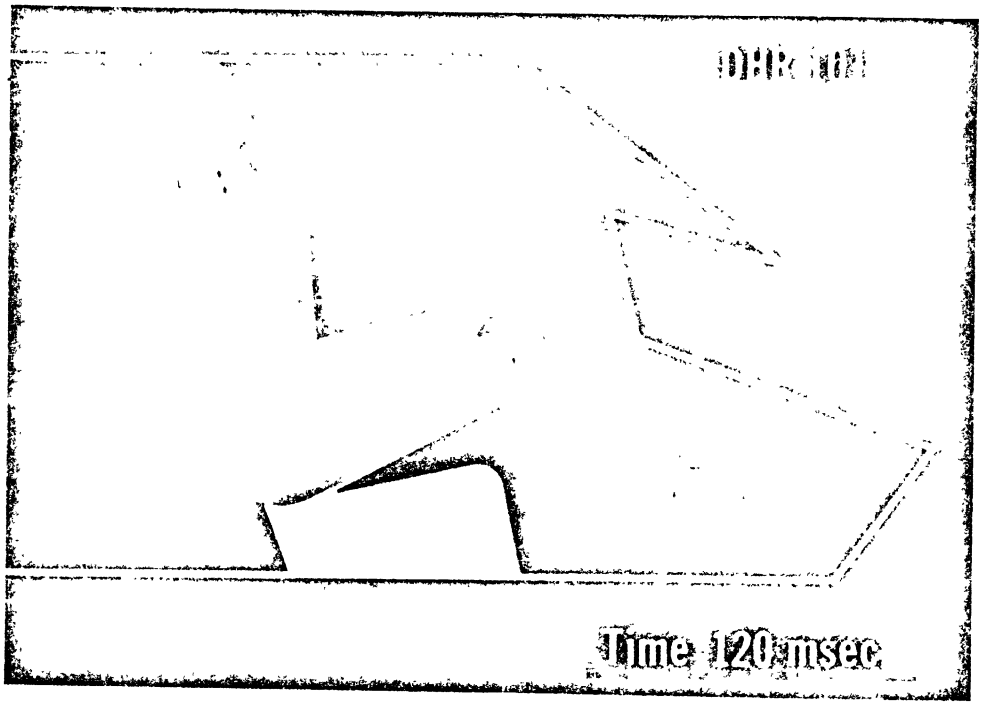

95th Percentile Male - no belts
Deployable Head Restraint Seat
Crash Pulse - 55 mph, Severy - Figure 3.
NOTE: In this simple graphic display the seat back remains in its original position, this was not the case in the actual computer simulation.

Figure 7. Computer Simulation Run DHR 101

TABLE 2. HEAD RESTRAINT COMPUTER SIMULATION MATRIX

%	RESTRAINT	PULSE
95	U	30 mph Severy
95	U	55 mph Severy
95	U	30 mph 10 G
95	U	30 mph 10 G (roof removed)
5	U	30 mph Severy
5	U	55 mph Severy
5	U	30 mph 10 G
95	SB	30 mph 10 G
5	SB	55 mph Severy
5	SB	55 mph Severy (roof removed)
95	U	55 mph Severy Double Stiffness System
95	U	55 mph Severy Half Stiffness System
95	U	55 mph Severy Half Stiffness System (roof removed)
95	U	30 mph 10 G Double Stiffness
95	U	30 mph 10 G Half Stiffness
95	U	5 mph 3.5 g Crash Test Simulation

Rear Seat Occupant Front Impact
Type 2 Head Restraint on Front Seat

%	RESTRAINT	PULSE
95	U	40 mph DOT

Legend % = Dummy size (5% female or 95% male)
Restraint = Restraint System (SB-seat belt, U-unrestrained)

decelerations during the initial contact phase of the crash and also to minimize the possibility of serious extension during rebound. The problem of head-roof contact for larger occupants must also be given consideration.

4. TASK 2. EVALUATION OF CRASH SENSORS

The purpose of this phase of the project was to evaluate various methods and devices for sensing crash conditions in which head restraint is required. Both commercially available devices and an experimental device were evaluated experimentally and in some cases analytically. The evaluation criteria included the following factors:

1. Reliable head restraint system initiation in the shortest possible time after the start of the collision consistent with reliable avoidance of inadvertent system initiation.
2. Simplicity, producibility, and minimum cost.
3. Tolerance to environmental conditions likely to be encountered while installed in automobiles in use in the United States for periods of time up to ten years.
4. Nonsusceptibility to vandalism or tampering.

Examples of the three commercial crash sensors presently available were obtained. They were:

1. Eaton Autoceptor Crash Sensor (shown in Figure 8) - a uniaxial mechanical spring-mass system which fires when the mass is displaced a predetermined distance. The spring holds the mass against an end of the sensor in order to produce a bias force against the mass.
2. Delco Electronics Mechanical Crash Sensor Model 8-1000 (shown in Figure 9) - a ball sear type mechanism fired by displacement of a mass which is restrained by magnetic force. The sensor is essentially omnidirectional in a plane and nominally set to trigger on a 11 G, 80 msec haversine shock wave.
3. Delco Electronics Safety Sentinel 4 Electronic Crash Sensor (shown in Figure 10)- a ball restrained by magnetic force is surrounded by a ring. The ball is displaced by deceleration until it contacts the ring thereby energizing the firing switch. The system is double redundant, self-diagnostic and is set to trigger on a 17 G, 60 msec haversine shock wave.

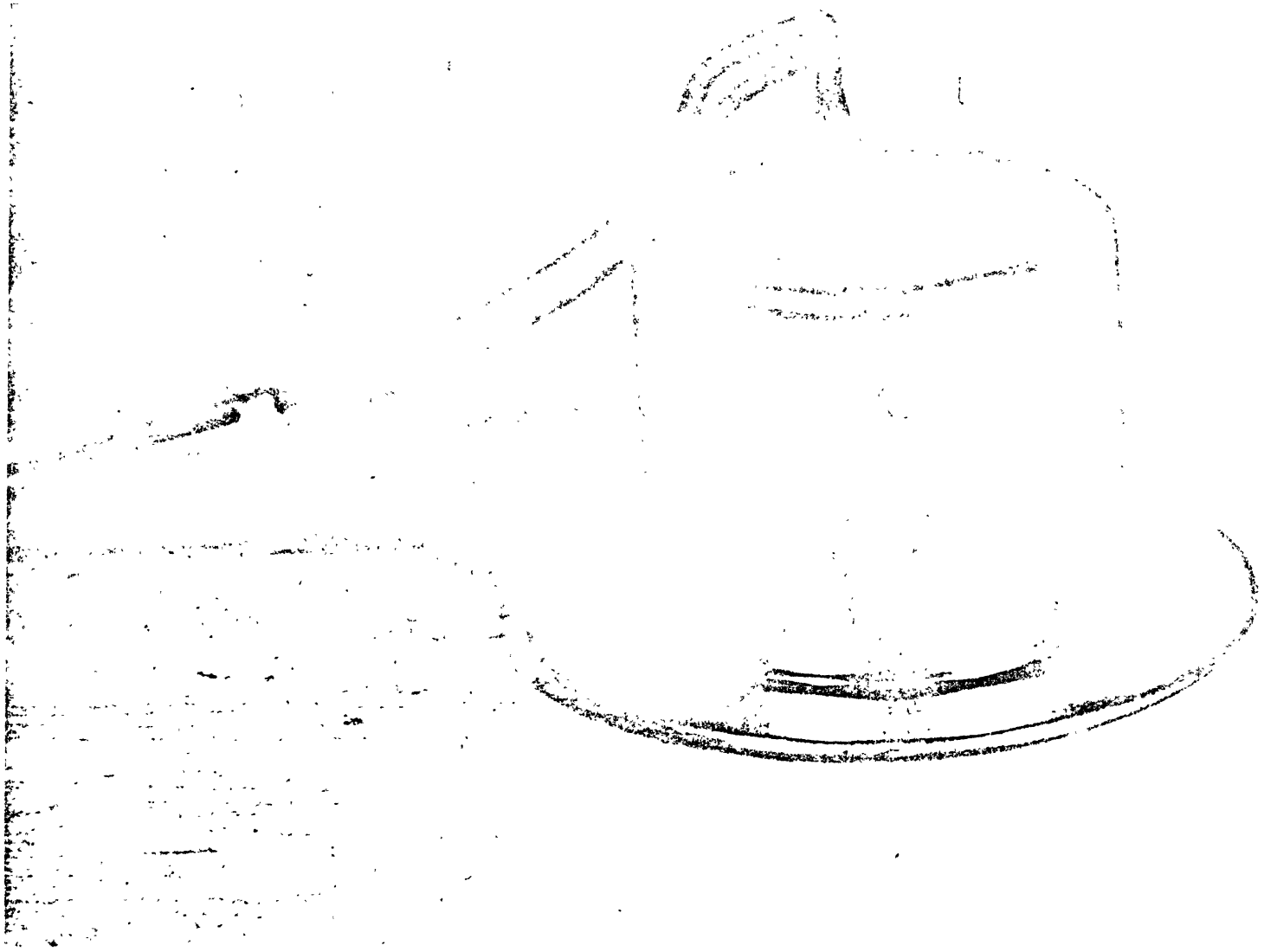

FIGURE 8. EATON CRASH SENSOR

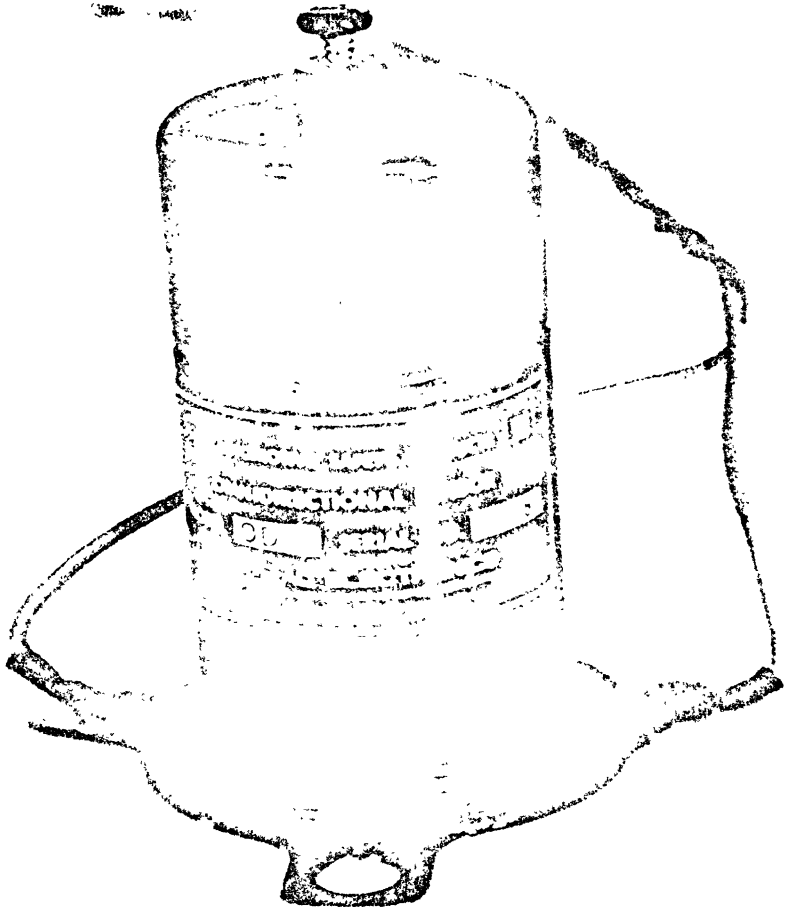

FIGURE 9. DELCO MECHANICAL CRASH SENSOR

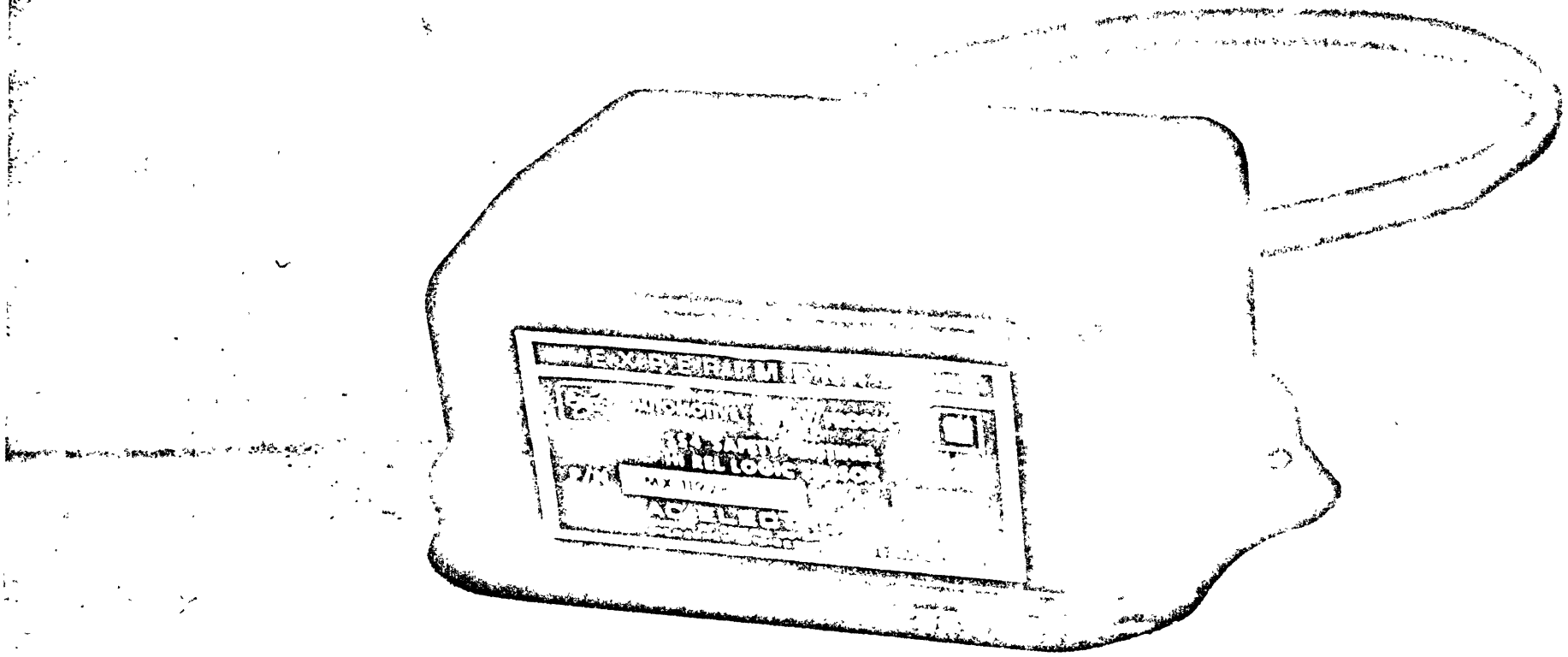

FIGURE 10. DELCO ELECTRONIC CRASH SENSOR

Each of the sensors was mounted on the ram of the Plastechon high speed universal testing machine as shown in Figure 11. This hydraulically actuated, electronically servo-controlled machine was programmed to subject the sensors to a variety of acceleration-time profiles. A Setra Model 110 accelerometer was mounted on the ram to measure the acceleration input to the sensor. The accelerometer output was filtered through a Burr-Brown filter meeting SAE J211 channel class 180 specifications. An automobile 12-volt battery was the power source for the crash sensors. Typical results for each of the three sensors subjected to the same pulse is shown in Figure 12. The majority of the input pulses used in this study were similar in shape to the one shown in Figure 12 because of their similarity to the initial portions of actual automobile rear-end crash profiles (Figure 3). In addition to the laboratory testing, an analytical study of the Eaton sensor was made in order to provide a format with which to present experimental data and to provide a means of projecting sensor performance over a broad range of conditions. An Eaton crash sensor was disassembled and the weight of the moving mass, the load-deflection curve of the spring, the free length of the spring, the static length of the spring, and the distance the mass must travel in order to make electrical contact were measured. From these quantities the following parameters necessary to model the system analytically were determined:

Weight of sensor mass	= 0.01368 lbs
Spring constant of sensor spring	= 0.0201 lbs/in
Equivalent acceleration bias on sensor mass	= 4.16 Gs
Distance the sensor mass must move to trigger	= 0.500 inches

Using these values, a computer study of the system, shown schematically in Figure 13, was made using a half sine acceleration pulse with pulse amplitude and duration as the variable input parameters. The results of the computer study are summarized in Figure 14 in the form of a plot of pulse peak acceleration versus pulse duration with lines of constant ratio of trigger time to pulse duration. Also shown on the plot are experimentally determined points for similar pulses indicating good correlation between the model response and the real system response. Using a similar format, the experimental data for all of the three sensors is shown in Figure 15. In the range of pulse shapes studied, the GM mechanical sensor was the quickest

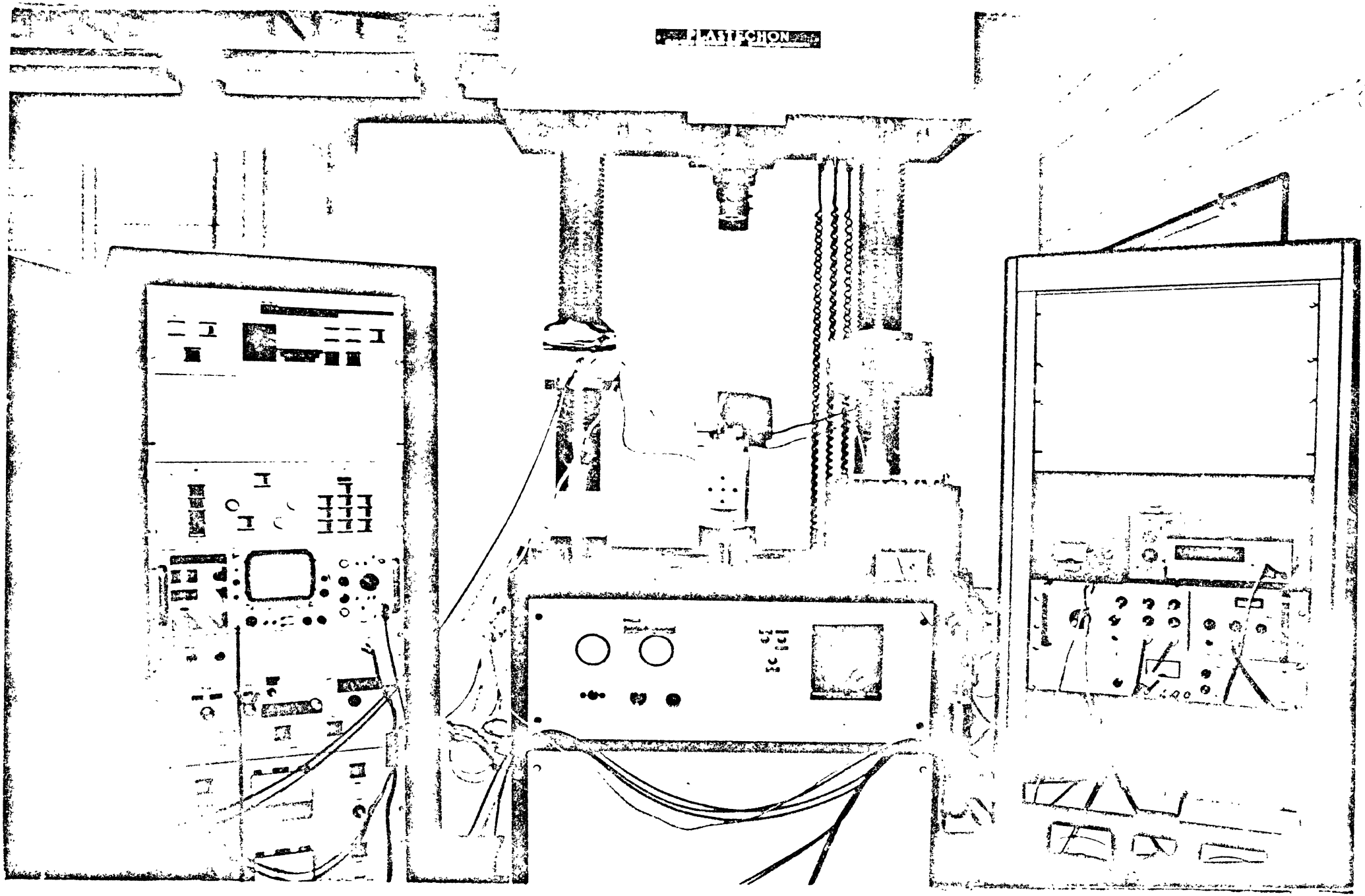

FIGURE 11. PLASTECHON TEST SET-UP FOR CRASH SENSOR TESTING

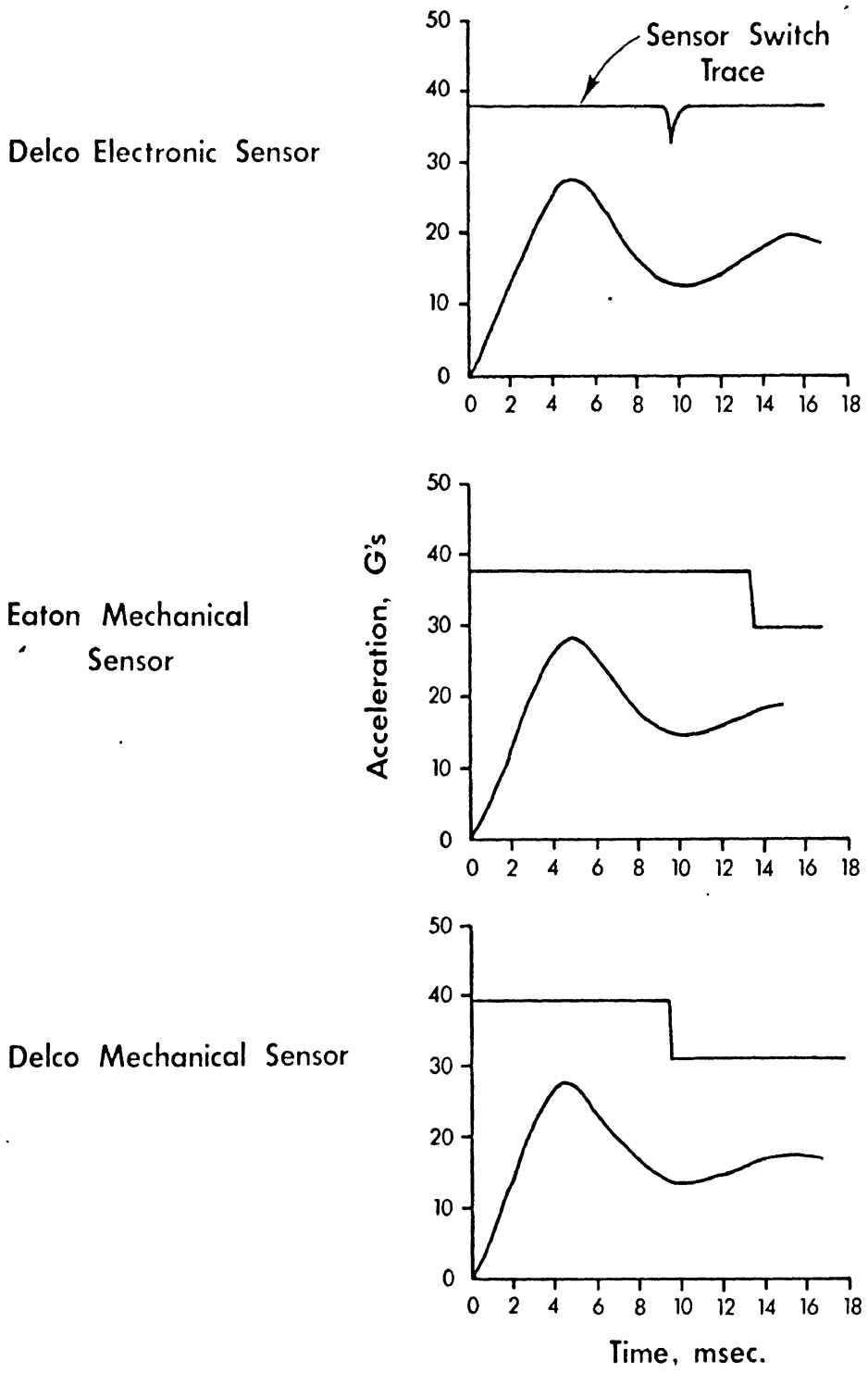

Figure 12. Crash Sensor Response Tests

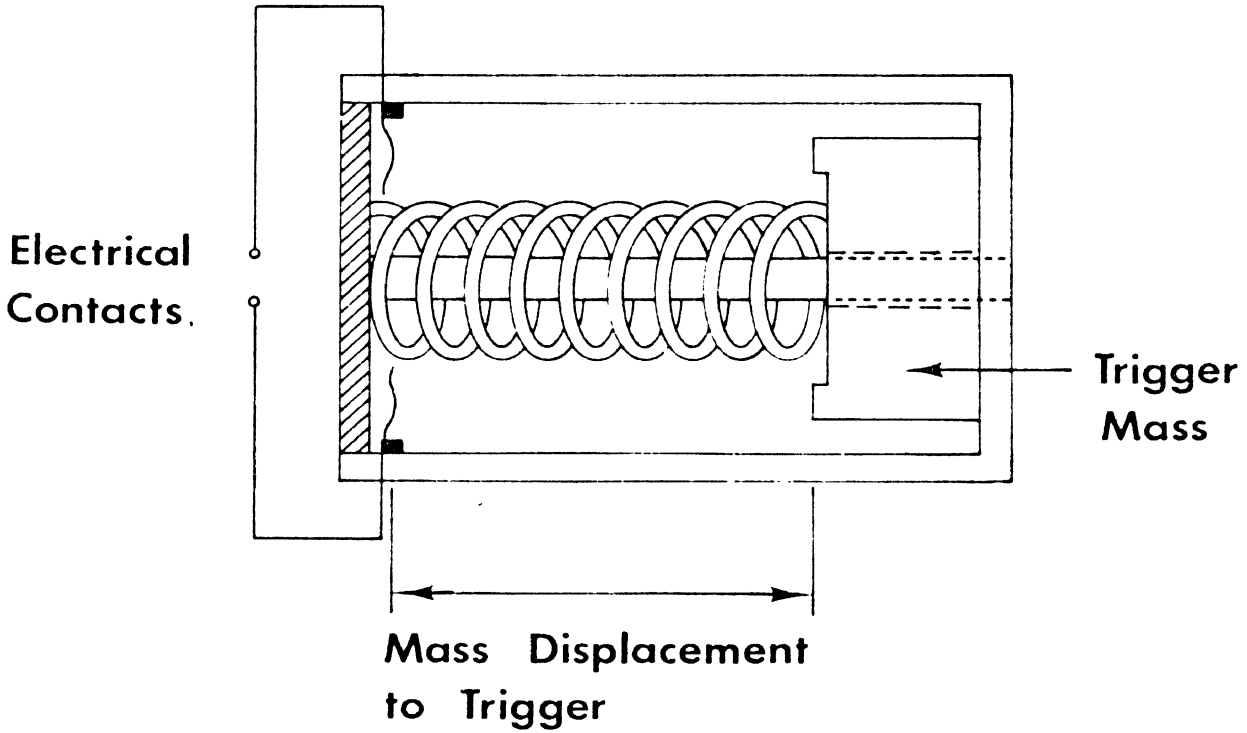

FIGURE 13. EATON CRASH SENSOR SCHEMATIC

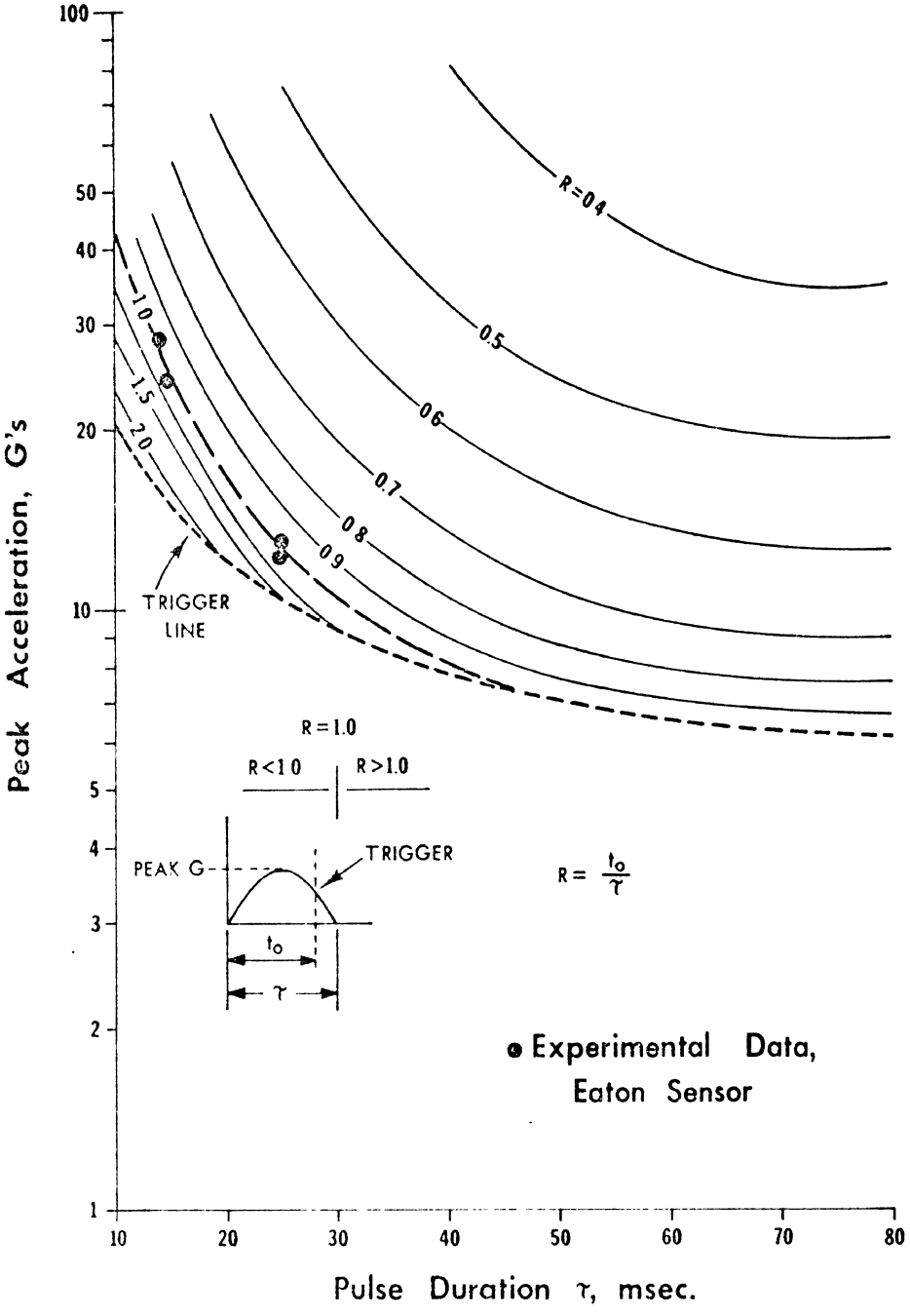

FIGURE 14 . THEORETICAL SENSOR TRIGGER RESPONSE CURVES FOR HALF SINE PULSES WITH THE EATON SENSOR

reacting system with the Delco electronic sensor matching its response at high acceleration amplitudes. The Eaton sensor was intermediate in response for amplitudes of 20 G or less. The general input pulse shape is also shown in Figure 15. Above 10 G's amplitude all the sensors fired at the end of the initial half sine portion of the pulse. For amplitudes below 10 G the two sensors that would trigger at these lower levels did so during the second portion of the pulse.

Tests were performed on the Eaton sensor to establish the effect of off-axis acceleration on the trigger time. Two different amplitude (11 G peak and 24 G peak) acceleration-time profiles were used. The sensor was subjected to the same pulse each time at angular increments of 10° off-axis starting at 0° and increasing until the sensor would not trigger. The trigger time should vary inversely with the acceleration component along the axis of the sensor. This component must include the effect of friction as its magnitude is significant for off-axis acceleration. The net component along the axis of the sensor is then of the form

$$ma(\cos\theta - \mu\sin\theta)$$

where a, is the magnitude of the acceleration vector

m, is the trigger mass of the sensor

θ, is the angle between the acceleration vector and the sensor axis

μ, is the sliding coefficient of friction between the trigger mass and its guide rod.

Thus the trigger time should vary as $1/(\cos\theta - \mu\sin\theta)$. The results of these tests are shown in Figure 16 along with curves corresponding to frictional effects with $\mu = 0.33$ (a typical value for hard plastic on steel). For the high acceleration level tests the trigger time increased along the theoretical curve up to 30° off-axis while in the low acceleration level tests the trigger time increased more rapidly than predicted above 10° off-axis. The increasing departure of the actual trigger time from the theoretical time is most likely due to cocking of the disc-like mass of the sensor on its guide rod thereby increasing the frictional force.

Inadvertent firing due to structural vibrations of the sensor mounting structure has to be considered in the total picture of sensor performance. Any panel that a sensor might be mounted on must not have resonant frequencies during road use that correspond to any critical resonant frequencies of the

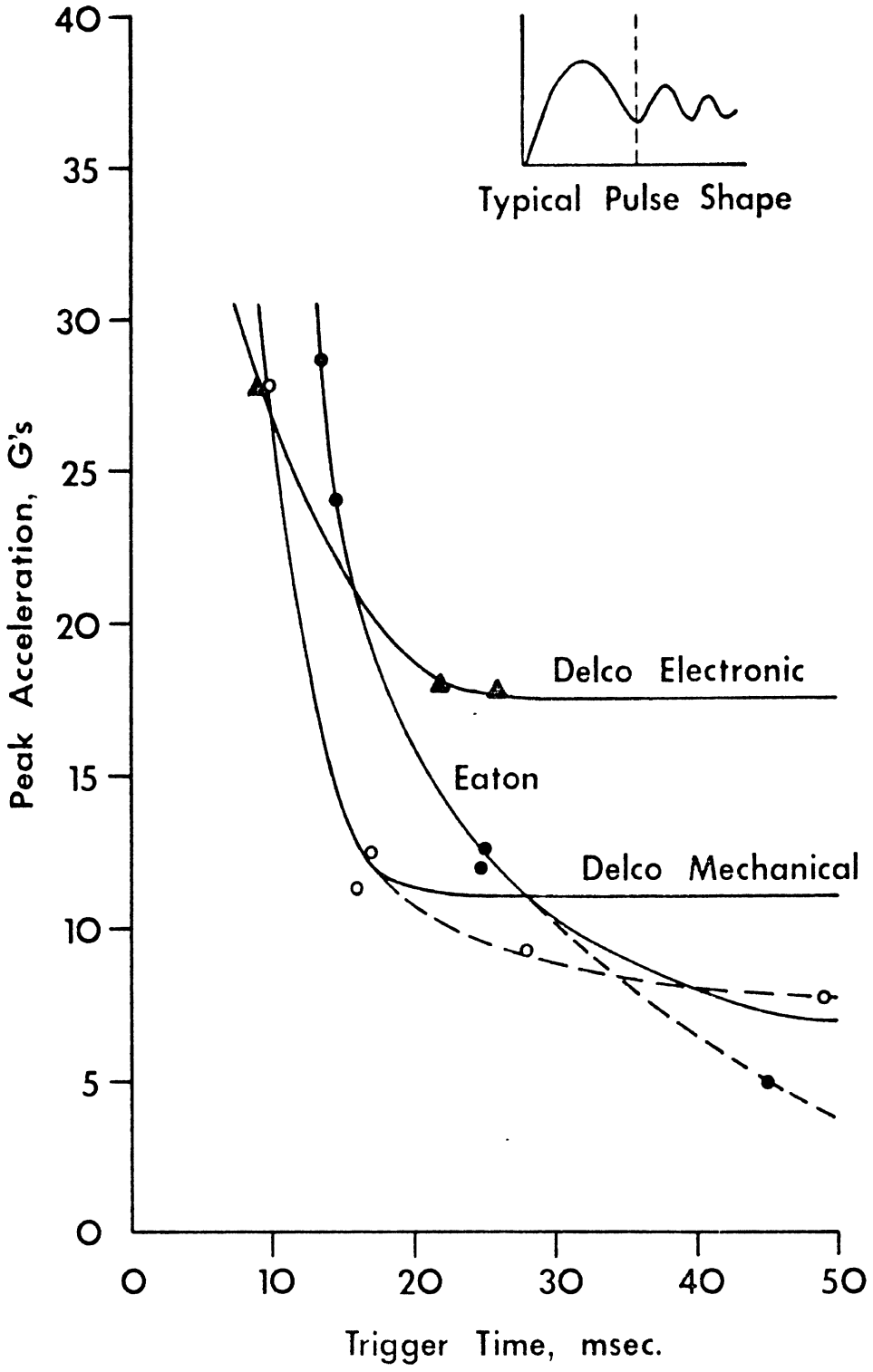

FIGURE 15. EXPERIMENTAL SENSOR TRIGGER RESPONSE CURVES

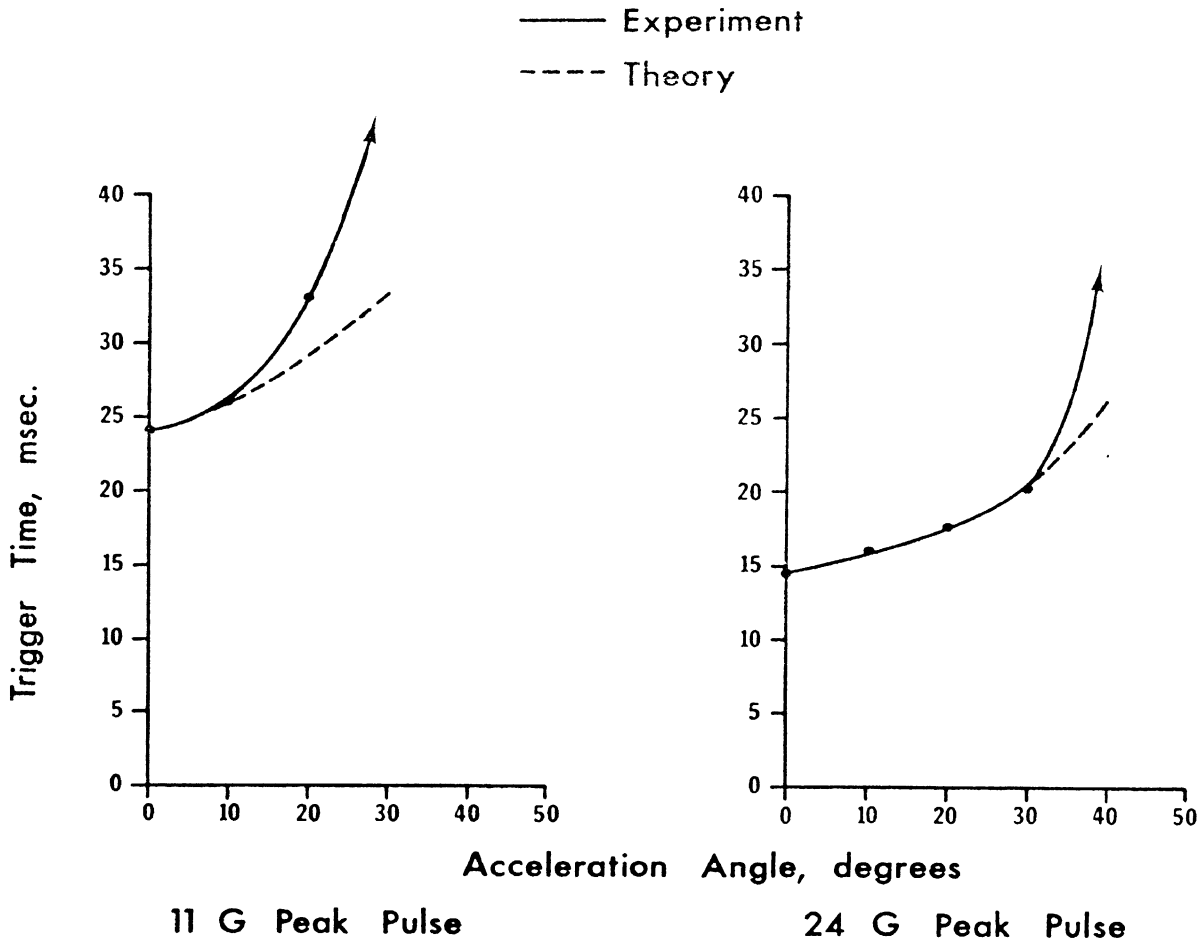

FIGURE 16. EATON SENSOR RESPONSE TO OFF-AXIS ACCELERATION

sensor system. For the case of the Eaton sensor the resonant frequency as calculated from the trigger mass and spring constant is of the order of 4 Hz. The acceleration bias force against this mass is equivalent to 4.16 G. Thus, although the resonant frequency is low, it would require a panel vibration amplitude of 5 inch peak to peak at that frequency to achieve an acceleration level high enough to begin to move the trigger mass. Such a vibration in the fore and aft mode is not likely in an automobile. Using the Plastechon as a shaker and sweeping from 50 Hz up to 115 Hz with a constant 9.6 G peak to peak acceleration sine wave, triggering was found to occur in the Delco electronic sensor at 100 Hz. The ground input into the sensor is equivalent to a 0.018 inch peak to peak displacement at 100 Hz. Although the Delco electronic sensor is set to trigger at the 17 G peak level on single impulses, it appears that certain steady state vibrations at lower acceleration levels can cause the trigger mass to resonate and fire. It is our understanding that this sensor has since been redesigned.

It is evident from results shown in Figure 15 that the Delco mechanical system or the Eaton system would be adequate to use as rear-end crash sensors in their present state for crash profiles such as the 55 mph and 30 mph profiles of Figure 3 (that is, 10 G peak initial half sine wave). However, the head restraint is required to provide protection in low velocity, low acceleration rear-end crashes as well as in more severe collisions. In this context none of these three sensors is suitable for activating a deployable head restraint over the entire range of possible crash profiles where protection is required.

It is possible to modify the characteristics of the sensors (G bias, mass displacement limit, etc.) to sense low level crashes such as the 4.8 mph 1962 Rambler pulse of Figure 3, but then other problems arise. In order to investigate this further, a 1967 Ford was instrumented with a Setra accelerometer mounted on the rear fender-well structure in the trunk as shown in Figure 17. The car was then driven over pot-holed roads, washboard road surfaces, and a railroad tie which simulated a roadside curbing. The most severe conditions recorded were a 30 mph panic stop on a washboard gravel road surface where rear axle hop was induced, and frontward and rearward single impacts running over a railroad tie at 20 mph. The corresponding accelerometer traces for these tests are shown in Figure 18. Of these three

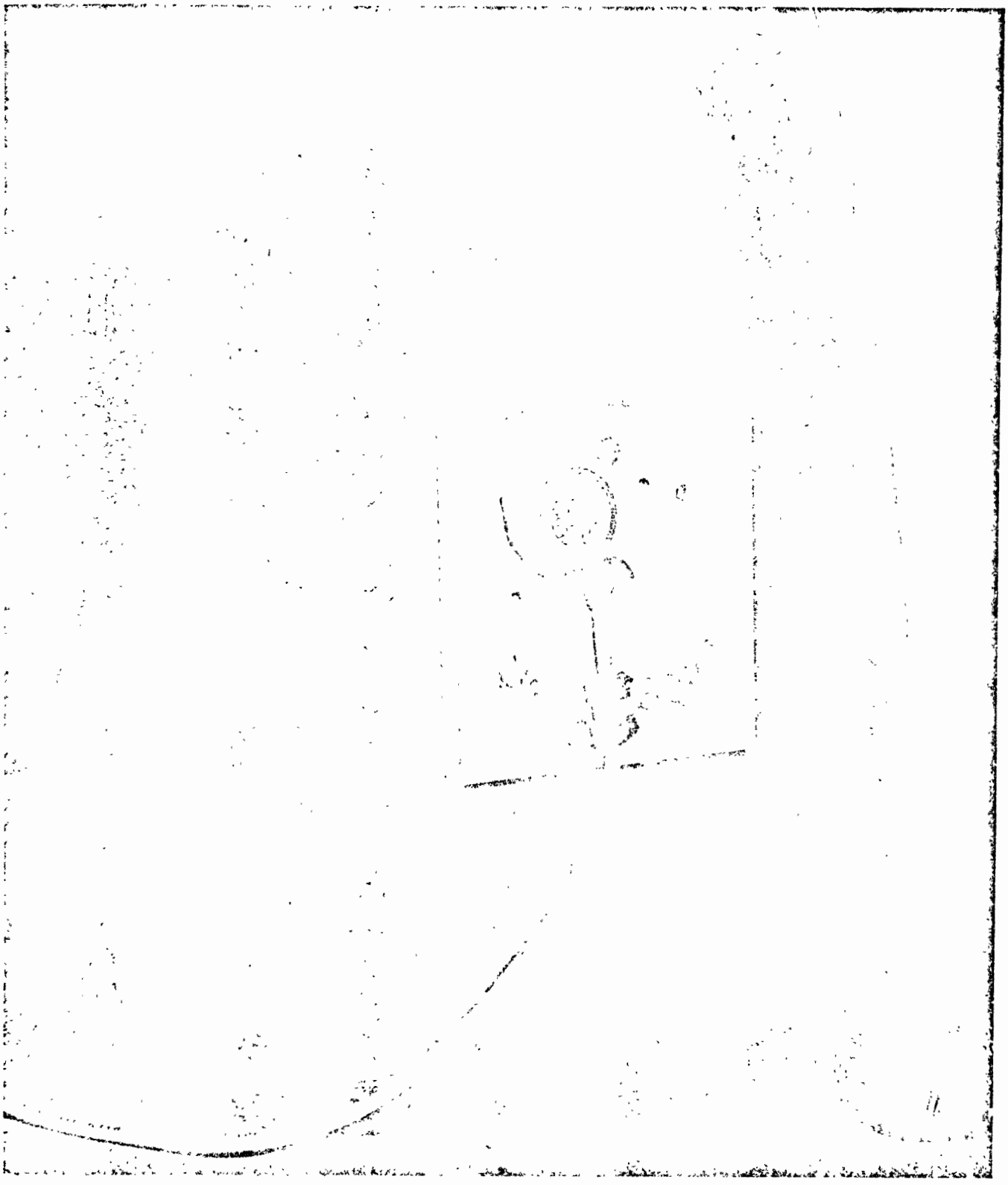

Figure 17. Accelerometer Mounting on Rear Fender Well for Road Noise Study

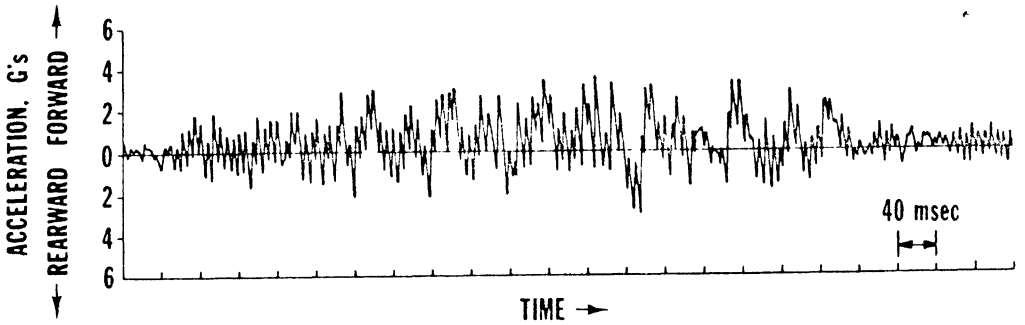

30 mph PANIC STOP ON WASHBOARD GRAVEL ROAD

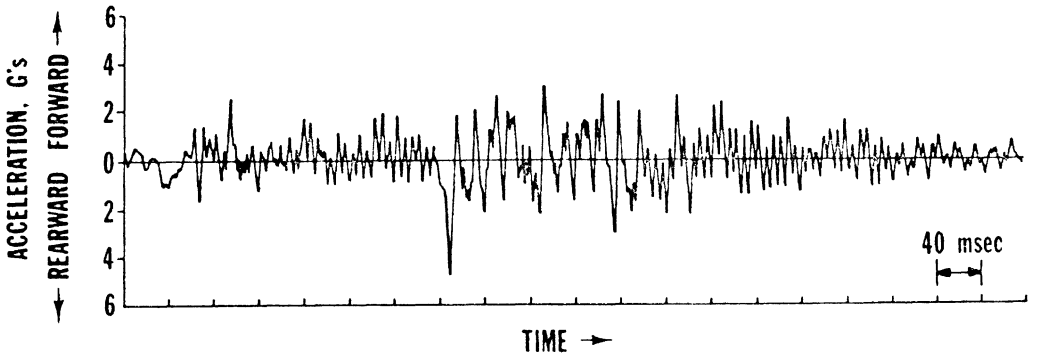

20 mph FRONTWARD OVER RAILROAD TIE

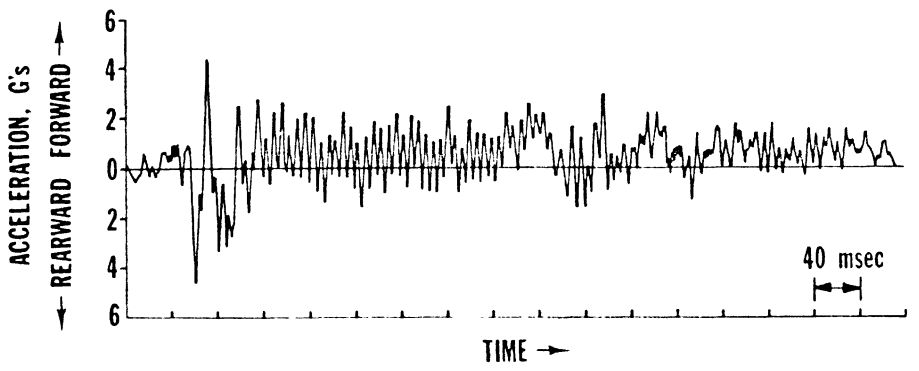

20 mph REARWARD OVER RAILROAD TIE

FIGURE 18. ACCELEROMETER TRACES OF ROAD NOISE

traces, the trace of running backward over a railroad tie produced the largest accelerations in the forward direction (over 4 G's). This is the direction that an inertial rear-end crash sensor would be activated. Comparison of this region of the trace with the acceleration trace from the 1962 Rambler collision test filtered at the same frequency indicated that the initial 40 msec of the crash pulse was very similar to the 40 msec portion of the road test that included the forward acceleration peaks. From this it would appear that using modifications of existing inertial crash sensor designs would not provide an appropriate means of discriminating between low speed crash and moderate speed non-crash situations.

Road tests of the Eaton sensor were made to check for inadvertent actuation during everyday use by mounting three of them in vehicles of widely differing design; a 1967 Ford sedan, a 1969 Triumph TR-6 sports car and a 1965 Jeep Wagoneer. The sensors were mounted on the firewalls of the cars and connected to warning units that would sound a small electronic siren if the unit triggered. The mileage accumulated during the test was nominally equally divided between the three vehicles and totalled 10,573 miles. None of the sensors were actuated during the road test program.

It would appear that one of the most difficult technical problems associated with deployable head restraints is developing a suitable crash sensor. One possibility is incorporation of proposed energy-absorbing rear bumpers as a means of sensing a crash. Because the mechanical characteristics of a bumper will be well defined in order to perform its main energy absorbing function in low speed collisions, these characteristics could serve to provide transducers with information adequate to discriminate and sense a crash quickly. The question of oblique rear crashes would still pose a problem, however, if the bumpers are intended primarily for longitudinal impacts. A sensor which may have application with regard to rear-end crash sensing was developed independently of this project by a graduate student in the Mechanical Engineering Department of The University of Michigan as a master's degree project. A detailed discussion of this sensor and tests performed on it is included as Appendix A of this report. The sensor basically senses the velocity of a constant force energy absorber at a predetermined displacement. Such a device could be developed to provide the proper discrimination and sensing necessary for low speed rear-end crashes and the quickness of responses (5 msec) necessary for 80 mph rear-end collisions with 40 G crush structures.

All of the commercial sensors tested were of basically simple design, although the Delco electronic sensor had sophisticated electronic components associated with it. The sensors were potted in tough plastic and hermetically sealed to such an extent that the effects of environment and tampering on the basic sensor components are minimal.

5. TASK 3. EVALUATION OF DEPLOYABLE HEAD RESTRAINT SYSTEMS

Information was obtained on the following three existing deployable head restraint designs:

1. Ensign-Bickford Co. - an airbag type restraint mounted on the top of the seat back and inflated pyrotechnically.
2. Olin Corp. - an airbag type restraint mounted on the top of the seat back and inflated with augmented bottled gas.
3. Whip-Lash Arrestor Corp. - a rigid type restraint consisting of a vertically rising plane deployed by cocked springs and activated by a counter-weighted hair trigger mechanism (shown in Figure 19). The unit is built into the seat back as shown in Figure 20.

The first two designs consist of small cylindrical airbags about 1 cu. ft. in volume. The two systems were evaluated briefly by viewing high speed movies of crash sled tests using dummies. Both systems deployed quickly but required the dummies to undergo significant rearward head-neck rotation (extension) relative to the torso before they began to load the heads of the dummies by being trapped vertically between the top of the seat back and the dummy heads. This was due to very low fore-aft resistance to motion on the part of the restraint. In discussions with the manufacturers of these two systems, a minimum deployment time of 20 msec was established.

The third head restraint type, a prototype rigid system developed by an inventor, was received and tested on the HSRI Impact Sled Facility. The test involved deployment characteristics only and was performed by attaching the system to the frame of the impact sled which was being run for other purposes. The performance of the Whip-Lash Arrestor during a 30 mph total velocity change crash simulation indicated that it had some difficulty deploying under severe deceleration environments and it deployed late in the crash pulse requiring some 70 msec to sense the crash and an additional 70 msec to deploy.

The evaluation of deployable head restraint systems was based on the following criteria:

1. Adequate distribution of head restraint forces, control of head accelerations, and control of head/neck displacement and flexure for the prevention of injury.
2. Rapid deployment, in conjunction with crash sensor and system initiation time requirements,to provide effective protection.

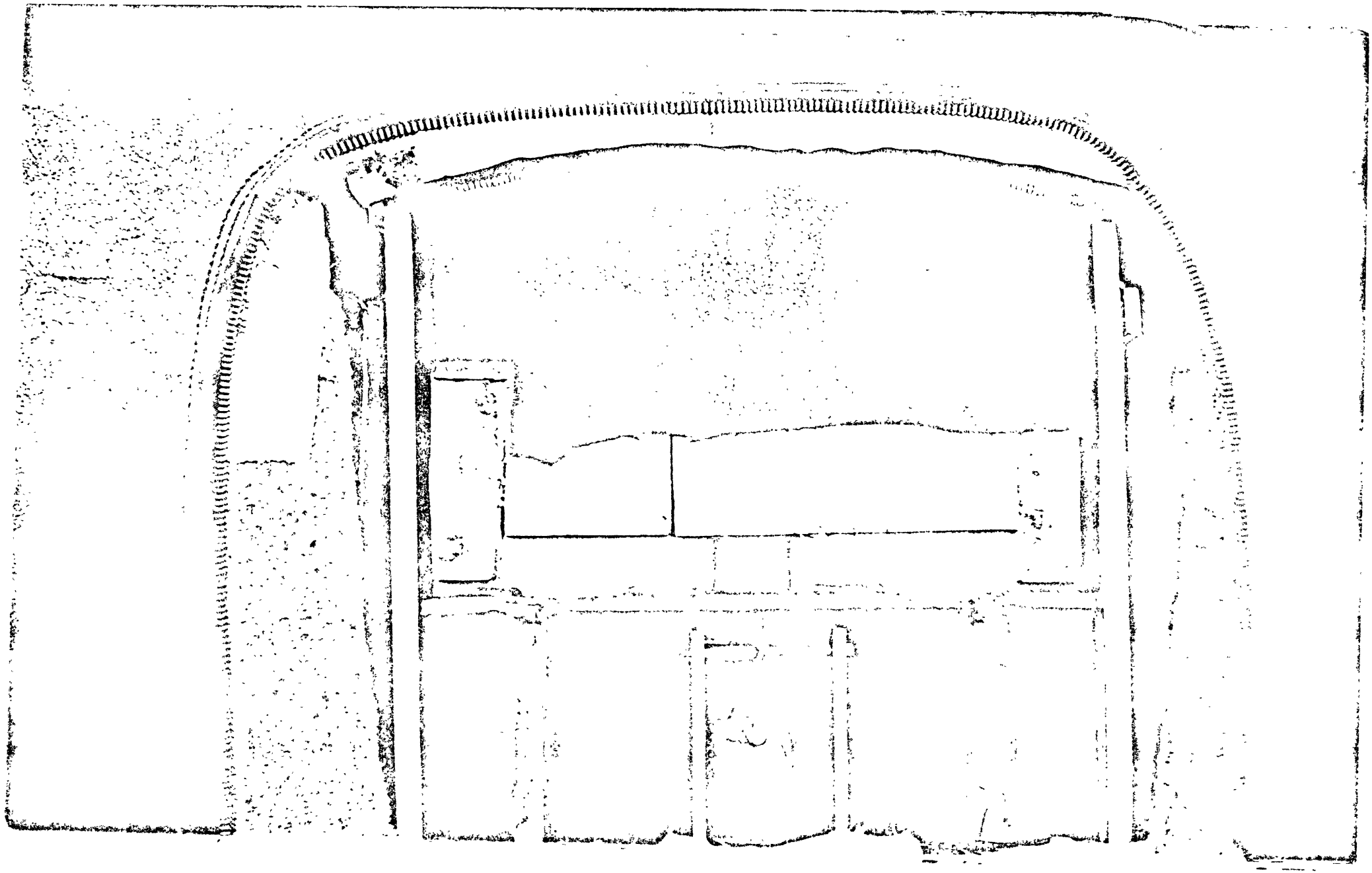

Figure 19. Whiplash Arrestor in Cocked Position

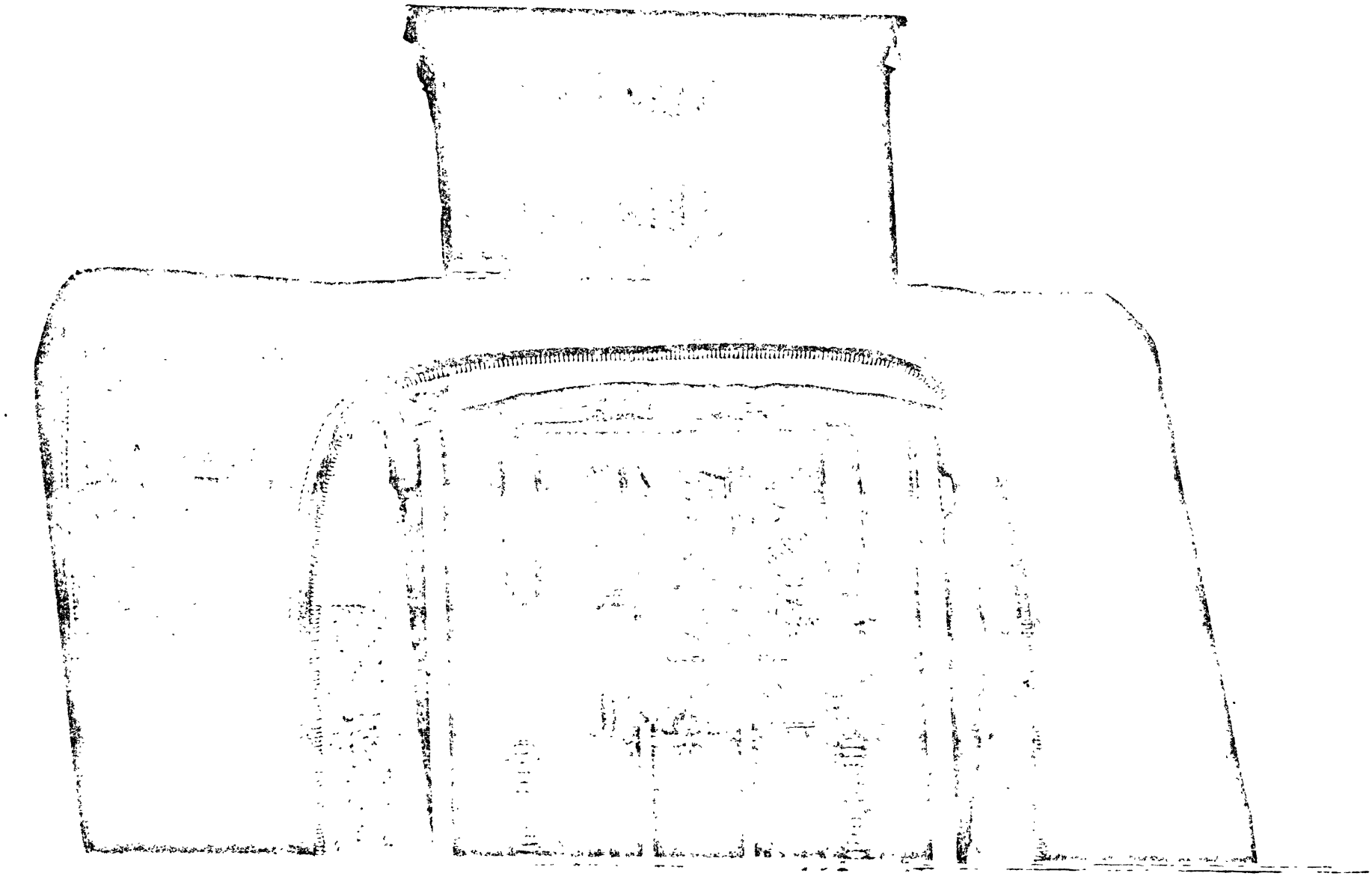

Figure 20. Deployed Whiplash Arrestor

3. Minimization of hazard to vehicle occupants in various possible positions and locations, both during a crash and during inadvertent activation.

4. Reliable activation on signal from the crash sensor, and reliable avoidance of inadvertent activation.

5. Simplicity, producibility, and minimum cost.

6. Requirements relative to other vehicle systems, such as seat structures.

7. Tolerance to environmental conditions likely to be encountered while installed in automobiles in use in the United States for periods of time up to ten years.

8. Nonsusceptibility to vandalism or tampering.

For the most effective analysis, the results of the rear-end crash simulations were presented to a multidisciplinary panel of experts for discussion. The panel consisted of Dr. Verne Roberts and Dr. James McElhaney for biomechanical considerations, Dr. Richard Snyder for anthropometric considerations and Dr. Harold Portnoy for neurosurgical considerations. In discussing the above criteria, the panel felt that the performance of the deployable head restraint system should not be just equivalent to existing fixed head restraints but, if possible, its performance should exceed that of conventional systems. Based on recent work by Dr. Portnoy (Portnoy,1970) in which minimal separation between head and fixed restraint was found to be highly desirable, it was concluded that the simulation results should be analyzed with the aim of defining a system time-space configuration which would minimize the occupant's total head motion. This goal, combined with inputs from Tasks 2 and 3 in the form of crash sensing and discrimination time allowance of 20 msec and a deployment time allowance of 20 msec , was used to define a surface extending above the seat back against which no occupant's head would come into contact in less than 40 msec after crash initiation in the conventional rear-end crash conditions that were studied. For the case of the 80 mph 40 G crash structure simulation the same occupant configuration occurs at 25 msec after crash initiation. Since a 20 msec deployment time appears to be at the limit of the present state of the art, it is apparent that a much quicker means of sensing such a severe crash is necessary to meet a 5 msec sensing and discrimination time budget.

The requirement of occupant protection during rear-end collisions defines a space-time deployment configuration which would insure that it would be deployed in adequate time for its necessary functions in frontal crashes as discussed in Task I.

The configuration of the deployable head restraint system is also subject to stored and deployed height requirements. These basically anthropometric requirements were determined from the existing literature (Meldrum, 1965). Figure 21 shows the locations of the baseline requirements for the seating system that was used in the experimental phase of this project. The eyellipse lower line defines a maximum stored height that the system may have and still give adequate rear vision for small drivers (21.5 inches above the H-Point). The upper line locates the top of the head for large occupants (32 inches above the H-Point). A deployed restraint height approximately two inches below this line was used in the design of deployable head restraint systems.

Two basic deployable head restraint configurations were designed, one inflatable, the other rigid. The inflatable system is shown schematically in Figure 22. The rotating hatch which covers the restraint in its stored position serves to shape the initial deployment of the bag and, following full deployment, provides fore and aft stiffness to the system in its vertical position. The rigid system is basically a vertical sliding plane and is shown schematically in Figure 23. It was decided that the head restraints would remain in place following the initial crash pulse in order to provide protection from possible subsequent secondary collisions, since the configuration of the restraints would not significantly impair driver control of the vehicle.

The configurations of the deployed head restraint systems chosen for this study, when considered with their associated seat structure, are intended to produce the equivalent of a load distribution couch for riding down the acceleration profile of a rear-end collision in the most efficient means possible.

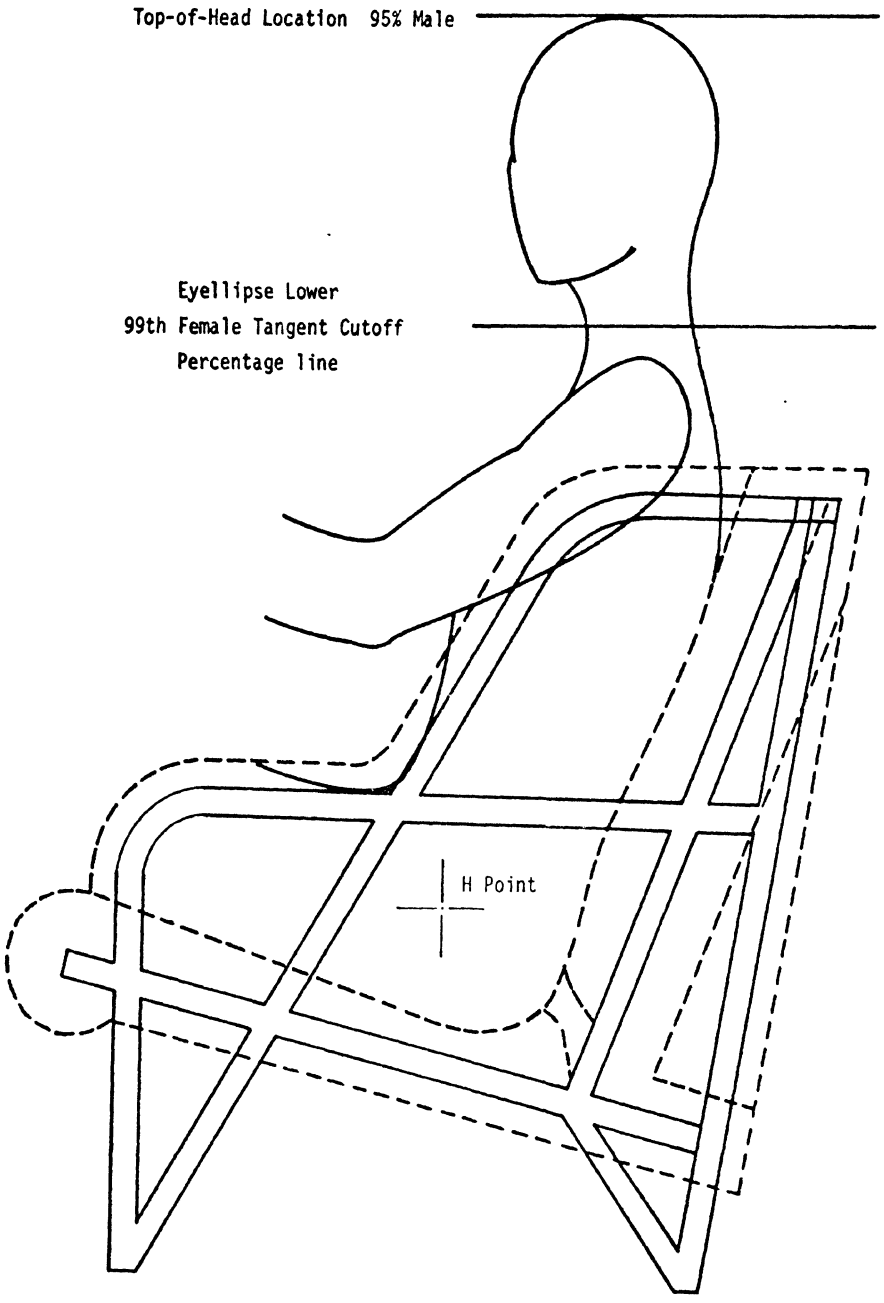

FIGURE 21. ANTHROPOMETRIC CONSIDERATIONS FOR HEAD RESTRAINT

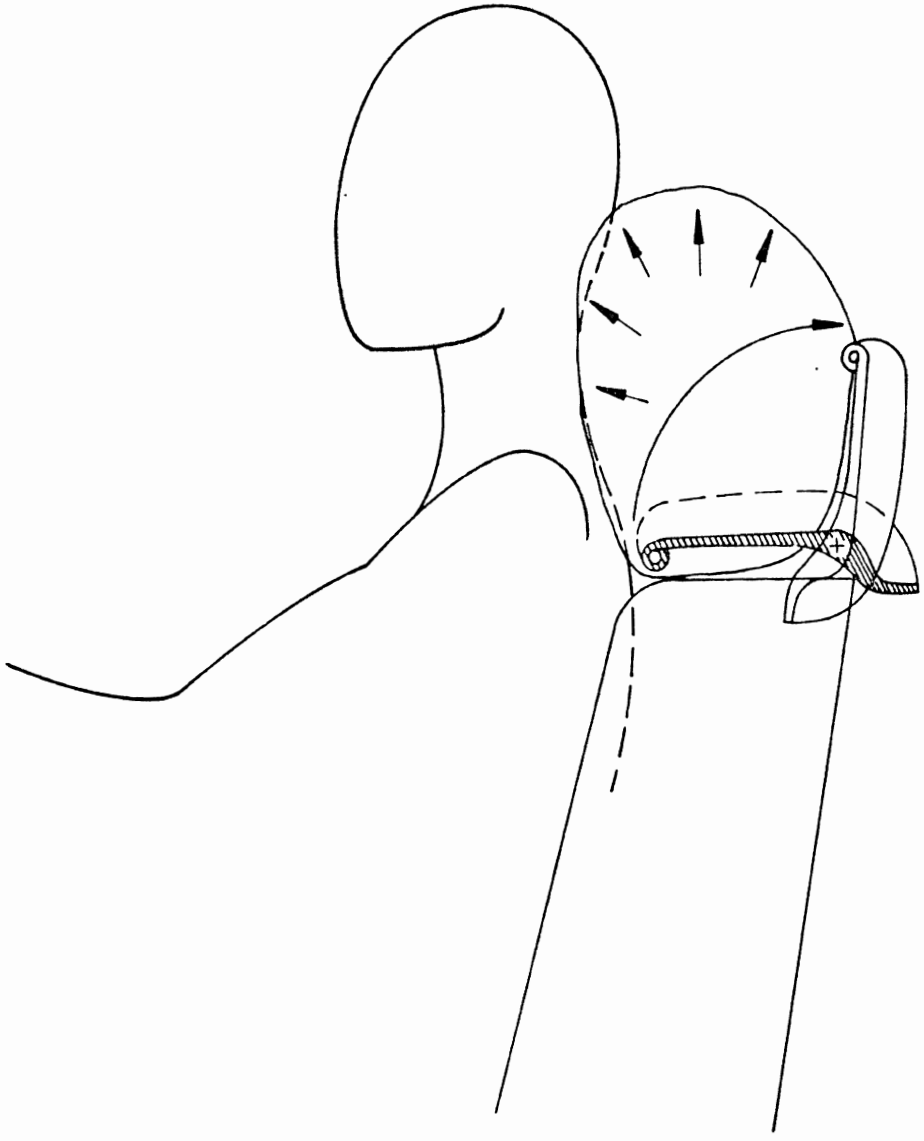

FIGURE 22. INFLATABLE HEAD RESTRAINT CONFIGURATION

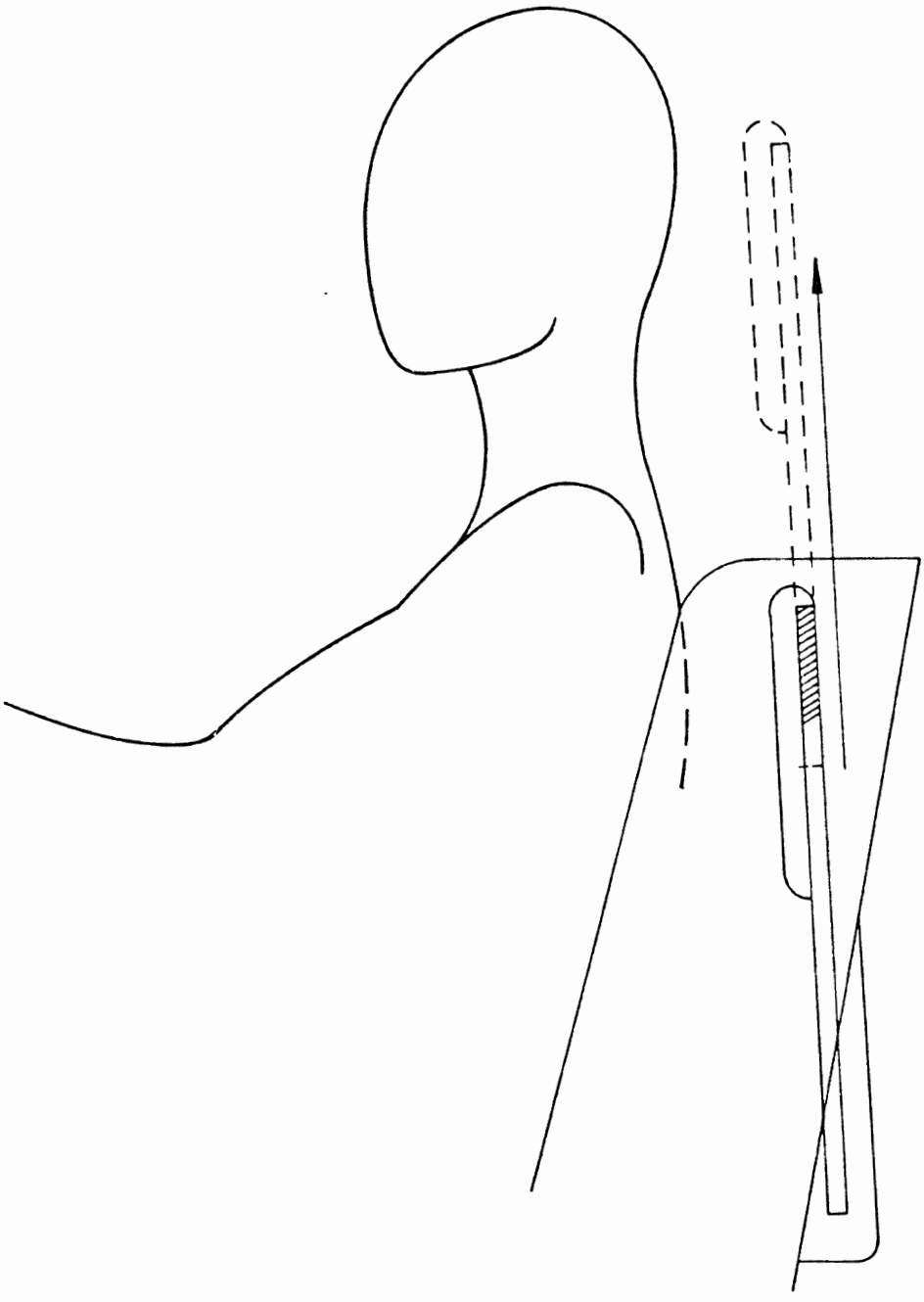

Rigid Deployable Head Restraint Configuration

Figure 23

6. SYSTEM DESIGN

This section discusses the design and fabrication of the two types of deployable head restraints used in this study. One prototype of a rigid sliding deployable head restraint was constructed, whereas, three types of inflating deployable head restraints were constructed.

6.1 INFLATING DEPLOYABLE HEAD RESTRAINT DESIGN

6.1.1 Eaton Deployable Head Restraint System. The inflatable head restraint system supplied by the Eaton Corp. consisted of an inflator system utilizing the inflation bottle and diffuser from their existing steering wheel airbag system and a special 12-inch diameter cylindrical head restraint 18 inches long specified by HSRI. The large diameter of the bag was necessary in order to achieve the proper vertical travel above the undeployed package height which included the inflator system as it is internal to the bag in the Eaton design. The accompanying rotating stabilization flap was designed and fabricated by HSRI. The flap was a curved sandwich panel pivoted at its outboard ends. The core material was balsa wood and the skin material was aluminum. The combined restraint and flap system is shown in Figure 24; the restraint bag is wrapped around the inflator-diffuser system and the flap is lightly taped down over it.

Figure 25 shows the system in its deployed configuration, in this particular picture a preinflated version. In the preinflated test series the bag was used without the inflator system and instead, a polyethylene bag was put inside the dacron restraint bag to eliminate air leakage.

6.1.2 Olin Deployable Head Restraint System. The Olin Corp. supplied special inflator units for use with head restraint bags made by Uniroyal. The bags were made of rubber-coated fabric with vulcanized seams and were elliptical in cross-section -- 8 inches deep, 10 inches high and 18 inches wide. The inflator was designed to mount below the bag in order to minimize the stored height of the restraint package. The inflator bottle was a special rechargeable design by Olin using the augmented air principle of inflation. Prior to testing, the inflator bottle was pressurized to

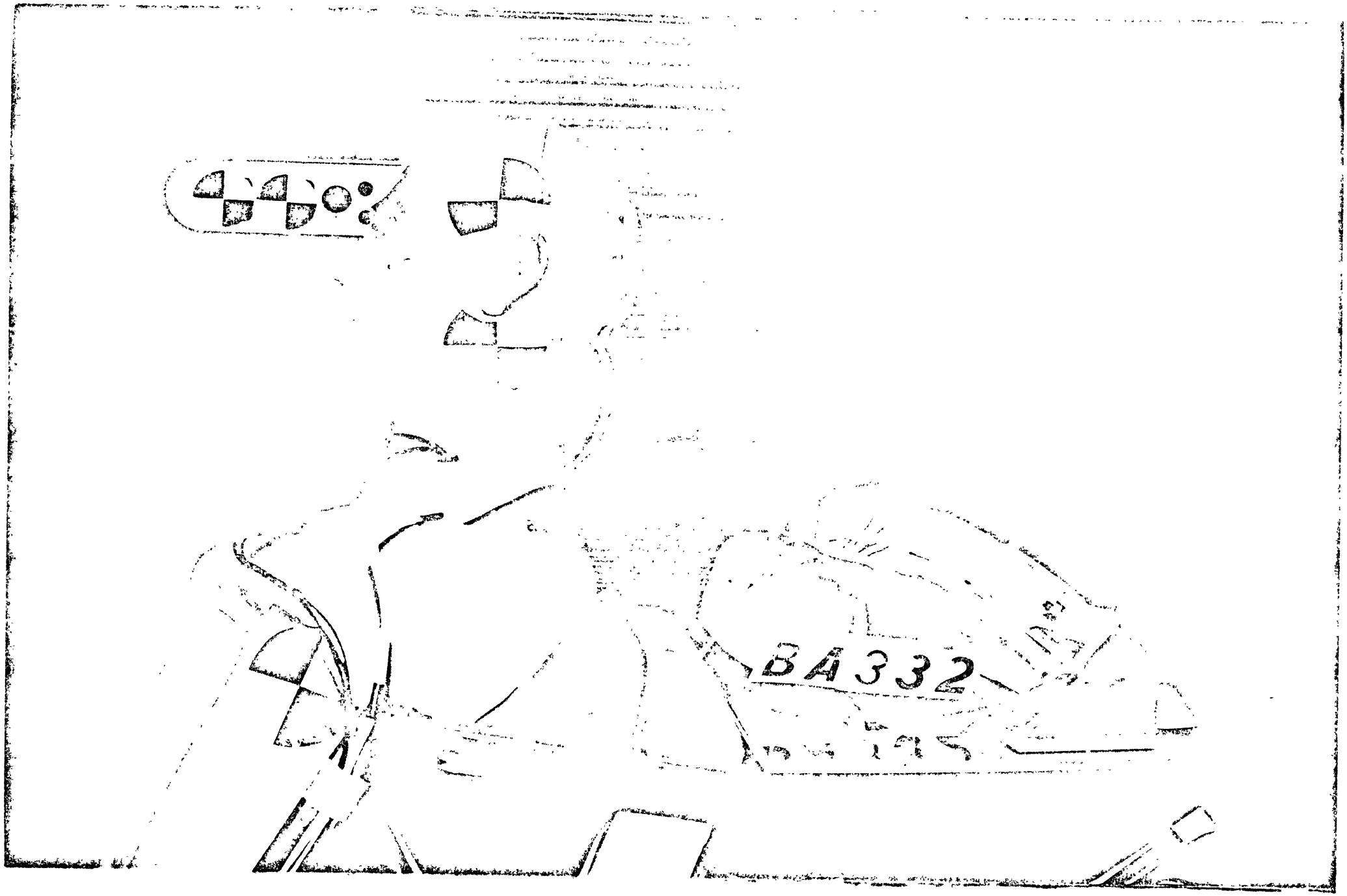

Figure 24. Eaton Inflatable Head Restraint with Stabilizing Flap

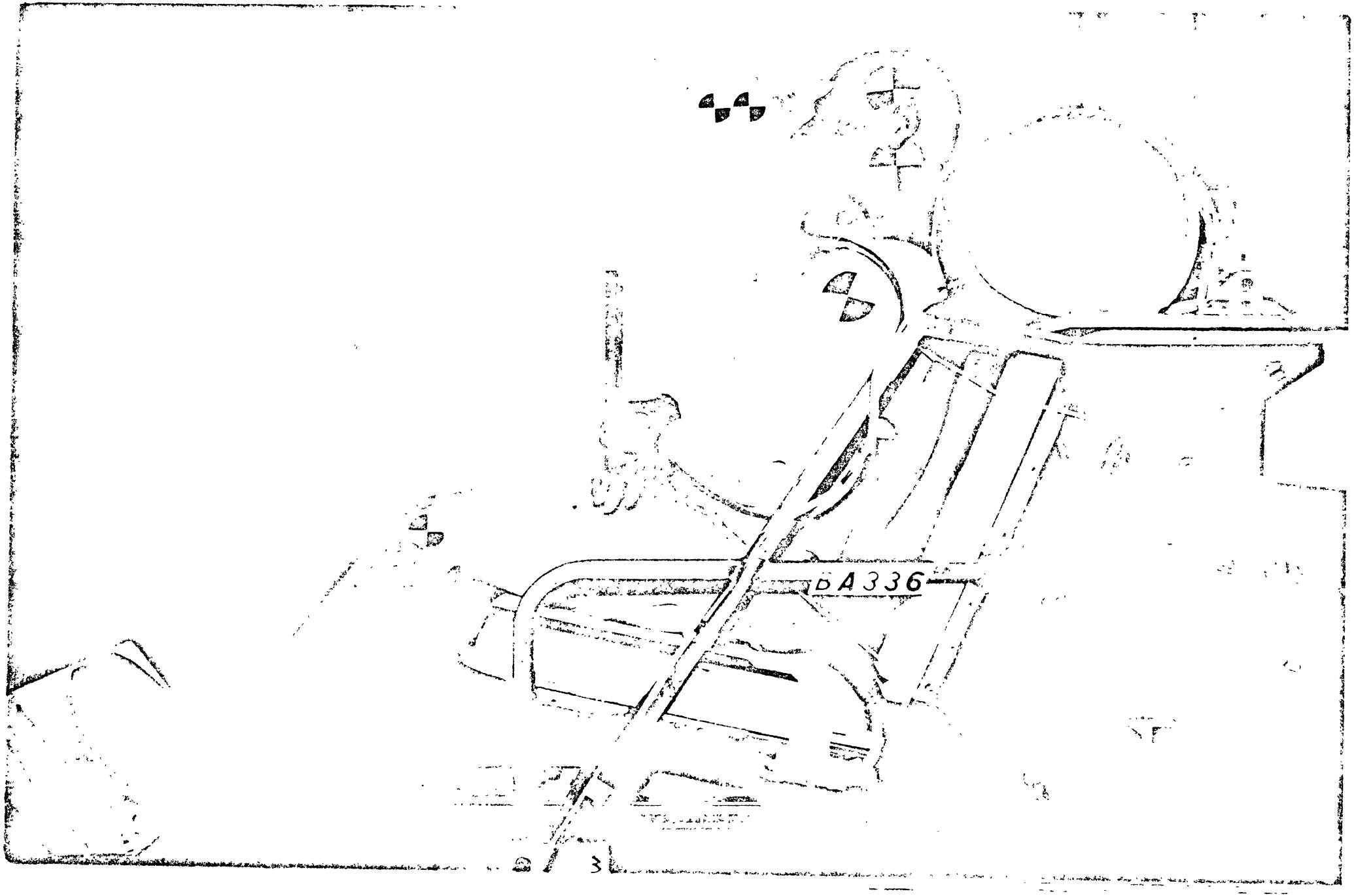

Figure 25. Deployed Configuration of Eaton System (Pre-inflated)

1800-2400 psi with compressed air. The sequence of events following activation of the system is:

1. A squib is ignited in the pyrotechnic portion of the inflator.
2. Pyrotechnic pressure is built up rupturing a disc which allows the hot gas to enter the chamber where the high pressure air is stored.
3. The heating of the high pressure air causes a second disc to rupture allowing the gases to fill the restraint bag.

The stabilizing flap used with the Eaton system was also used for the initial tests of the Olin system. These tests utilized preinflated bags without the inflators. The system configurations for these tests are shown in Figures 26 and 27.

Following the tests of the preinflated systems, modifications of both the bag mounting plate and the stabilization flap design were made. The flap was redesigned for compactness and low weight by making it a single curved plate of 3/16 inch thick aluminum. The number of pivot points was increased to four by the addition of two inboard pivot bearings. The bag mounting point was raised as high as possible within the confines of the maximum package height defined in Figure 21. The predeployed configuration of the modified Olin system is shown in Figure 28, Figure 29 shows the inflator mounting position and the pressure transducer location, and Figure 30 shows the system configuration following deployment. The placement of the system relative to the 95th percentile male dummy is shown in Figure 31.

6.1.3. Air Mat Inflatable Head Restraint System. An unusual concept in inflatable structures was brought to our attention late in the program and because of the limited time available it was utilized without the benefit of much development. The basis for the unusual characteristics of this material, known as dropweave fabric, is the manner in which it is woven. Figure 32 shows such a material in an unfinished form. The material is woven three-dimensionally with the tightly woven upper and lower surfaces forming fabrics and the dropwoven threads serving to tie the two surfaces together. When the sides of the material are sealed by bonding fabric to provide an air tight system, the resulting inflatable structure is much more stiff in bending than a comparable baglike inflatable system due to the three dimensional nature of the dropweave fabric. A head restraint made of

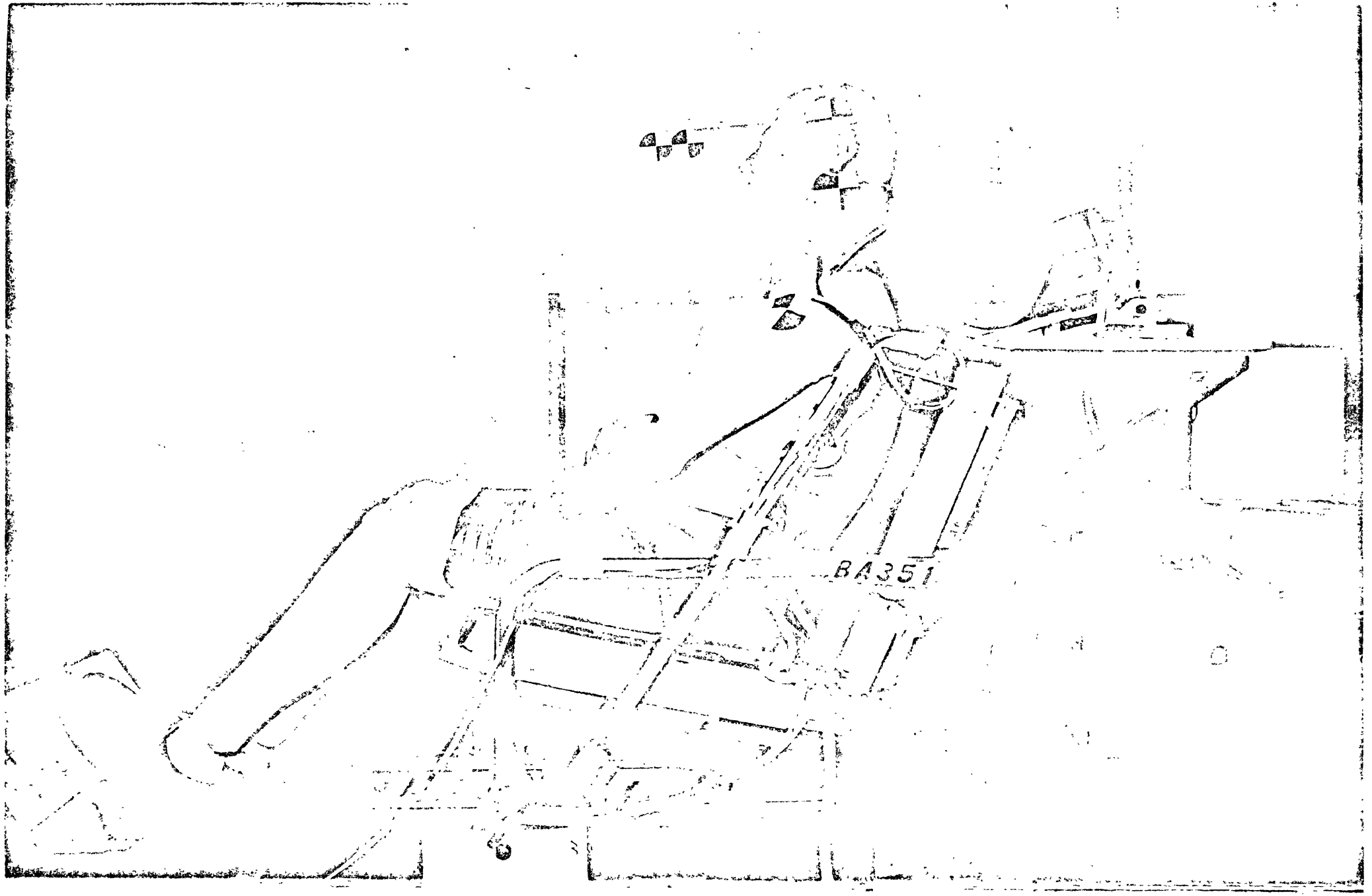

Figure 26. Olin Inflatable Head Restraint with Stabilizing Flap
(Shown with a 95th Percentile Male Dummy)

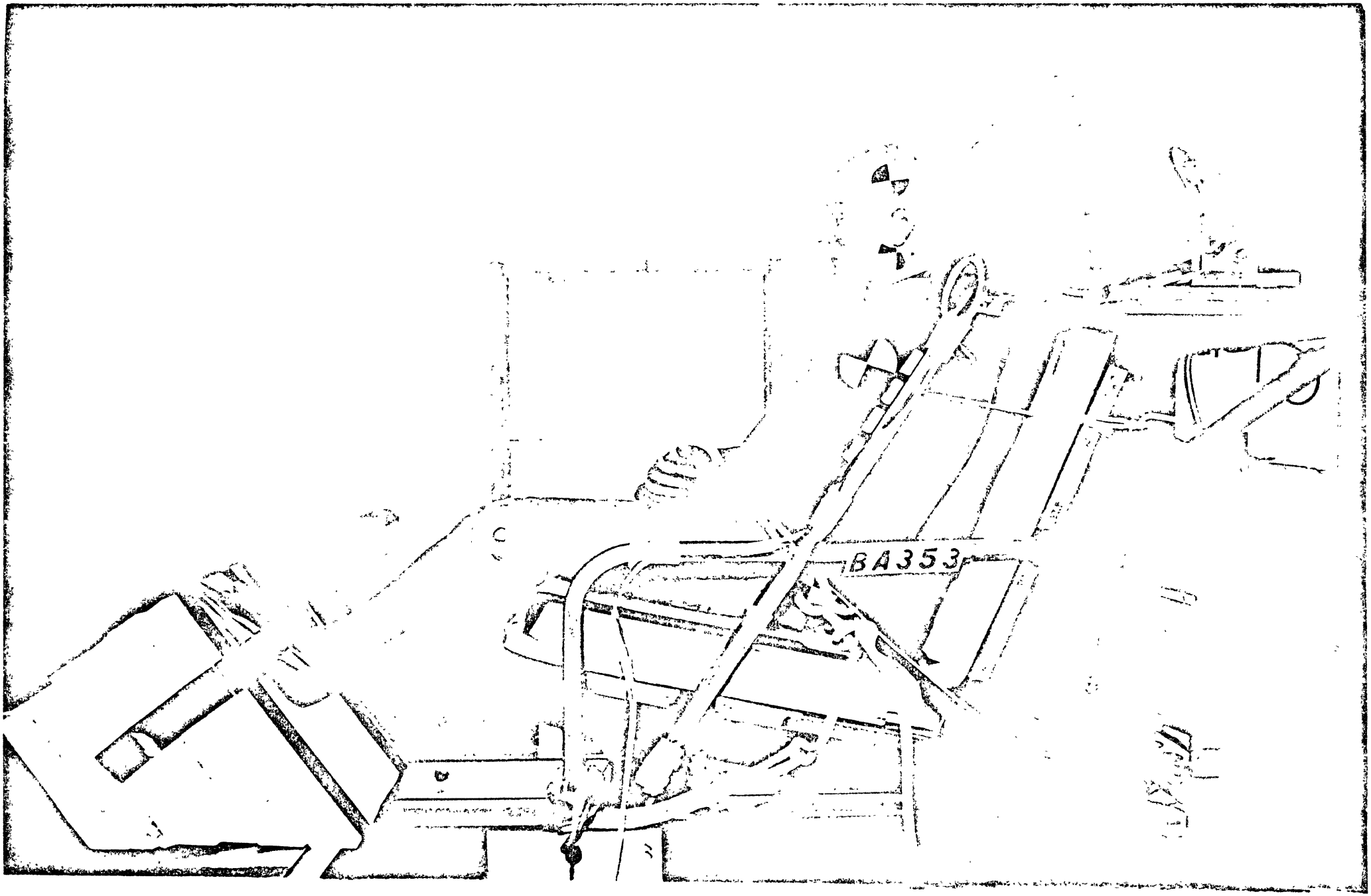

Figure 27. Olin Inflatable Head Restraint with Stabilizing Flap
(Shown with a 5th Percentile Female Dummy)

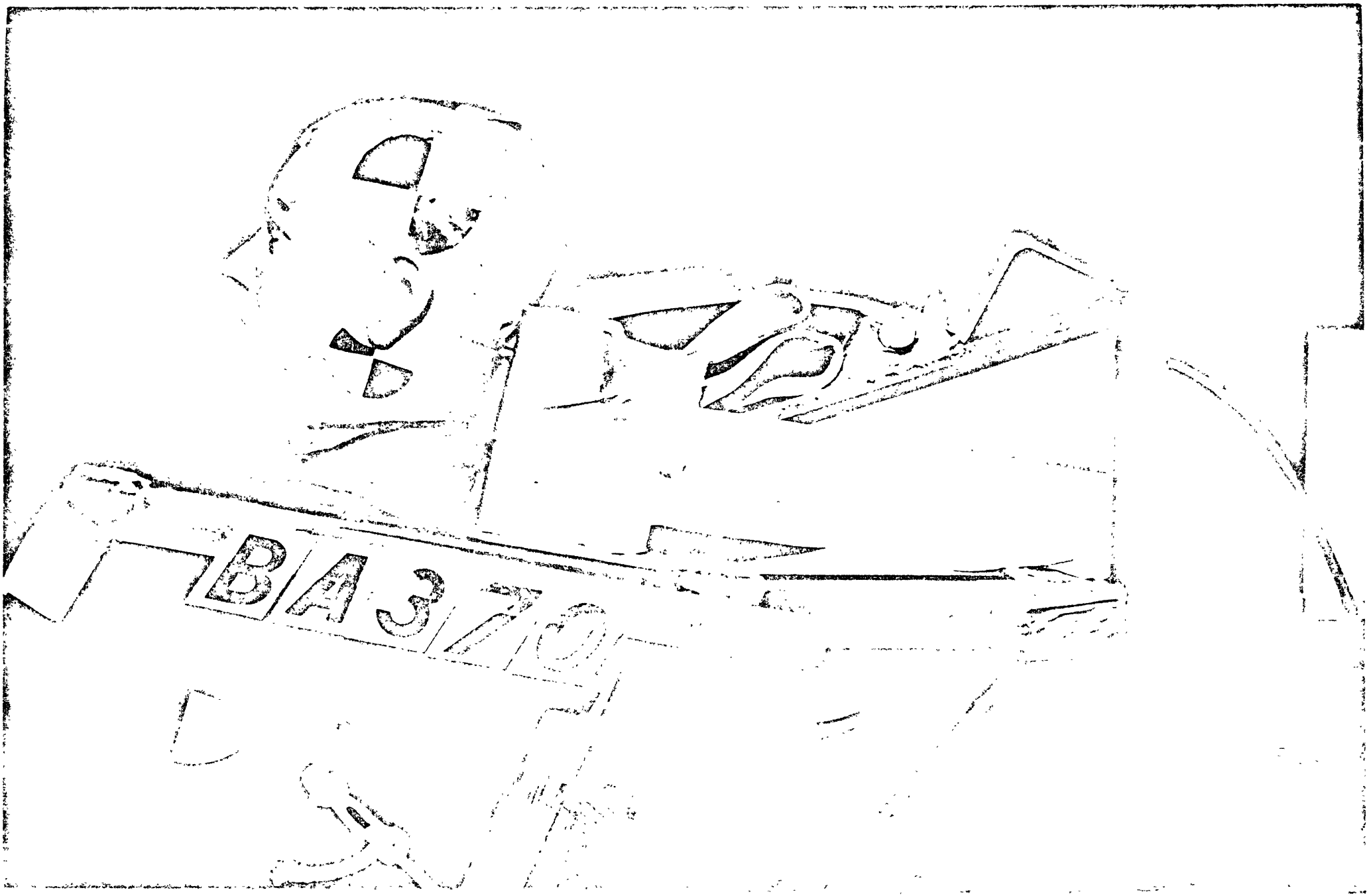

Figure 28. Olin Inflatable Head Restraint with a Modified Stabilizing Flap and Restraint Mounting

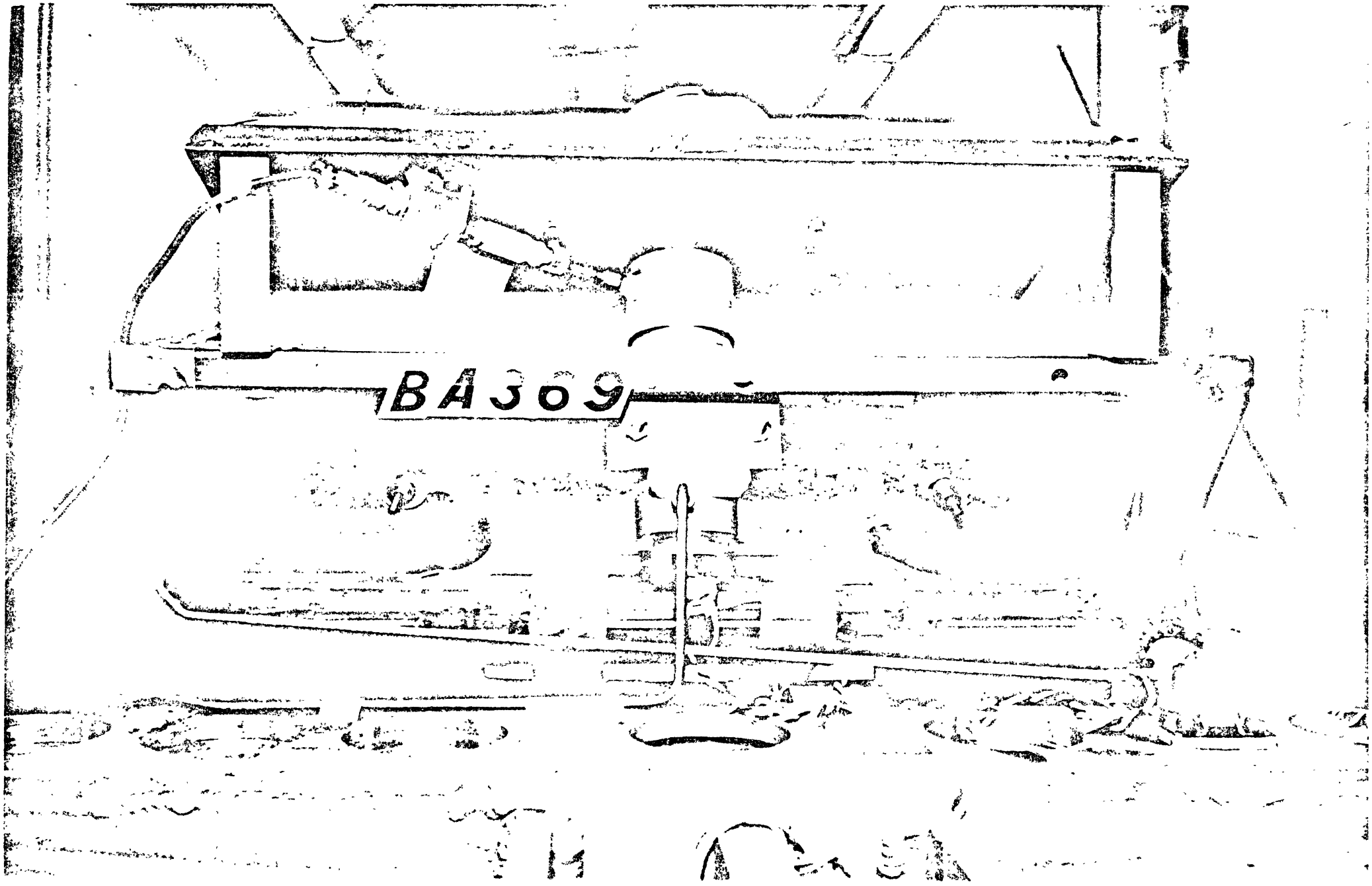

Figure 29. Olin Inflator Mounting with Connected Pressure Transducer

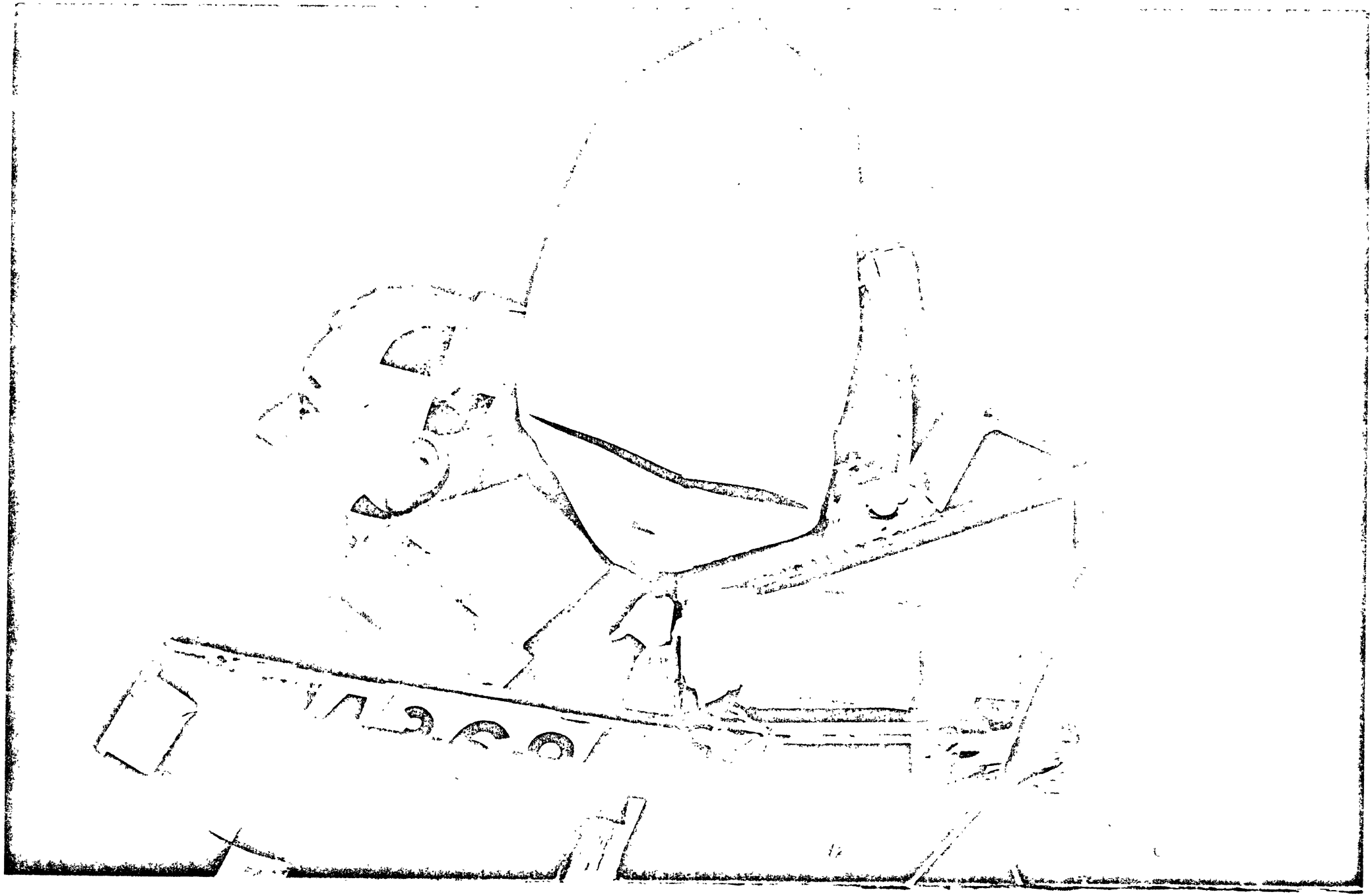

Figure 30. Olin Inflatable Head Restraint After Deployment

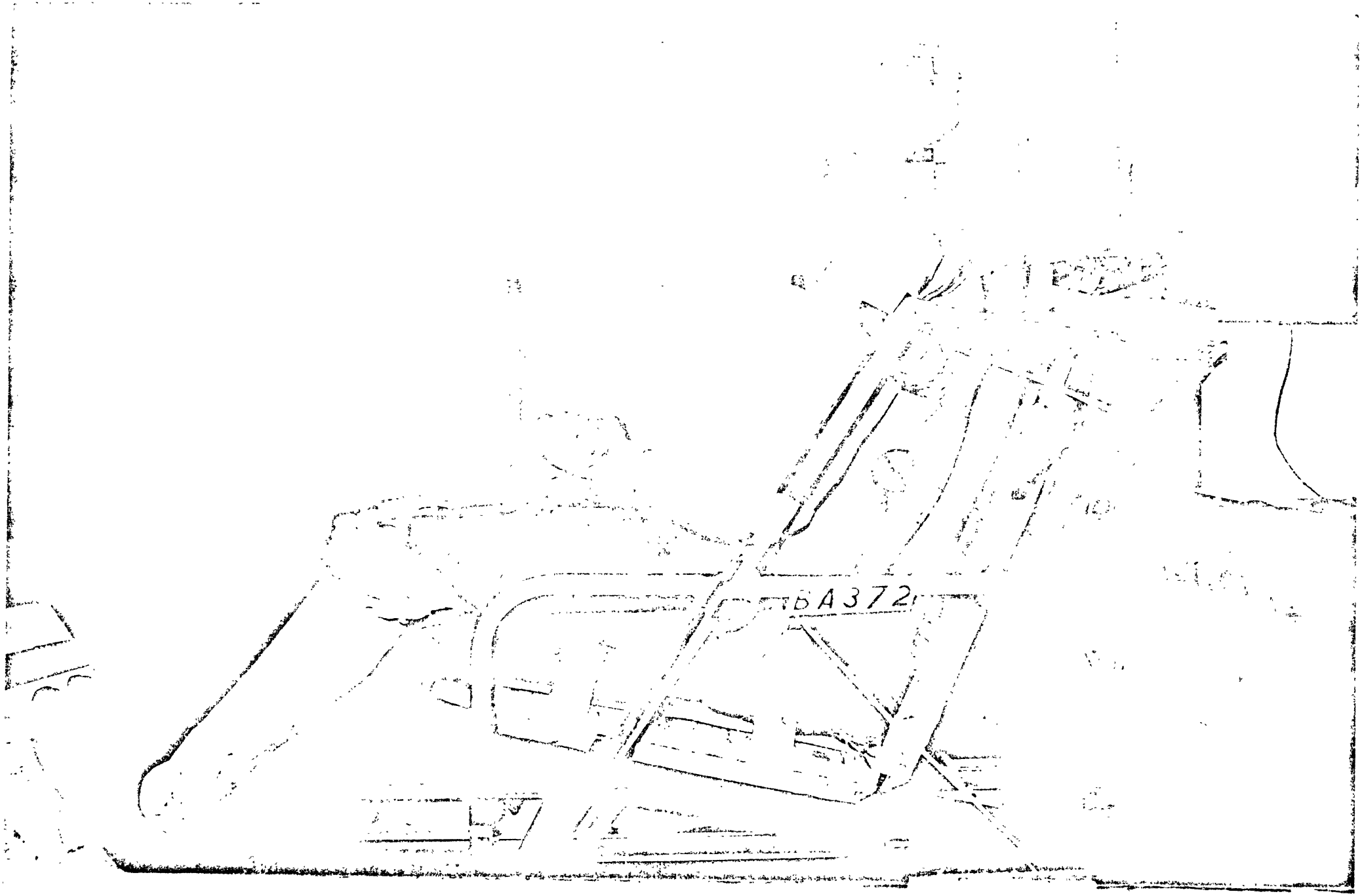

Figure 31. Olin Inflatable Head Restraint Package Prior to Deployment with a 95th Percentile Male Dummy

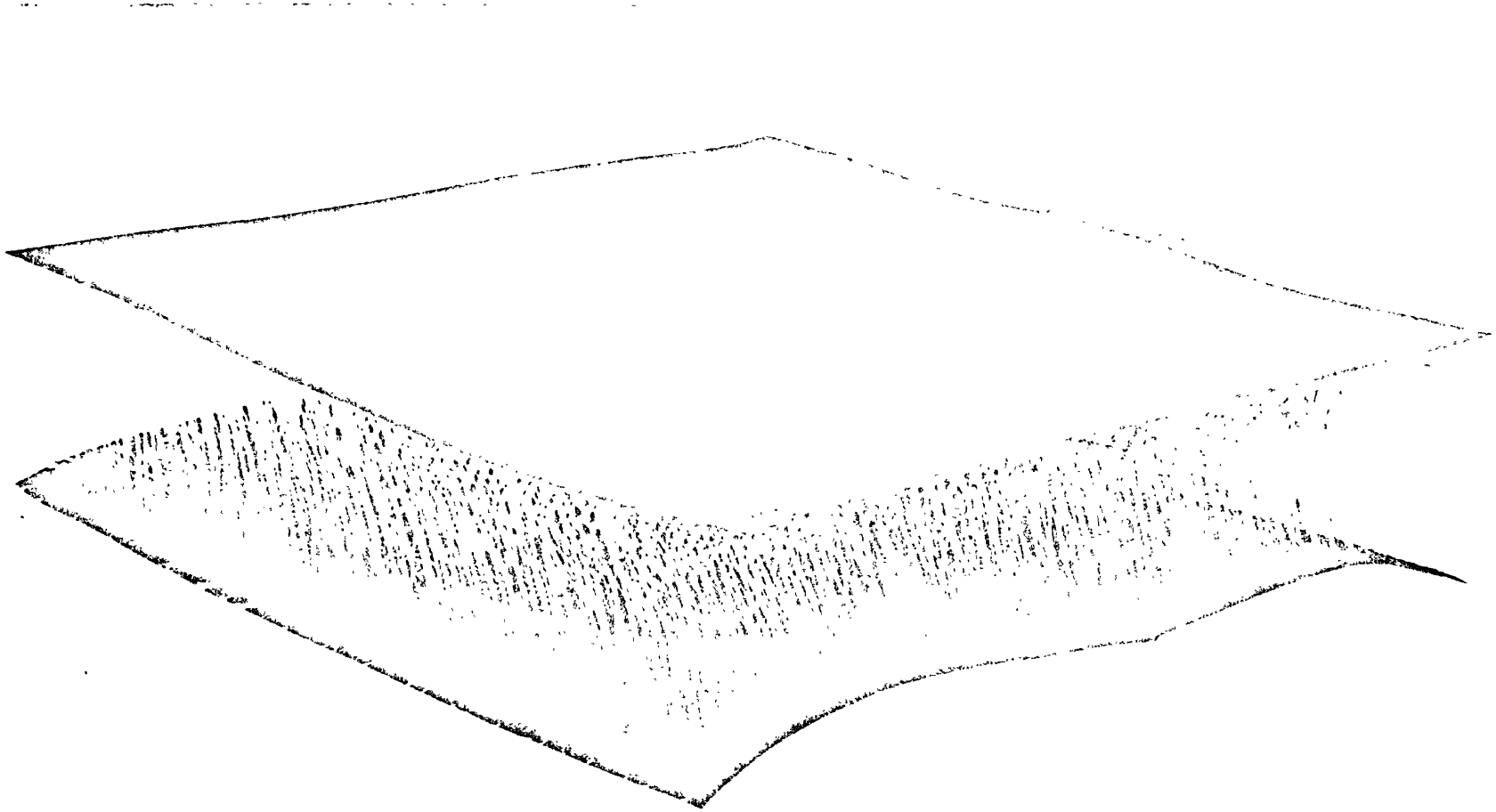

Figure 32. Typical Dropweave Fabric

such a material offers the possibility of providing its own fore and aft stiffness, thereby eliminating the need for an auxiliary rigid stabilizing flap.

The material can be woven into a variety of surface shapes, but most of the examples readily available were of a flat planar nature. Such an example was obtained from Goodyear Aerospace Corporation in the form of a 3-inch thick, 10-inch high, 20-inch wide unit of their version of dropweave fabric called Air Mat. This unit was sealed and mounted by Goodyear onto a rigid mounting plate and was intended for preinflation testing only. The system was adapted to the seat structure but it could not be mounted as far forward as possible for the most effective use in limiting head motion. The mounted system is shown in Figure 33.

6.2 RIGID DEPLOYABLE HEAD RESTRAINT DESIGN

The design of a rigid sliding head restraint of the type shown schematically in Figure 23 is basically quite straight-forward until consideration is given to a means of deploying such a device. Considerable time and effort was spent on evaluation of possible sources of actuation of the system, the majority of which were based on types of piston and cylinder arrangements actuated with compressed gas. It became evident that the requirement of a 20 msec deployment time ruled out conventional pneumatic devices. The use of springs was considered but the requirements of force level and stroke were not compatible with compact design. Fortunately, a device was brought to our attention by the Contract Monitor which possessed characteristics similar to those necessary for the requirements of the deployment device (i.e. 20 msec response for a stroke of 10 inches). The device was a drogue chute thruster manufactured by the Propellex Chemical Corporation for use with aircraft ejection seats. This unit is a limited stroke piston and cylinder arrangement that is powered pyrotechnically. It has an active stroke of 5.25 inches and a nominal response time of 10 msec for that stroke when working against a mass of 8.75 lbs. One of the units was purchased and the design of the remainder of the head restraint was carried out around the requirements of the thruster.

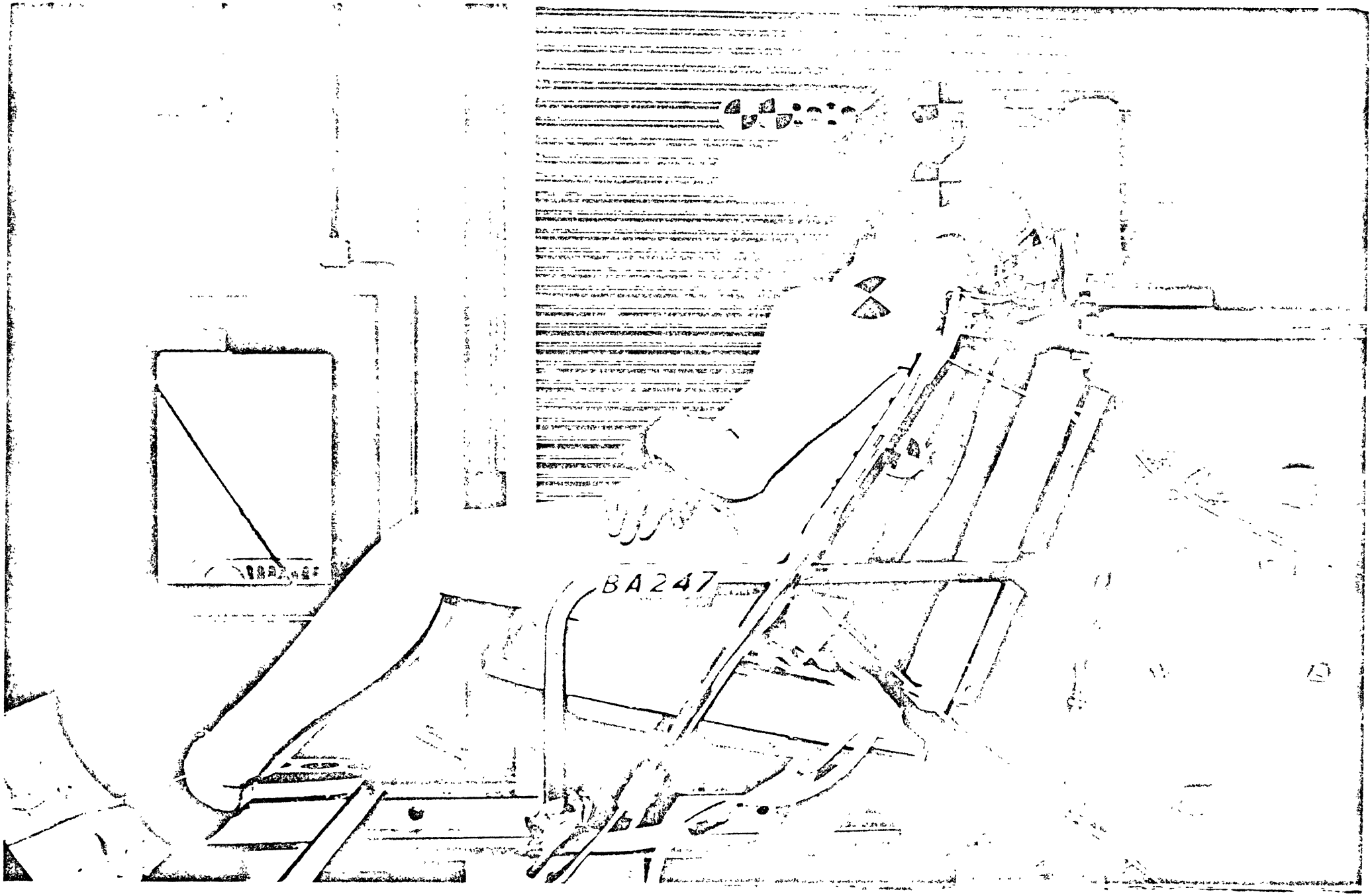

Figure 33. Air Mat Inflatable Head Restraint Configuration

The head restraint package consisted of an aluminum channel support frame with steel guide rods at each side with the movable head restraint contained within the frame. The head restraint itself consisted of a horizontal rectangular steel tube with nylon bearings at each end and rising from the center of the horizontal member was a round steel tube tee which served as the load carrying member of the head restraint. The tubular steel tee was filled in with balsa wood and covered with sheet aluminum to present a rectangular surface in front view. Figure 34 shows the assembled system prior to final mounting on the seat. The thruster was mounted centrally to the aluminum frame and extended up into the vertical tube of the steel tee. The upper end of the thruster rested against a rubber plug interior to the tube which allowed the thruster to push against the head restraint to propel it upward, but it was not attached to the restraint so that the restraint could continue upward past the limited stroke of the thruster to reach its full upward motion of 10 inches. This movement is shown in Figure 35. The nylon lined bearing surfaces at each end of the restraint guided the upward motion of the restraint along the guide rods. Steel tubing was used in the head restraint portion of the system in order to make the mass of the system close to the 8.75 lb. design requirement of the thruster. It is obvious that an adequately stiff system could have been fabricated from lightweight metal that would have weighed in the 4 to 5 lb. range if it were not for the mass requirement of the thruster. The front surface of the restraint was covered with a two-inch thick slab of 9 lb. per cu. ft. polyethylene open-celled foam for cushioning purposes.

The final mounting position of the rigid head restraint package is shown in Figure 36 and its deployed configuration shown in Figures 37 and 38.

6.3 SEAT-HEAD RESTRAINT DESIGN CONSIDERATIONS

As noted in the computer simulation studies of Section 3.7, the matching of seat back mechanical response and head restraint mechanical response is necessary for optimal performance of the system as a whole. The desired effect of this matching is to have the occupant move into and back out of the system with basically linear translation of the head, neck and torso during a rear-end crash. The mechanical properties of the seat back cushioning material, the seat back structure, the head restraint mechanical properties, and the geometric

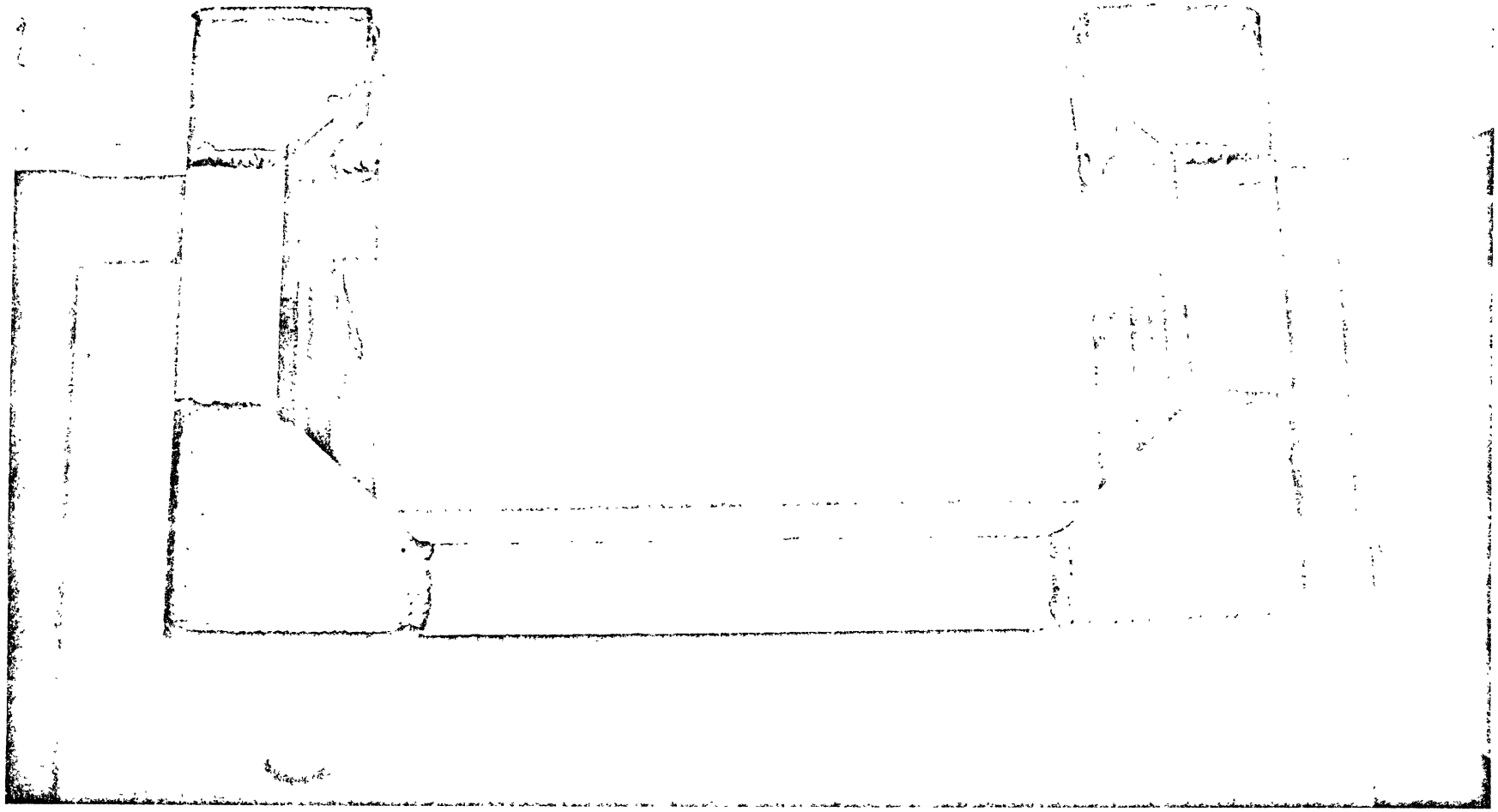

Figure 34. Rigid Sliding Head Restraint System Package

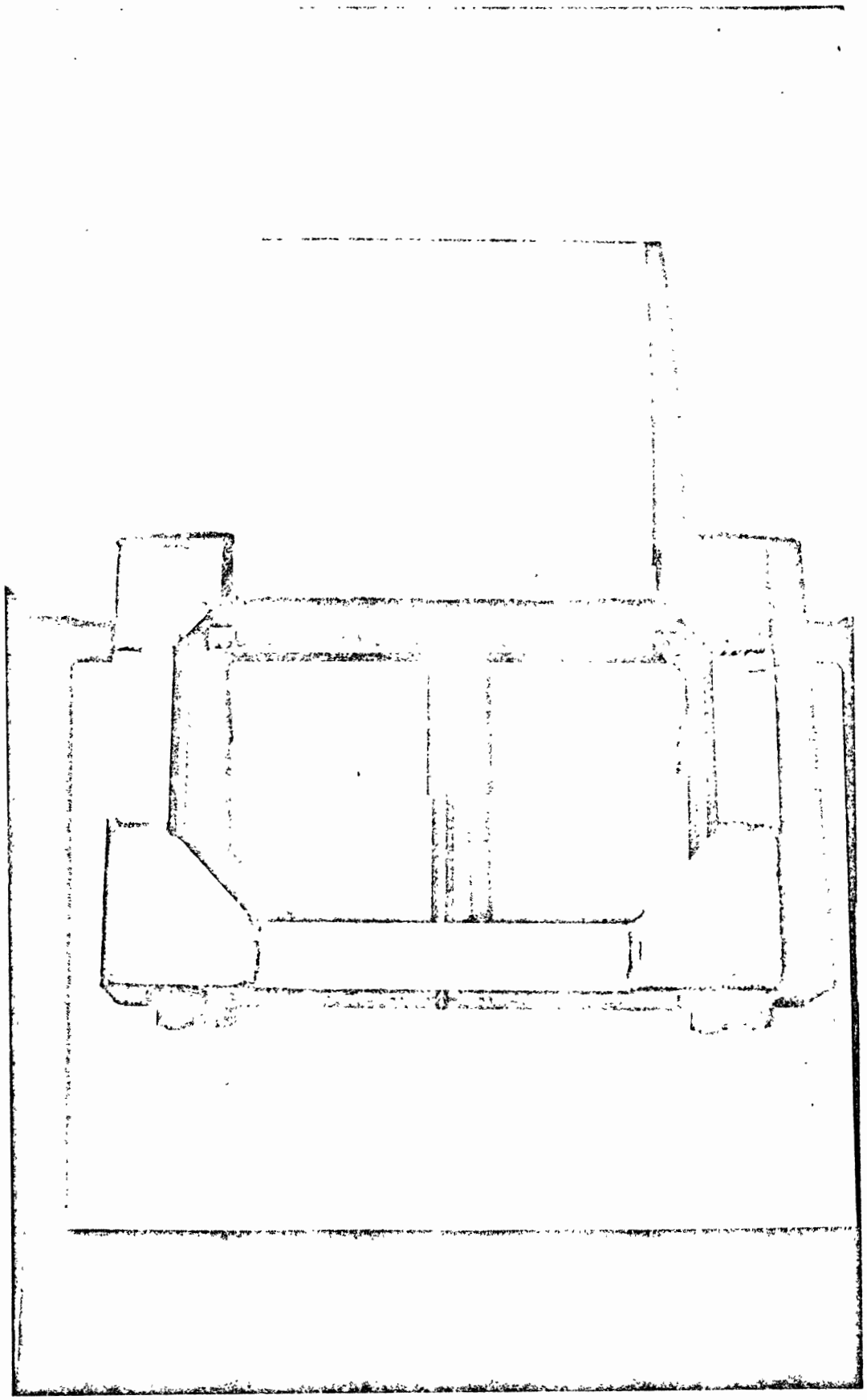

Figure 35. Rigid Sliding Head Restraint in Deployed Position

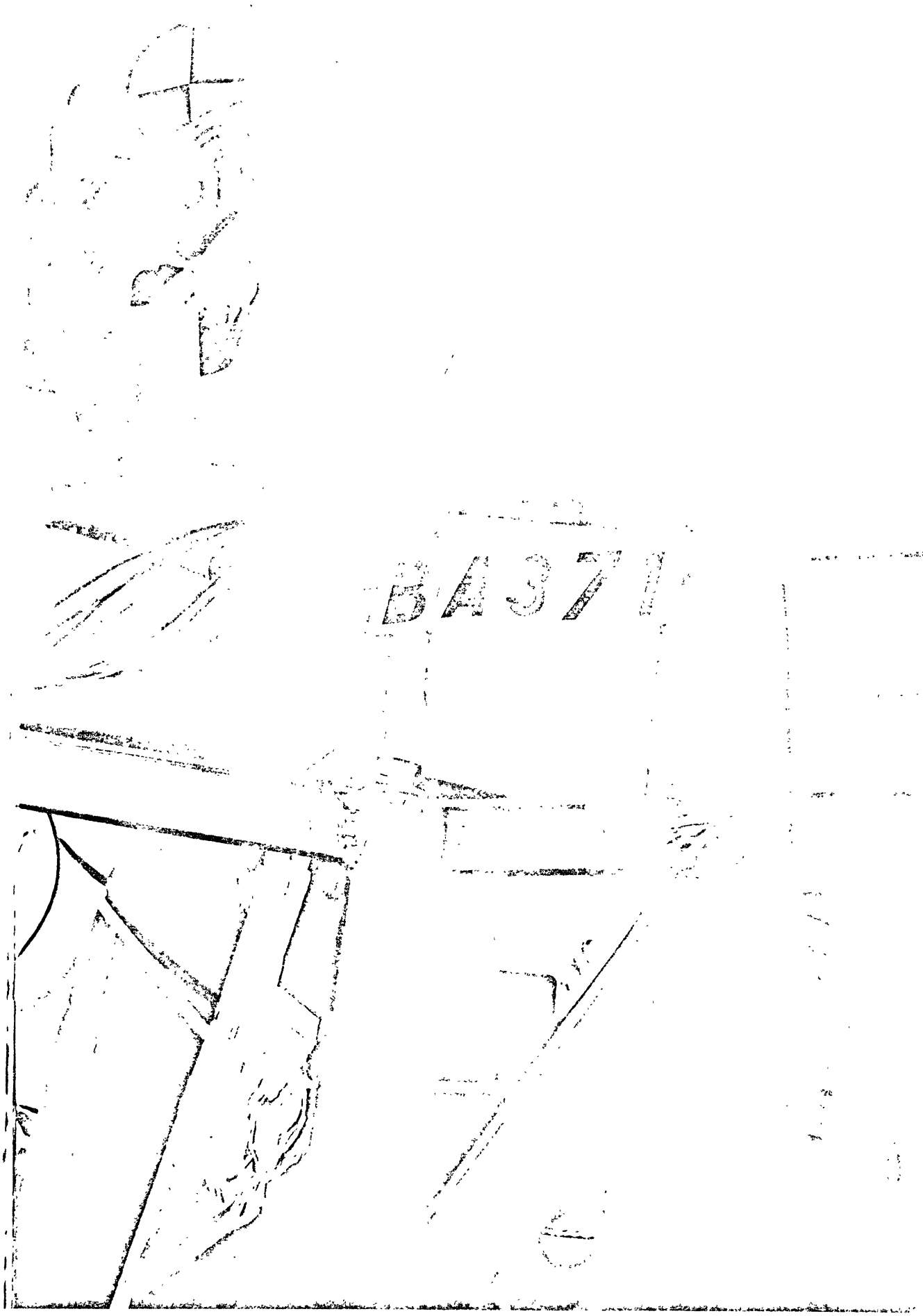

Figure 36. Rigid Sliding Head Restraint Test Configuration

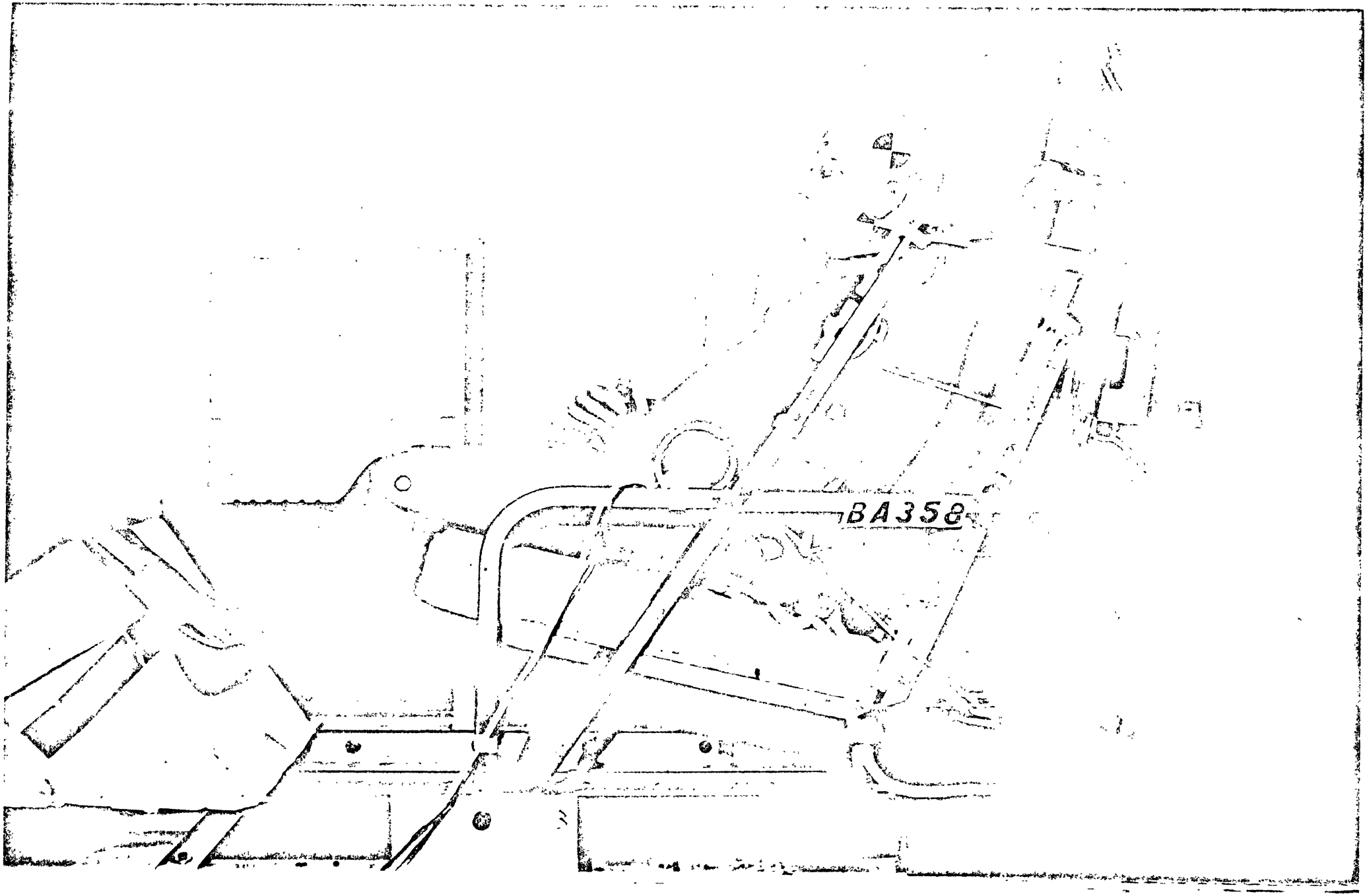

Figure 37. Rigid Sliding Head Restraint in Pre-deployed Test Configuration with 5th Percentile Female Dummy

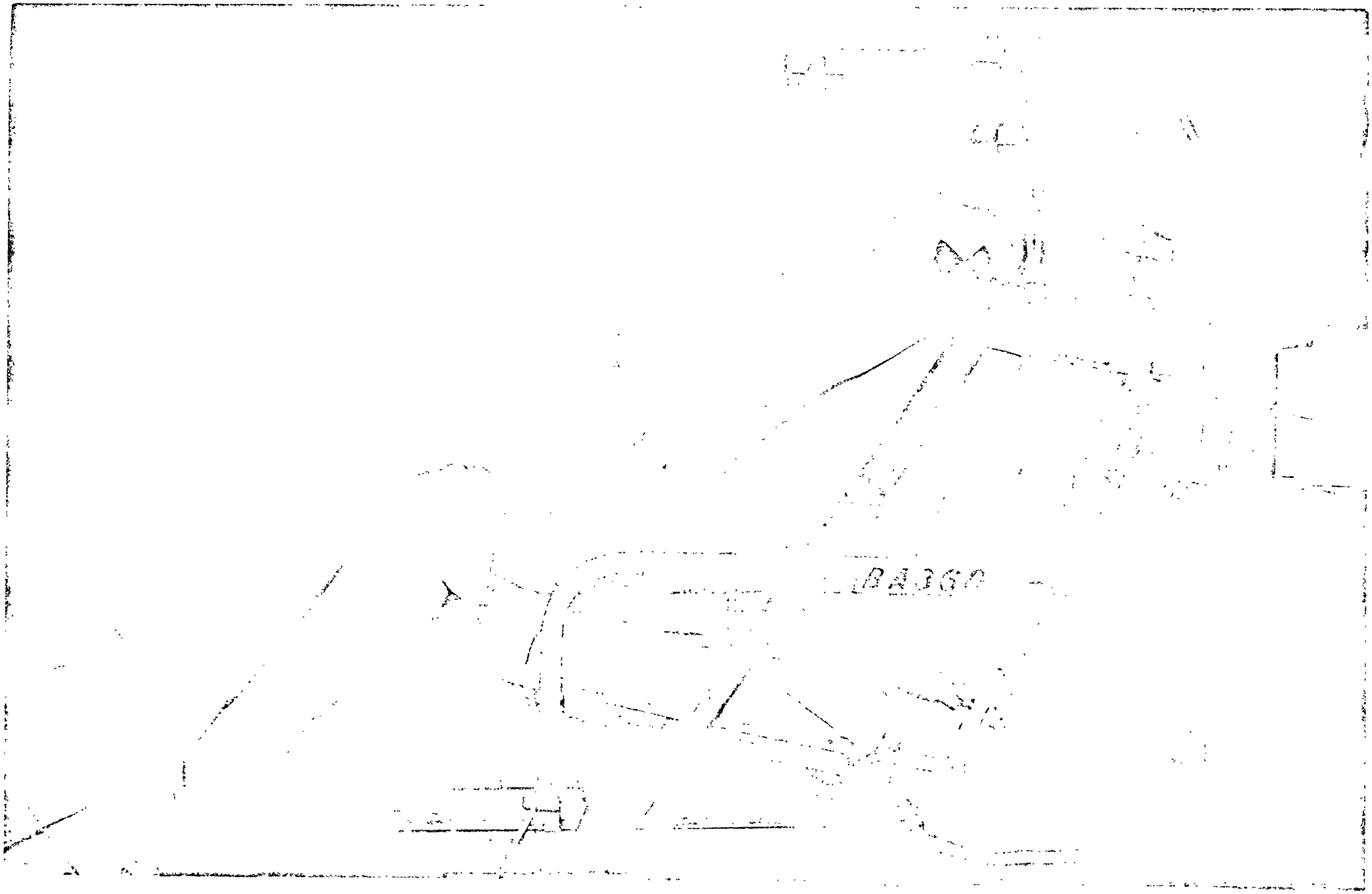

Figure 38. Rigid Sliding Head Restraint in Pre-deployed Test Configuration with 95th Percentile Male Dummy

placement of the restraint relative to the seat back all influence the final response of the system.

The seat structure used in all of the tests in this program was designed as part of another DOT sponsored program on integrated restraint systems. It was constructed from one-inch square steel tubing welded into the configuration shown in the drawing of Figure 21. This structure is extremely strong and rigid when compared to conventional seat designs. A pan of thin sheet metal was attached to the frame to provide mounting for the seat back and seat bottom which consisted of 0.75 inch plywood sheet covered with one inch of Ensolite AH energy absorbing foam and then 1.5 inch of soft sponge rubber for comfort. The entire cushioning composite was upholstered with a vinyl covering.

The mounting of the head restraints to the seat was achieved by welding substructures to the basic seat frame as shown in Figures 25, 29 and 36.

Mechanical property tests were performed on both the inflatable head restraint system and the seat back cushion to determine their characteristics. The head restraint test was performed by mounting a 6-inch diameter hemispherical head form on a load cell and deflecting the head form into the head restraint bag while it was mounted in an Instron. A typical load-deflection curve is shown in Figure 39. The results of the testing showed the system to behave as a linear spring and that it was also linear with respect to inflation pressure thereby allowing extrapolation of the data to other pressures. The Instron was also used to get the load-deflection properties of the seat back cushion, but instead of a head form for a loading surface, a flat surface one foot square was attached to the load cell. The result of the test is shown in Figure 40 for both loading and unloading. The load-deflection curve is typical of cushioning materials in compression with its rapidly increasing slope as the material approaches a bottoming out condition.

From comparison of the load-deflection curves for the restraint and the seat back cushion it is evident that they are quite different in response at the same deflection. In order to produce a uniform response it is necessary to introduce adjustments in bag pressure and relative offset in position. By placing the bag slightly forward of the seat back and adjusting the bag pressure it is possible to achieve maximum restraint of rearward head motion at the same time that the seat back begins to strongly limit rearward torso movement thereby preventing significant relative motion of the head-neck

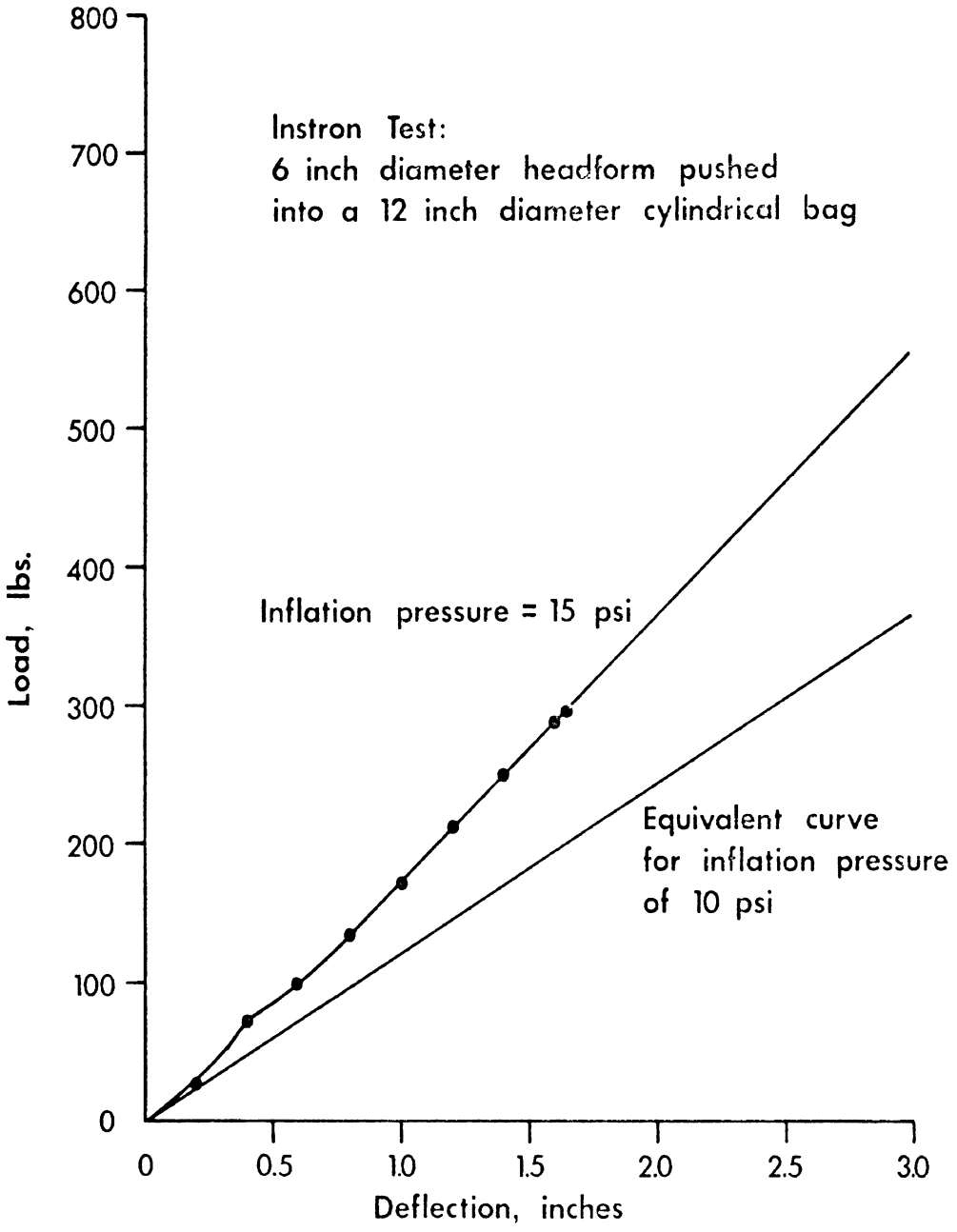

FIGURE 39. HEAD RESTRAINT BAG LOAD DEFLECTION CURVES

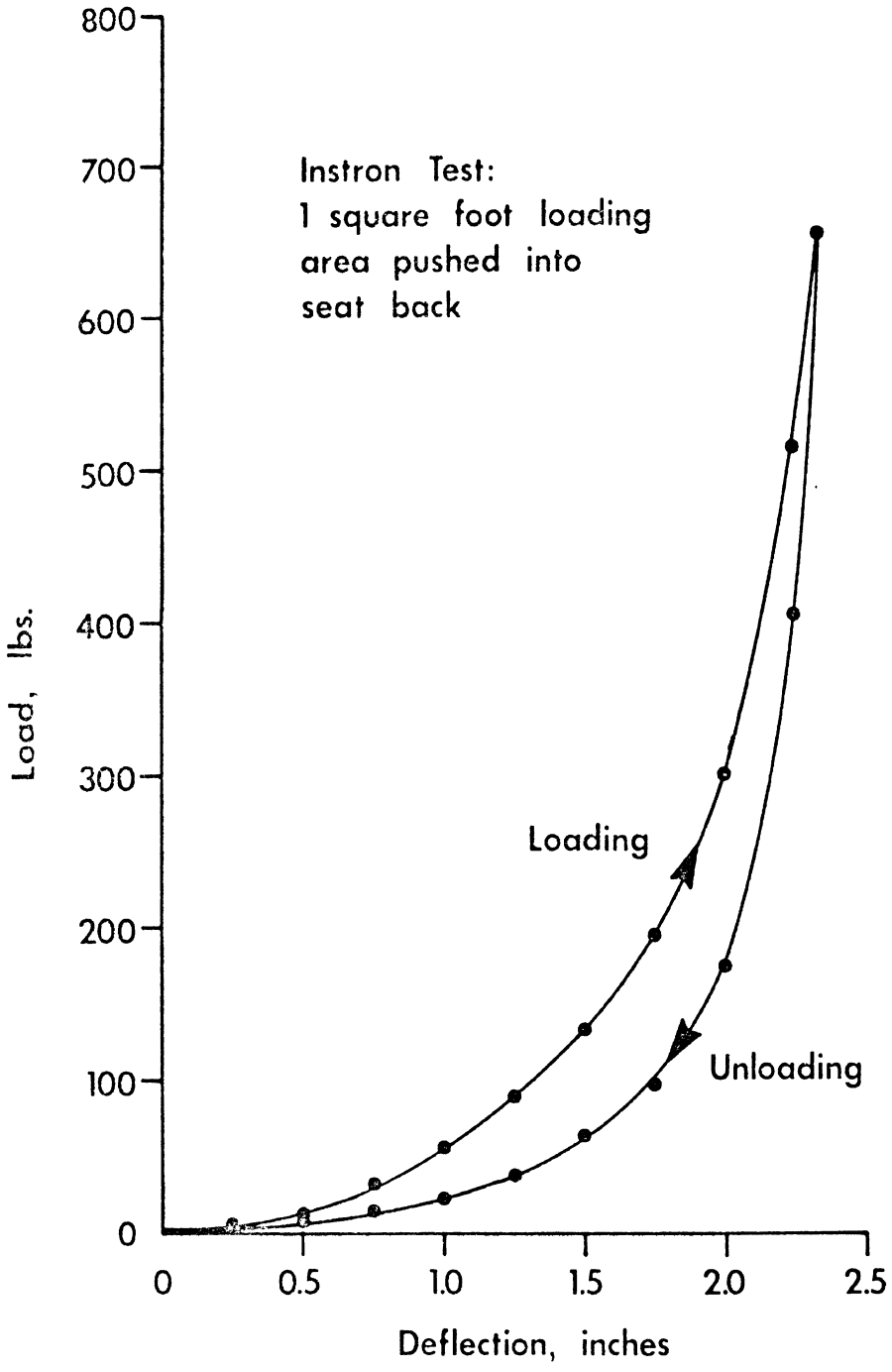

FIGURE 40. SEAT BACK CUSHION LOAD DEFLECTION CURVE

region. It is not possible to achieve this state for all acceleration levels without a variable bag pressure. An appropriate compromise is to adjust the bag pressure to achieve the desired effect under the most severe crash condition to be considered.

The test program discussed in the following section utilized these concepts in an effort to optimize the system based on dynamic tests using the impact sled.

7. TEST, DEVELOPMENT AND DEMONSTRATION PROGRAM

The purpose of the test, development and demonstration program was to establish system feasibility for the deployable head restraint components and systems described in the previous section. The primary tool used in this phase of the project was the HSRI Impact Sled Facility shown in Figure 73. With the exception of some frontal crash simulation tests for belt rebound onto the head restraint, the impact sled was used primarily to simulate rear-end crashes of 20 mph, 60 mph and 80 mph car to car closing velocities. For the case of a stationary car being struck in the rear by an identical weight car, these closing velocities correspond approximately to the struck car undergoing velocity changes of 10 mph, 30 mph and 40 mph respectively. The nominal sled pulses used to simulate these conditions were 10 mph, ∿10 G's peak; 30 mph, ∿ 18 G's peak; and 40 mph, ∿ 40 G's peak. Typical acceleration-time profiles for these three pulses are shown in Figure 41. Also shown in Figure 41 for comparison is a 55 mph crash profile from Severy (1968). Note that the 30 mph sled pulse has higher acceleration than the car crash pulse in the time region from 25 to 75 msec. The consequence of this higher acceleration in the early portion of the pulse is to produce occupant kinematics of a somewhat more severe nature than would be the case in an actual rear-end collision. Thus, the sled tests taxed the capabilities of the head restraints to a greater extent than would a car crash with the same velocity change.

7.1 TEST EQUIPMENT AND INSTRUMENTATION

Two sizes of anthropometric dummies were used in the test program; Sierra No. 292-895 95th percentile male, weight 217 lb, height 73.3 in., and Sierra No. 592-805 5th percentile female, weight 106 lb, height 59.8 in. Rubber necks designed and manufactured by General Motors were used in both dummies for all of the tests. These necks were used primarily to minimize variations between tests due to the changes in neck behavior associated with adjustable ball and socket necks.

Triaxial accelerometer packs were mounted in the dummy chests and heads. The locations of the head accelerometer planes are shown in Figure 42 for the two dummies. The accelerometers used in the packs were Kistler Piezotron Model 818. The specifications and calibration procedures for these

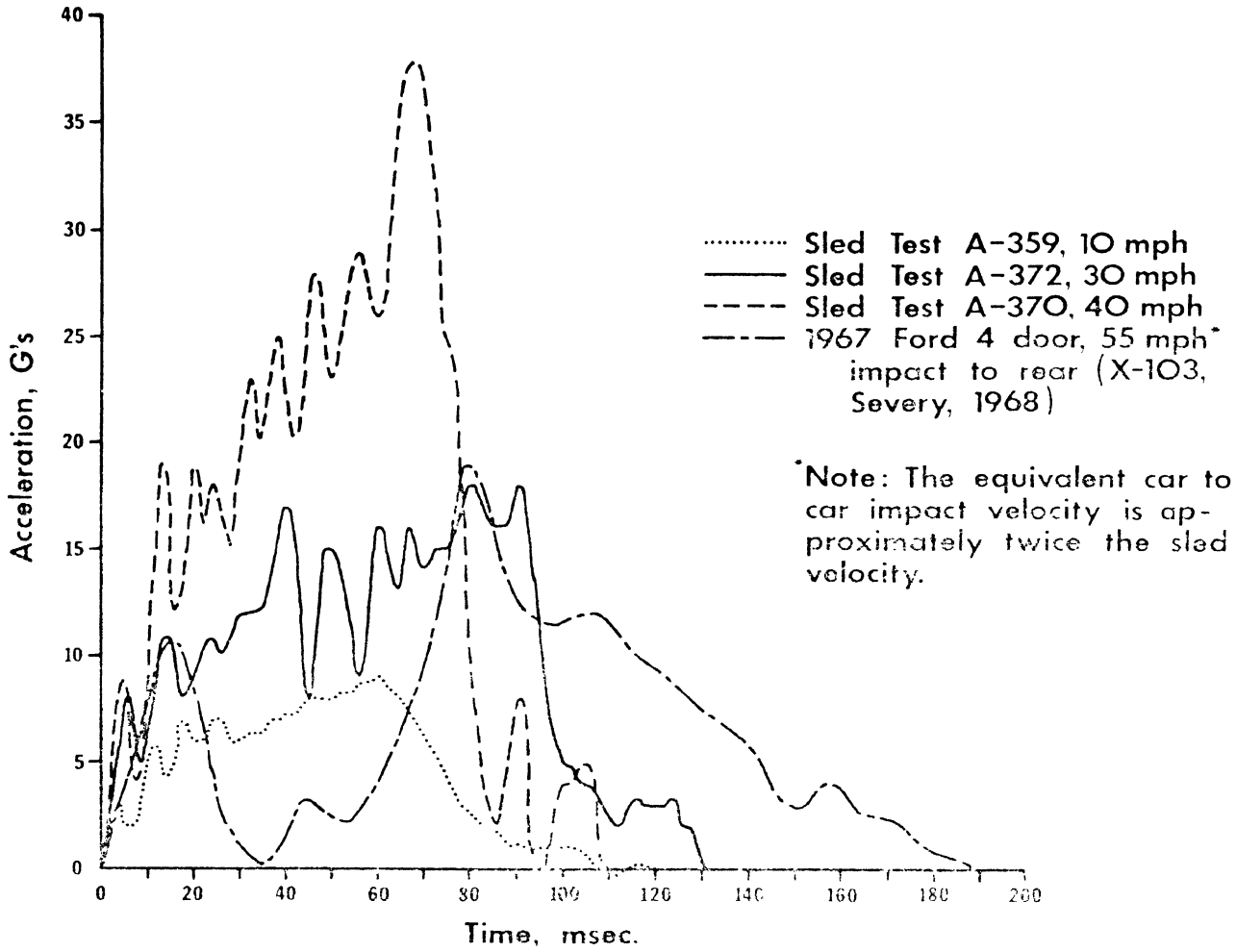

FIGURE 41. TYPICAL SLED ACCELERATION PULSES

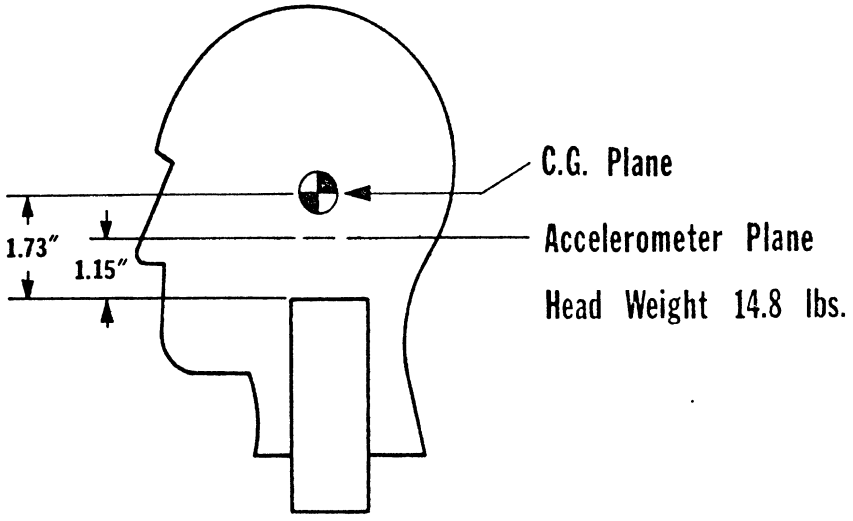

95% Male

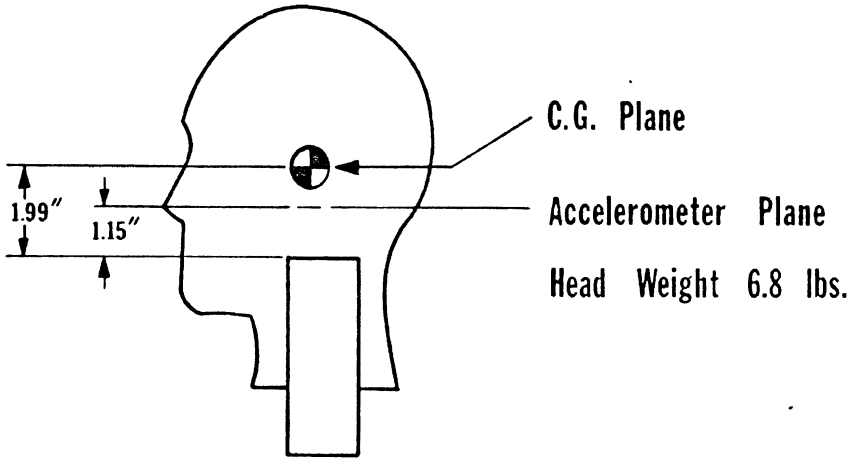

5% Female

FIGURE 42. ACCELEROMETER LOCATIONS IN DUMMY HEADS

accelerometers, the sled accelerometer and the signal conditioning and recording equipment are given in Apendix B. The photographic coverage of each test consisted of high speed 16 mm movies (overhead and side views), a Graph-chek sequence camera side view for immediate photographic evaluation and before and after-test still photographs of the test set up. The high speed movies were made with Photosonics cameras and in some cases a Hi-Cam camera with nominal frame rates of 1000 fps.

In those tests which required dynamic deployment, detonation of the device was accomplished by a set of electrical contacts that were actuated as the sled passed by them. The placement of the contacts was adjustable so that the timing of the detonation could be selected at any point during the sled pulse. The bag pressure readout in these tests was accomplished using a strain-gaged diaphragm type pressure transducer designed by Eaton and built in-house at HSRI. In all tests the dummy was not restrained by any belts; however, loose tethering at the hip was used to limit excessive excursions.

7.2 DATA HANDLING AND ANALYSIS

The data from the accelerometers was recorded directly on magnetic tape (Honeywell Model 7600 tape recorder) and a filtered version (Burr-Brown filters, SAE J211 channel class 180) was recorded on a Honeywell Model 1612 Visicorder light beam oscillograph. The Visicorder traces were used directly for data analysis. A careful and detailed photometric analysis was performed on the side view high speed movie film of selected tests of particular significance to the program. The basic measuring device used in this work was the Vanguard film analyser model M-160 W. Four-place accuracy in linear and angular measurements is obtainable with this instrument. The linear and angular displacements of the target points on the head, neck and shoulder of the dummy were measured every fifth frame ($\sim$5 msec time increments) The film analyser was coupled to an IBM 29 card punch unit and computer cards were automatically punched with the displacement data. Computer programs which have been developed to analyze photometric data at HSRI, were used to compute head angular velocities and accelerations from the digitized displacement data by means of appropriate smoothing and filtering operations.

The sign conventions for the accelerations of the dummies are as follows;

1. Linear accelerations in the forward direction (towards the front for an occupant seated in a car) are positive
2. Linear accelerations in the upward direction are positive

3. Linear accelerations to the right are positive

4. Forward angular accelerations are positive

In discussion of whiplash, the extension of the head-neck relative to the upper torso is of interest. Thus, when discussing extension in this report the extension angle will be denoted as a positive quantity while flexion will be a negative quantity. Thus, angles between the head-neck and the upper torso rearward of the zero degree line are positive while angles forward of the zero degree line are negative. Because of the difficulty in determining the exact angle of the upper torso segment during a test the angle of the seat back itself is used as the zero angle line. Because the seat structure used in all the tests was exceptionally stiff it is felt that this is a valid basis for analyzing the tests where the dummies contacted the seat back in a normal seated position.

7.3 SLED TEST RESULTS

The results of the sled crash simulations are presented in this report in three forms: a descriptive summary of each test, a numerical summary table of pertinent data and, in the case of particularly important tests, Graphchek sequence photographs, accelerometer traces and kinematic analysis graphs obtained from the high speed movie coverage of the tests.

The summary of the numerical data for each test is found in Table 3. The descriptive summaries of each test follow below. Detailed analysis of particularly pertinent test results is found in the discussion of results section of the report.

SLED TEST A-332 - 30 mph, 13 G peak pulse, rear impact, 95th percentile male dummy.

An Eaton inflatable head restraint package with stabilizer flap was mounted but was not deployed in order to provide baseline whiplash data. Severe hyperextension occurred accompanied by ramping of the dummy up the seatback. The ramping was limited by the hip tether belt. Rebound of the dummy was upward as well as forward.

SLED TEST A-333 - 30 mph, 14 G peak pulse, rear impact, 95th percentile male dummy.

An Eaton inflatable head restraint package with stabilizer flap was accuated at the start of the crash pulse (t=0). The restraint started to inflate at t = 2 msec. and was fully in place at t = 20 msec. The average bag

TABLE 3. DEPLOYABLE HEAD RESTRAINT SLED TEST SUMMARIES (Page 1)

Test Number	Dummy Size	Head Restraint Type	Average Inflation Pressure psi	Peak Sled Pulse G @ msec	Peak Head A-P Accel. G @ msec	Peak Head S-I Accel. G @ msec	Peak Chest A-P Accel. G @ msec	Peak Chest S-I Accel. G @ msec	Maximum Extension Angle Degrees @ msec
A-332	95% M	None	-	13 @ 115	36 @ 138	-22 @ 133	18 @ 70	- 7 @ 130	+62.3 @ 139
A-333	95% M	Eaton Deployed	7.5	14 @ 100	26 @ 77	-14 @ 62	27 @ 60	- 6 @ 50	+11.7 @ 89
A-334	95% M	Eaton Preinflated No Flap	7.0	14 @ 102	24 @ 133	-30 @ 110	28 @ 77	- 8 @ 122	+43.4 @ 122
A-335	95% M	Eaton Preinflated	7.0	15 @ 97	27 @ 73	-15 @ 70	25 @ 60	-11 @ 67	+ 3.6 @ 85
A-336	95% M	Eaton Preinflated	15.0	16 @ 92	26 @ 77	-10 @ 86	23 @ 56	-10 @ 70	- 8.6 @ 84
A-337	95% M	Eaton Preinflated	7.5	16 @ 88	29 @ 70	-11 @ 55	27 @ 55	-10 @ 57	+ 7.7 @ 78
A-338	95% M	Eaton Preinflated	7.5	17 @ 93	31 @ 80	-13 @ 63	28 @ 63	-10 @ 71	+ 7.6 @ 78
A-339	95% M	Eaton Preinflated	3.5	18 @ 92	30 @ 80	-14 @ 65	30 @ 65	-12 @ 68	+17.4 @ 76
A-347	95% M	Air Mat Preinflated	10.0	18 @ 80	28 @ 50	-25 @ 80	27 @ 45	- 9 @ 60	+14.7 @ 77
A-348	95% M	Air Mat Preinflated	4.0	18 @ 84	27 @ 97	-27 @ 85	38 @ 53	- 9 @ 87	+39.2 @ 103
A-349	95% M	Air Mat Preinflated	10.0	18 @ 85	33 @ 97	-22 @ 90	43 @ 57	-10 @ 56	+29.1 @ 99
A-350	95% M	Olin Preinflated	7.0	18 @ 84	48 @ 84	-66 @ 119	40 @ 102	-20 @ 64	+58.5 @ 134 ramp
A-351	95% M	Olin Preinflated	7.0	18 @ 80	32 @ 68	-16 @ 83	27 @ 56	-- 8 @ 62	+12.6 @ 87

TABLE 3. DEPLOYABLE HEAD RESTRAINT SLED TEST SUMMARIES (Page 2)

Test Number	Dummy Size	Head Restraint Type	Average Inflation Pressure psi	Peak Sled Pulse G @ msec	Peak Head A-P Accel. G @ msec	Peak Head S-I Accel. G @ msec	Peak Chest A-P Accel. G @ msec	Peak Chest S-I Accel. G @ msec	Maximum Extension Angle Degrees @ msec
A-352	95% M	Olin Preinflated	7.0	10 @ 50	15 @ 75	- 7 @ 63	16 @ 86	- 4 @ 70	+ 1.0 @ 92
A-353	5% F	Olin Preinflated	7.0	21 @ 82	20 @ 67	10 @ 48	26 @ 48	-10 @ 58	-25.0 @ 82
A-354	5% F	Olin Preinflated	7.0	10 @ 52	15 @ 60	10 @ 61	17 @ 60	- 6 @ 70	-26.0 @ 32
A-356	5% F	Olin Preinflated	7.0	36 @ 66	47 @ 58	-15 @ 66	46 @ 42	-17 @ 46	-13.7 @ 65
A-357	95% M	Olin Preinflated	10.0	37 @ 69	50 @ 73	-47 @ 52	45 @ 46	-17 @ 59	+13.0 @ 80
A-358	5% F	Rigid Predeployed	-	21 @ 76	33 @ 50	-20 @ 54	23 @ 53	-12 @ 57	+ 8.6 @ 64
A-359	5% F	Rigid Predeployed	-	9 @ 59	15 @ 54	- 3 @ 50	10 @ 47	- 5 @ 72	+ 3.6 @ 75
A-360	95% M	Rigid Predeployed	-	8 @ 55	22 @ 72	- 2 @ 63	12 @ 61	- 7 @ 66	+ 3.2 @ 80
A-361	95% M	Rigid Predeployed	-	19 @ 83	30 @ 108	- 8 @ 110	50 @ 104	-13 @ 55	+31.4 @ 130 ramp
A-362	95% M	Rigid Predeployed	-	20 @ 78	38 @ 60	- 3 @ 63	22 @ 47	-12 @ 73	+ 5.6 @ 66
A-369	5% F	Olin Deployed	9.0	21 @ 82	22 @ 42	-33 @ 56	23 @ 46	-13 @ 61	- 3.5 @ 102
A-370	5% F	Olin Deployed	-	38 @ 67	43 @ 53	-27 @ 62	43 @ 44	-17 @ 64	0 @ 84
A-371	95% F	Rigid Deployed	-	24 @ 50	50 @ 70	-45 @ 58	38 @ 43	-16 @ 70	- 7.2 @ 86

TABLE 3. DEPLOYABLE HEAD RESTRAINT SLED TEST SUMMARIES (page 3)

Test Number	Dummy Size	Head Restraint Type	Average Inflation Pressure psi	Peak Sled Pulse G @ msec	Peak Head A-P Accel. G @ msec	Peak Head S-I Accel. G @ msec	Peak Chest A-P Accel. G @ msec	Peak Chest S-I Accel. G @ msec	Maximum Extension Angle Degrees @ msec
A-372	95% M	Olin Deployed	10.0	18 @ 80	32 @ 67	-10 @ 78	25 @ 51	-10 @ 58	-14 @ 96
A-373	95% M	Olin Deployed	10.0	40 @ 77	42 @ 82	-24 @ 58	23 @ 47	-25 @ 56	-13 @ 102
A-374	95% M	None	-	19 @ 80	26 @ 97	-85 @ 105	25 @ 100	- -	+65 @ 109
A-376	95% M	Olin Deployed	10.0	19 @ 83	26 @ 62	-10 @ 66	21 @ 48	- 7 @ 74	+ 9 @ 75
A-377	95% M	None	-	28 @ 78	15 @ 324	- 4 @ 300	10 @ 280	- -	+35 @ 295
A-379	95% M	Olin Deployed	11.0	33 @ 64	12 @ 287	- 7 @ 240	10 @ 287	- -	+30 @ 240

pressure during the time the head of the dummy was in contact with it was 7 psi. Slight extension of the dummy head-neck occurred. The bag pocketed the dummy shoulders resulting in slight ramping. Rebound was moderate.

SLED TEST A-334 - 30 mph, 14 G peak pulse, rear impact, 95th percentile male dummy.

An Eaton inflatable head restraint without the stabilizer flap was preinflated to 7 psi. The dummy was leaning slightly forward out of position at the start of the crash pulse. The shoulders contacted the bag first and forced it rearward due to the absence of the stabilizer flap. Moderate head-neck extension occurred along with ramping. There was significant upward rebound along with forward rebound.

SLED TEST A-335 - 30 mph, 15 G peak pulse, rear impact, 95th percentile male dummy.

An Eaton inflatable head restraint with a stabilizer flap was preinflated to 7 psi. Slight head-neck extension occurred. The bag pocketed the dummy shoulders resulting in slight ramping. Rebound was mild.

SLED TEST A-336 - 30 mph, 16 G peak pulse, rear impact, 95th percentile male dummy.

An Eaton inflatable head restraint with a stabilizer flap was preinflated to 15 psi. There was minimal head-neck extension. The dummy motion was basically linear translation into and back out of the seatback-head restraint combination. The dummy shoulders were pocketed by the bag. Slight rebound occurred.

SLED TEST A-337 - 30 mph, 16 G peak pulse, rear impact, 95th percentile male dummy.

An Eaton inflatable head restraint with a stabilizer flap was preinflated to 7.5 psi. Slight head-neck extension occurred. The bag pocketed the dummy shoulders. Slight rebound occurred.

SLED TEST A-338 - 30 mph, 17 G peak pulse, rear impact, 95th percentile male dummy.

An Eaton inflatable head restraint with stabilizing flap was preinflated to 7.5 psi. Slight head-neck extension occurred. The dummy shoulders were pocketed by the bag. Moderate rebound occurred.

SLED TEST A-339 - 30 mph, 18 G peak pulse, rear impact, 95th percentil male dummy.

An Eaton inflatable head restraint with a stabilizer flap was preinflated

to 3.5 psi. Slight head-neck extension occurred. The bag did not pocket the shoulders well. Rebound was more pronounced than in test A-338 and it was more upward.

SLED TEST A-347 - 30 mph, 18 G peak pulse, rear impact, 95th percentile male dummy.

An Air Mat inflatable head restraint was preinflated to 10 psi. The dummy was poorly positioned in a slouching position against the head restraint. Slight head-neck extension occurred. There was no ramping and very slight rebound.

SLED TEST A-348 - 30 mph, 18 G peak pulse, rear impact, 95th percentile male dummy.

An Air Mat inflatable head restraint was preinflated to 4 psi. Severe head-neck extension occurred as the head restraint buckled and allowed rearward motion. There was no ramping and slight rebound.

SLED TEST A-349 - 30 mph, 18 G peak pulse, rear impact, 95th percentile male dummy.

An Air Mat inflatable head restraint was preinflated to 10 psi. Moderate head-neck extension occurred as the system deflected rearward. Slight rebound occurred.

SLED TEST A-350 - 30 mph, 18 G peak pulse, rear impact, 95th percentile male dummy.

An Olin inflatable head restraint with a stabilizer flap was preinflated to 7 psi. The dummy was poorly positioned - leaning forward. Upon impact the dummy rotated backward striking the head restraints high with its shoulders. The head missed the restraint resulting in severe head-neck extension followed by violent upward and forward rebound.

SLED TEST A-351 - 30 mph, 18 G peak pulse, rear impact, 95th percentile male dummy.

An Olin inflatable head restraint with a stabilizer flap was preinflated to 7 psi. Slight head-neck extension occurred along with some ramping. Rebound was moderate.

SLED TEST A-352 - 10 mph, 10 G peak pulse, rear impact, 95th percentile male dummy.

An Olin inflatable head restraint with a stabilizing flap was preinflated 7 psi. Very little head-neck extension occurred and the bag pocketed the dummy's shoulders. Rebound was mild.

SLED TEST A-353 - 30 mph, 21 G peak pulse, rear impact, 5th percentile female dummy.

An Olin inflatable head restraint with a stabilizer flap was preinflated to 7 psi. Little or no head-neck angle change occurred, and the dummy motion was almost completely linear translation. Rebound was slight.

SLED TEST A-354 - 10 mph, 10 G peak pulse, rear impact, 5th percentile female dummy.

An Olin inflatable head restraint with a stabilizing flap was preinflated to 7 psi. Little or no head-neck extension angle occurred, and the dummy motion was almost completely linear translation. Rebound was slight.

SLED TEST A-355 - 40 mph, 36 G peak pulse, rear impact, 5th percentile female dummy.

An Olin inflatable head restraint with a stabilizing flap was preinflated to 7 psi. Minimal head-neck angle changes occurred, and the dummy motion was almost entirely linear translation. The dummy head nodded slightly. Rebound was slight. Some of the accelerometer channels malfunctioned and the test was repeated as A-356.

SLED TEST A-356 - 40 mph, 36 G peak pulse, rear impact, 5th percentile female dummy.

A repeat of A-355. The dummy response was quite similar to the response of A-355.

SLED TEST A-357 - 40 mph, 37 G peak pulse, rear impact, 95th percentile male dummy.

An Olin inflatable head restraint with a stabilizing flap was preinflated to 10 psi. Slight head-neck extension occurred with moderate ramping limited by the bag loading the shoulders. There was significant upward as well as forward rebound.

SLED TEST A-358 - 30 mph, 21 G peak pulse, rear impact, 5th percentile female dummy.

The sliding rigid head restraint was fixed in its upward position prior to the test. Slight head-neck extension occurred due to rearward placement of the restraint. Ramping and rebound were slight.

SLED TEST A-359 - 10 mph, 9 G peak pulse, rear impact, 5th percentile female dummy.

The sliding rigid head restraint was fixed in its upward position prior

to the test. Slight head-neck extension occurred. Ramping was slight and rebound was minimal.

SLED TEST A-360 - 10 mph, 8 G peak pulse, rear impact, 95th percentile male dummy.

The sliding rigid head restraint was fixed in its upward position prior to the tes. Slight head-neck extension occurred. Ramping and rebound were very slight.

SLED TEST A-361 - 30 mph, 19 G peak pulse, rear impact, 95th percentile male. dummy.

The sliding rigid head restraint was fixed in its upward position prior to the test. The dummy was leaning forward out of position at the start of the pulse and rotated backward severely, resulting in the head going over the top of the head restraint with severe head-neck hyperextension. There was severe upward and forward rebound.

SLED TEST A-362 - 30 mph, 20 G peak pulse, rear impact, 95th percentile male dummy.

The sliding rigid head restraint was fixed in its upward position prior to the test. Slight head-neck extension occurred with some oscillation. Ramping and rebound were slight.

SLED TEST A-369 - 30 mph, 21 G peak pulse, rear impact, 5th percentile female dummy.

An Olin inflatable head restraint with a modified mounting configuration and modified stabilizer flap was deployed at t = 27 msec. The bag slapped the dummy head during the initial deployment phase causing a slight forward rotation and an acceleration spike. Pressure in the bag stabilized at 9 psi at t = 52 msec. The bag oscillated in shape causing rapid nodding of the dummy head. No head-neck extension occurred; the dummy exhibited basically linear translational motion. There was slight ramping and slight rebound. This test is discussed in detail in the Discussion of Results section.

SLED TEST A-370 - 40 mph, 38 G peak pulse, rear impact, 5th percentile female dummy.

An Olin inflatable head restraint with a modified mounting configuration and modified stabilizer flap was deployed at t = 15 msec. The bag appeared to slap the head less than in test A-369. There was no head-neck extension, but there was oscillation of the head. Rebound was significant. This test is discussed in detail in the Discussion of Results section.

SLED TEST A-371 - 30 mph, 24 G peak pulse, rear impact, 95th percentile male dummy.

The sliding rigid head restraint was deployed at t = 27 msec. by the drogue chute thruster. The restraint was fully up in 9 msec. There was no head-neck extension. Ramping was moderate and there was very slight rebound. This test is discussed in detail in the Discussion of Results section.

SLED TEST A-372 - 30 mph, 18 G peak pulse, rear impact, 95th percentile male dummy.

An Olin inflatable head restraint with a modified mounting configuration and modified stabilizer flap was deployed at t = 30 msec. The bag pressure stabilized at 10 psi at t = 59 msec. There was no head-neck extension, slight ramping and mild rebound. This test is discussed in detail in the Discussion of Results section.

SLED TEST A-373 - 40 mph, 40 G peak pulse, rear impact, 95th percentile male dummy.

An Olin inflatable head restraint with a modified mounting configuration and modified stabilizer flap was deployed at t = 9 msec. The bag pressure stabilized at 10 psi at t = 40 msec. There was slight rotation of the head, but no extension. Ramping was moderate and rebound was significant. This test is discussed in detail in the Discussion of Results section.

SLED TEST A-374 - 30 mph, 19 G peak pulse, 22 1/2° oblique rear impact, 95th percentile male dummy.

An Olin inflatable head restraint with modified stabilizer flap was mounted but was not deployed. Severe head-neck extension occurred. The dummy moved sidewards after the initial phase of impact and then began to rotate, the dummy shoulders hitting the side of the seat. Rebound was severe up, out and to the side of the seat.

SLED TEST A-376 - 30 mph, 19 G peak pulse, 22 1/2° oblique rear impact, 95th percentile male dummy.

An Olin inflatable head restraint with a modified stabilizer flap was deployed at t = 32 msec. There was slight head-neck extension. The head restraint minimized the sidewards motion of the dummy compared to test A-374. Rebound was significant. This test is discussed in detail in the Discussion of Results section.

SLED TEST A-377 - 30 mph, 28 G peak pulse, frontal impact, 95th percentile male dummy.

An Olin inflatable head restraint with a modified stabilizer flap was mounted but was not fired. The dummy was restrained by a lap belt and a diagonal shoulder harness. The dummy rebounded off the belt restraints back onto the seat back. There was slight head-neck extension prior to further moderate extension when the dummy struck the seat back.

SLED TEST A-379 - 30 mph, 33 G peak pulse, frontal impact, 95th percentile dummy.

An Olin inflatable head restraint with a modified stabilizer flap was deployed at t = 25 msec. The dummy was restrained by a lap belt and a diagonal shoulder harness. Following rebound off the belt system the dummy moved backward towards the seat. Head-neck extension of 30° occurred prior to the dummy hitting the head restraint. At t = 258 msec the dummy struck the head restraint stopping any further extension. The bag pocketed the shoulders well.

7.4 MALPOSITIONED OCCUPANT TESTS

A special series of three malpositioned occupant tests were performed with the Olin inflatable head restraint system. These tests involved dynamic deployment of the restraint with the seat mounted in the interior of a stationary automobile. The three tests involved the 5th percentile female dummy leaning forward from the seat against an Eaton frontal airbag restraint which was deployed in order to drive the dummy back into the head restraint, a 50th percentile male dummy with its head laying back on the head restraint package prior to deployment and a 3-year old child dummy standing behind the seat with its head resting just above the head restraint package prior to deployment.

In the test involving the frontal airbag, both inflator systems (Eaton bottled gas for the frontal bag and Olin augmented air for the head restraint bag) were activated simultaneously. The dummy was pushed back into the seat with a motion very similar to that of the 95th percentile male dummy in the belt rebound test A-379 (that is, as the dummy approached the seat back the head-neck was already in mild extension. Unfortunately the head restraint bag ruptured during inflation and subsequently did not cushion the dummy head. However, the similarity of this test to that of A-379 in terms of dummy kinematics indicates that had the head restraint been in position it would have performed as successfully as it did in A-379.

The 50th percentile male dummy, used to simulate a sleeping occupant leaning back on the packaged head restraint, was fitted with a standard ball and socket neck rather than the rubber neck used in all the other tests. This was done to facilitate the head placement of the dummy. Upon initiation of inflation, the dummy's head, which was in direct contact with the rigid stabilizing flap, received a severe head A-P acceleration spike of over 180 G's for a duration of 8 msec and an accompanying head S-I acceleration spike of 95 G's. These high accelerations were due to the rigid nature of the stabilizing flap and the initial high pressure peak of the inflator system. The high pressure peak acting over the surface area of the rigid flap (4-3/4 inches by 18-3/4 inches) produced the high forces that were transmitted against the dummy's head. Modification of the inflator pressure-time characteristics and elimination of the rigid flap through the use of a self-stiffening inflatable system would most likely minimize this type of malpositioned occupant problem.

In the case of the three-year old child dummy standing behind the seat, the rigid rotating stabilizing flap produced a sharp impact to the dummy's face upon inflation but the limited rearward motion of the flap was such that the dummy did not achieve an appreciable rearward velocity but instead, simply fell backward against the rear seat back ending up in a sitting position on the seat. The problem of the malpositioned child would appear to also be minimized by modifications of the inflator characteristics and elimination of the rigid stabilizing flap.

8. DISCUSSION OF TEST PROGRAM RESULTS

This section discusses and analyzes in detail the pertinent features of the test development and demonstration program that are of particular significance to the development of deployable head restraints.

The first sled test of the program (A-332) was a baseline test to evaluate the whiplash characteristics of the 95th percentile male dummy with a rubber neck interacting with the basic seat and deployable head restraint mounting structure. The sequence photographs in Figure 43 show that the head-neck extension was severe (+62.3°) in this 30 mph 14 G peak crash pulse even though the head restraint package served to limit further extension. Associated with the angular motions of the head were angular accelerations of close to 1000 rad/sec^2 in both the backward and forward modes as determined by the results of the photometric analysis shown in Figure 44. The angular acceleration peak in the forward mode is during the whiplash phase of the head motion and it is accompanied by the peak head accelerometer readings shown in the visicorder traces of Figure 45.

The results of this baseline test will serve as a standard of comparison for the following head restraint tests. Note, however, that this test had a slightly lower peak sled acceleration than the subsequent head restraint tests at 30 mph.

8.1 EATON CYLINDRICAL INFLATABLE HEAD RESTRAINTS

The first test of this system (A-333) was a dynamic deployment test which served to establish the basic viability of inflating head restraint performance (e.g., the restraint deployed in 20 msec, and the dummy began to load the bag at about 40 msec). The results of this test were used as the basis for a development series of preinflated head restraint tests (A-334 through A-335). This series of tests (see Table 3) established the necessity of fore and aft stabilization for proper system performance (A-334) and also established inflation pressure requirements in the range of 7 to 15 psi for adequate bag stiffness. These tests also demonstrated the important role that the geometry of the front portion of the head restraint plays in minimizing ramping of the occupant up the seat back by pocketing the shoulders.

8.2 OLIN INFLATABLE HEAD RESTRAINTS

Development of the inflatable head restraint system supplied by Olin

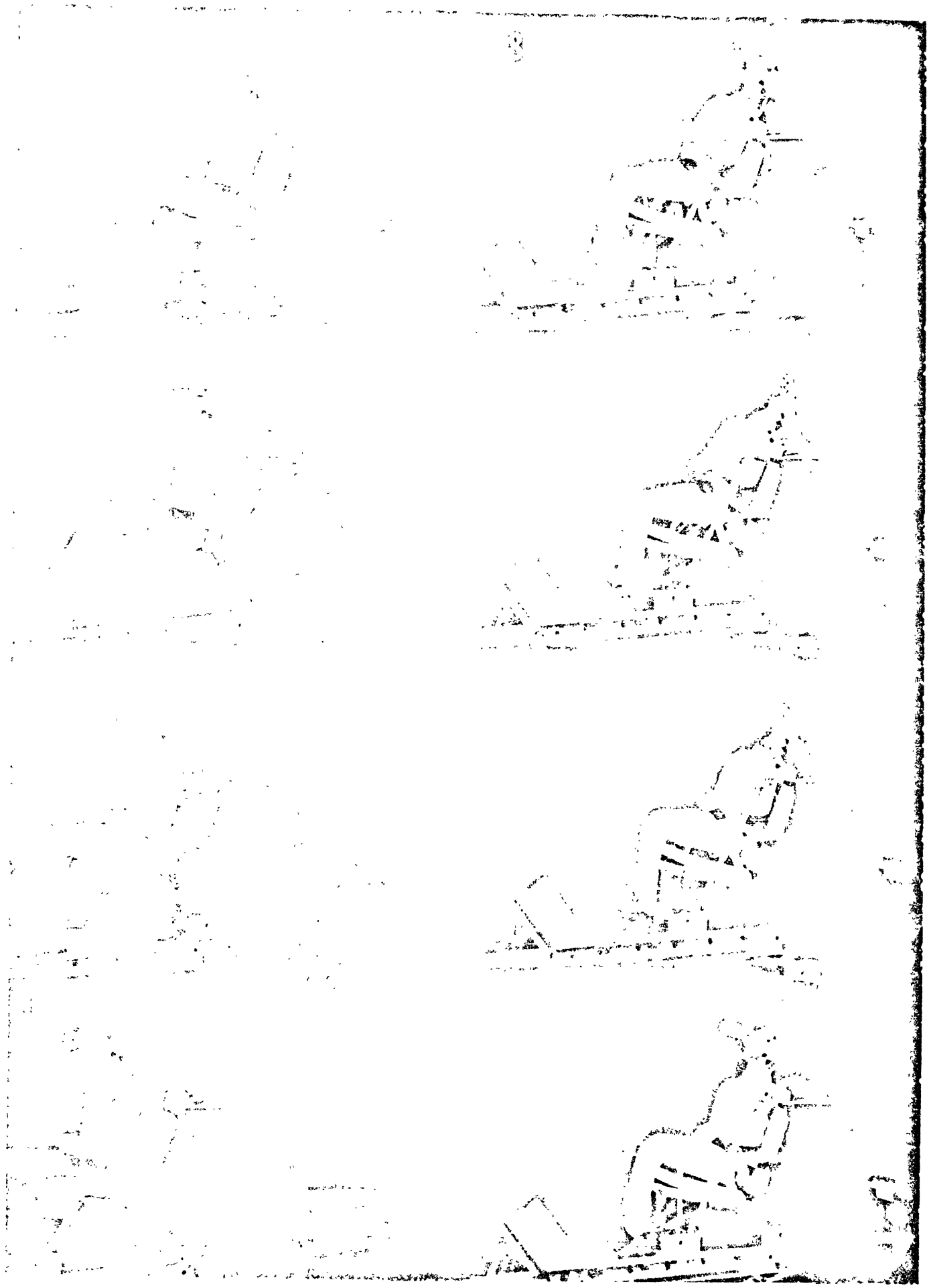

Figure 43. Sequence Photographs of Test A-332
(~ 25 msec. between Pictures)

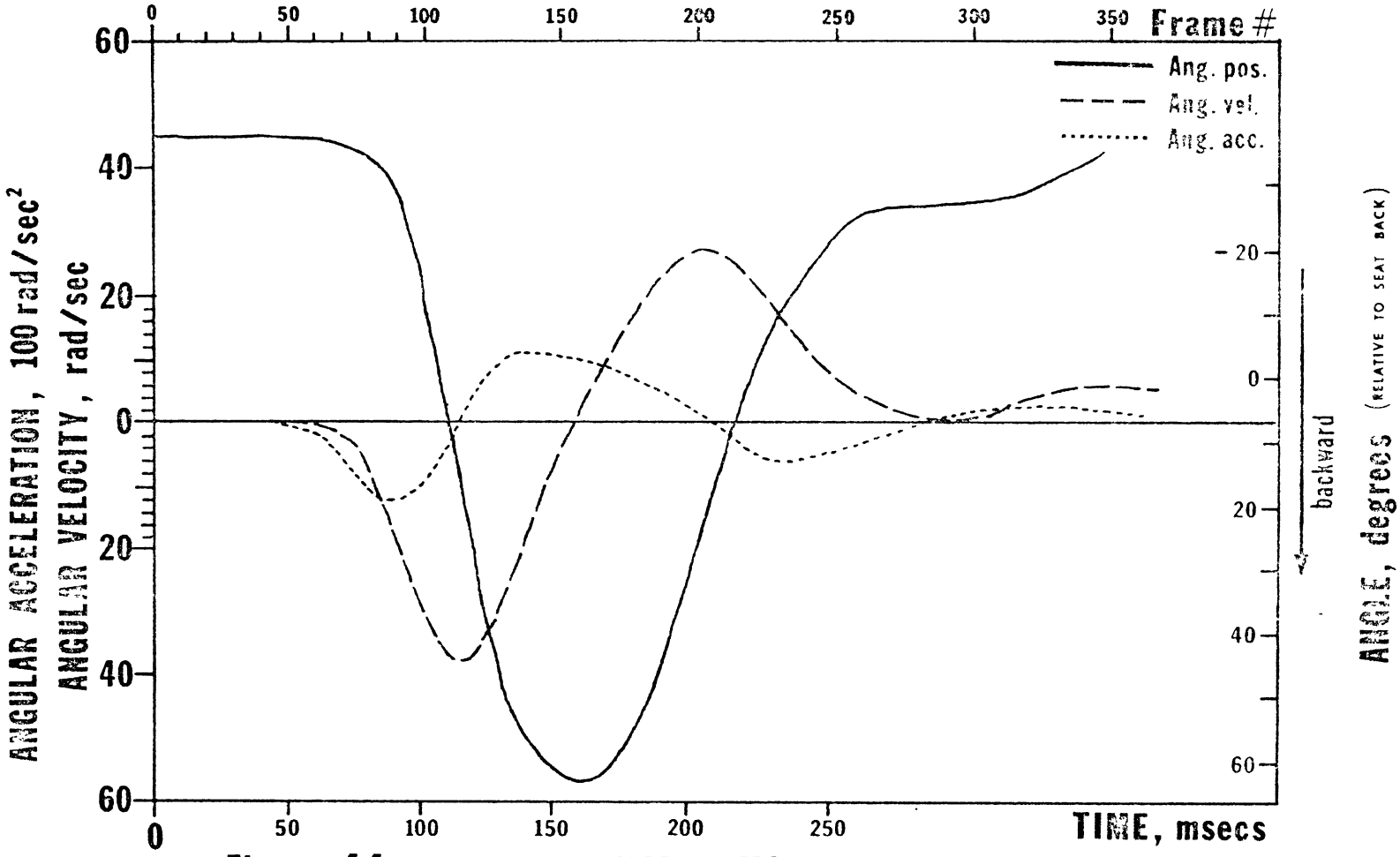

Figure 44 HEAD MOTION Run No. A-332

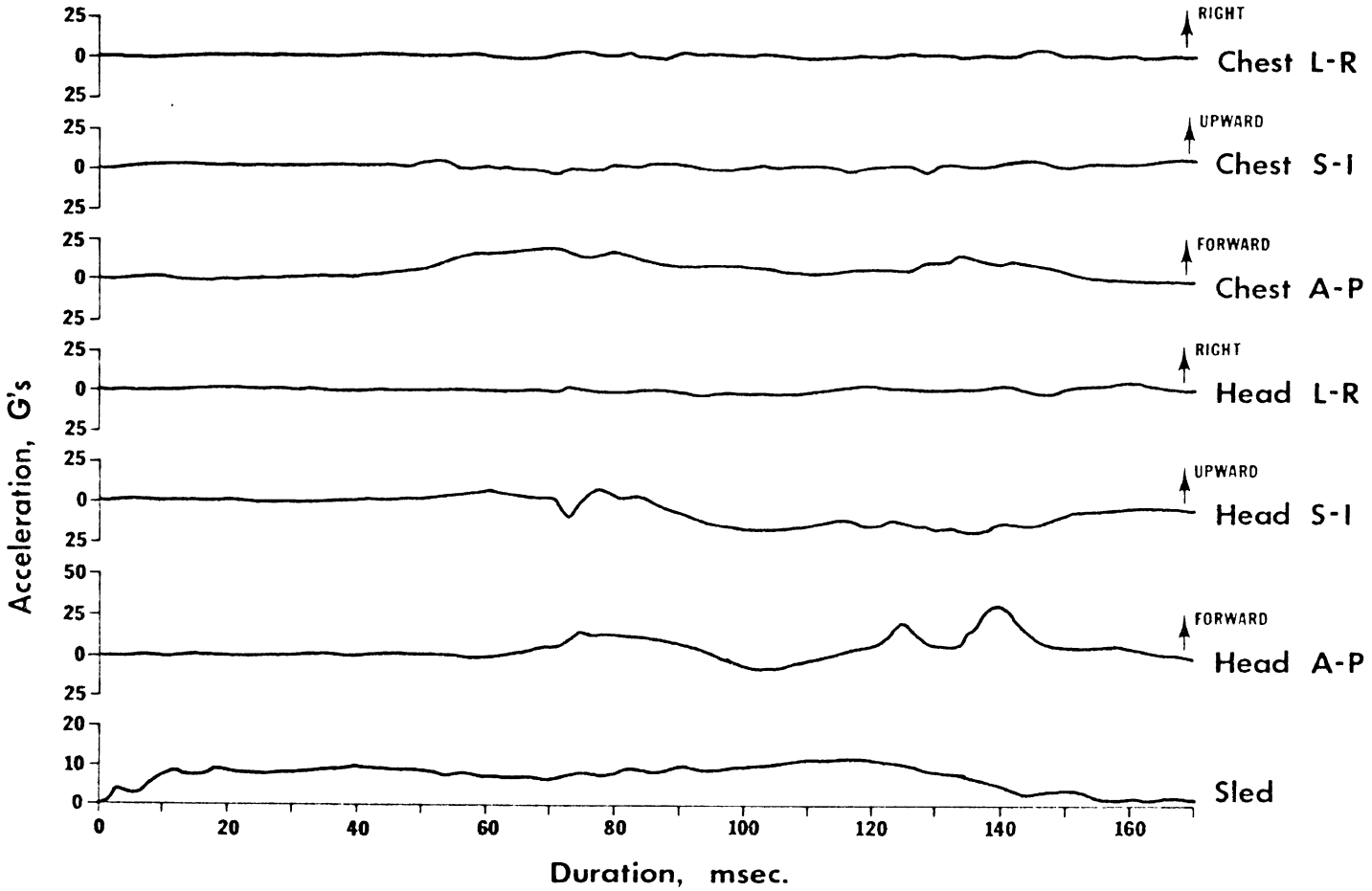

FIGURE 45. VISICORDER TRACES OF SLED TEST A-332

proceeded in two phases; a series of preinflated tests followed by a series of dynamic deployment tests.

The purpose of the first series (A-350 through A-357) was to evaluate the effectiveness of the bag shape for both the 95th percentile male dummy and for the 5th percentile female dummy. System performance was checked at both 10 mph and 30 mph sled velocities with 7 psi inflation pressures. The results as shown in Table 3 were quite comparable to the previous tests with the larger cylindrical bag. The system's effectiveness was further tested by particulary severe tests of 40 mph sled velocity to simulate advanced crush structure characteristics. Again the performance of the system was very satisfactory.

The second series of tests (A-369, A-370, A-372, A-373, A-376 and A-379) involved evaluation of dynamically deploying systems with realistic, state-of-the-art crash sensing time delays before deployment initiation. These tests proved the system to be highly effective in minimizing head motion with results that were even more satisfactory than the excellent results of the preinflated tests (see Table 3).

The results of tests A-369 and A-370 are presented in Figures 46,47,48, 49, and 50. In these tests with the 5th percentile female dummy, the bag slapped the dummy's head during initial deployment causing a 50 G acceleration spike of 9 msec duration in the A-P direction (see Figures 47 and 50). The bag slap also resulted in forward angular acceleration prior to the typical backward angular acceleration of a rear impact shown in Figures 46 and 49 . It was evident from the high speed movies of these tests that the bag was undergoing an oscillation in shape after inflation that was causing the dummy head to nod rapidly back and forth resulting in the pronounced oscillating of the traces of the linear and angular accelerations of the head shown in Figures 46, 47, 49 and 50. In spite of this nodding phenomena, the peak angular accelerations were only 473 rad/sec^2 and 653 rad/sec^2 in the rearward direction for the 30 mph (A-369) and 40 mph (A-370) runs respectively. Except for the nodding, the motion of the 5th percentile female dummy was amazingly uneventful with the main motion being linear translation back into the seat and rebound out. The rebound velocities of the dummy out of the seat were 1.1 mph and 2.5 mph for the 30 mph and 40 mph tests respectively, and the ramping of the dummy up the seat back was limited by the head restraint to 1.33 inches for the 30 mph test and 2.16 inches for the 40 mph test.

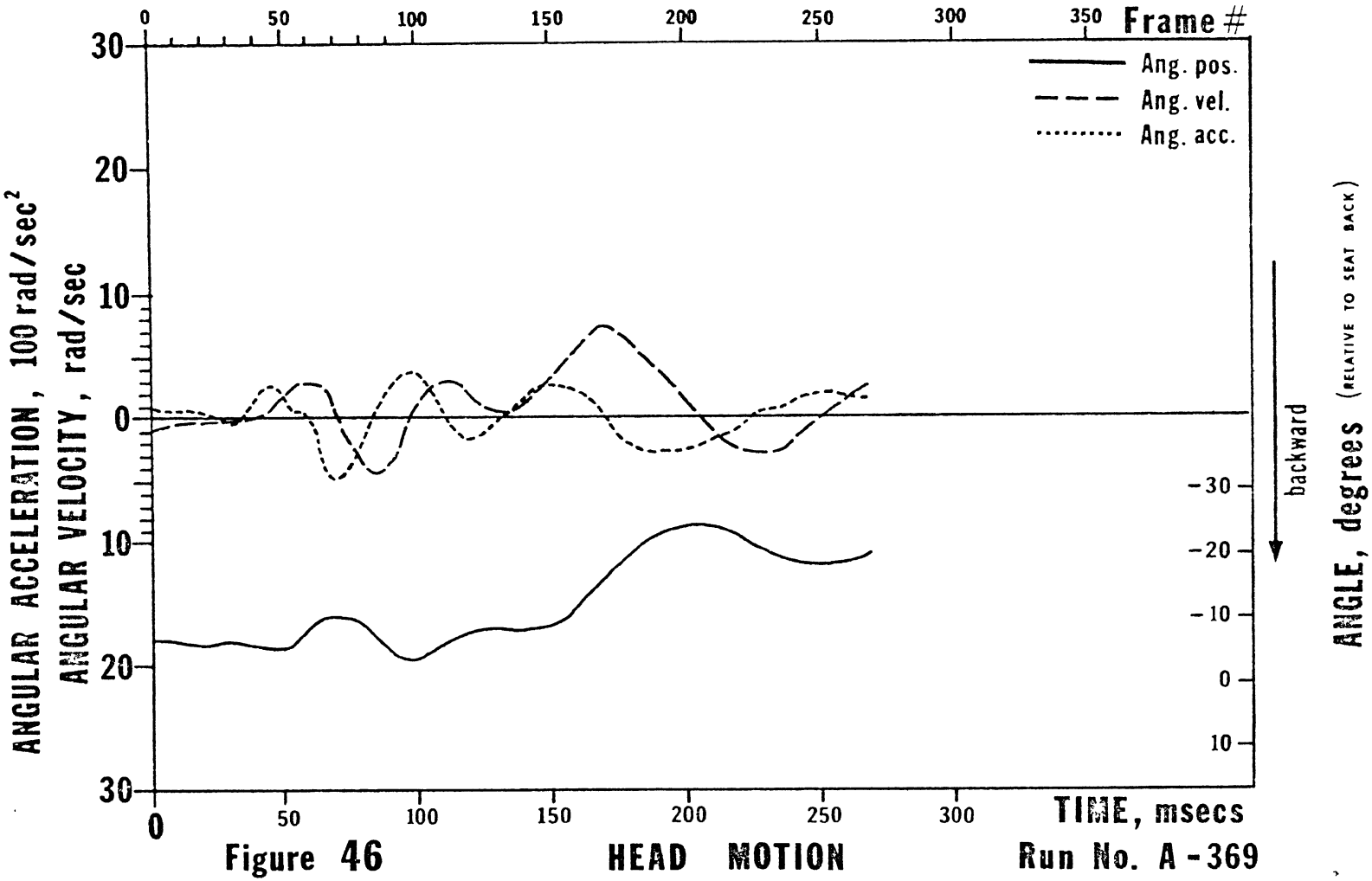

Figure 46 HEAD MOTION Run No. A-369

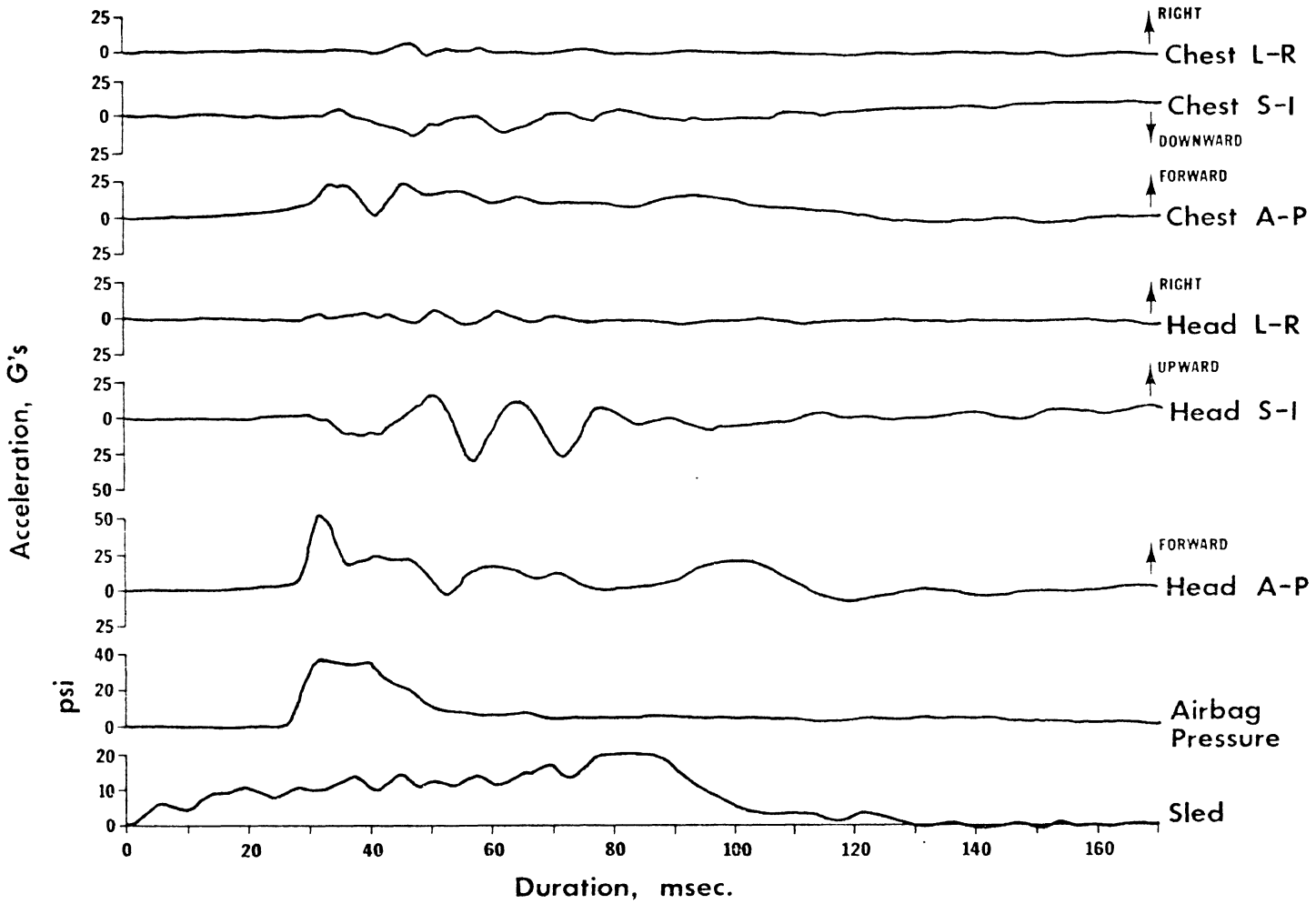

FIGURE 47. VISICORDER TRACES OF SLED TEST A-369

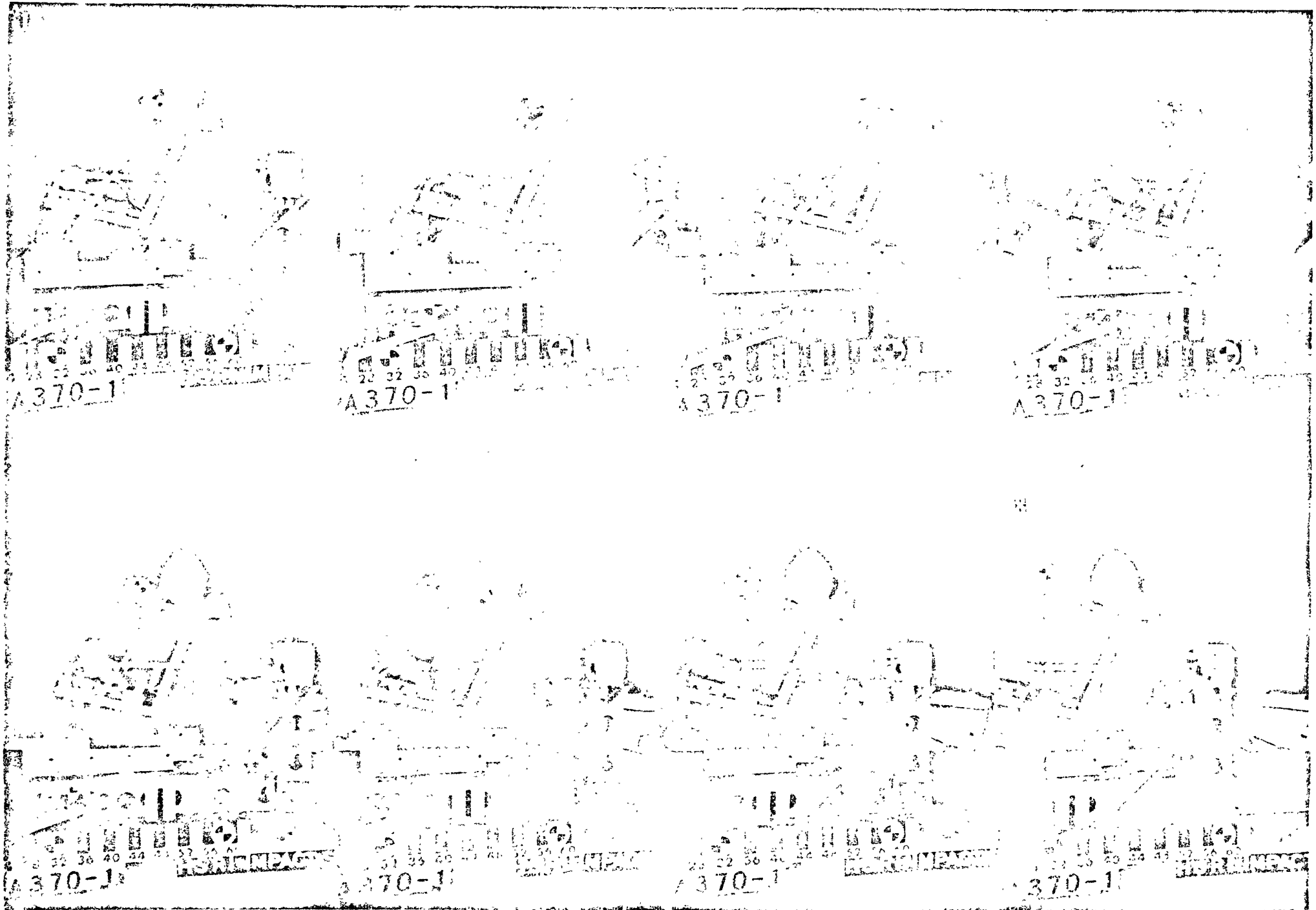

Figure 48. Sequence Photographs of Test A-370 (~ 25 msec. between pictures)

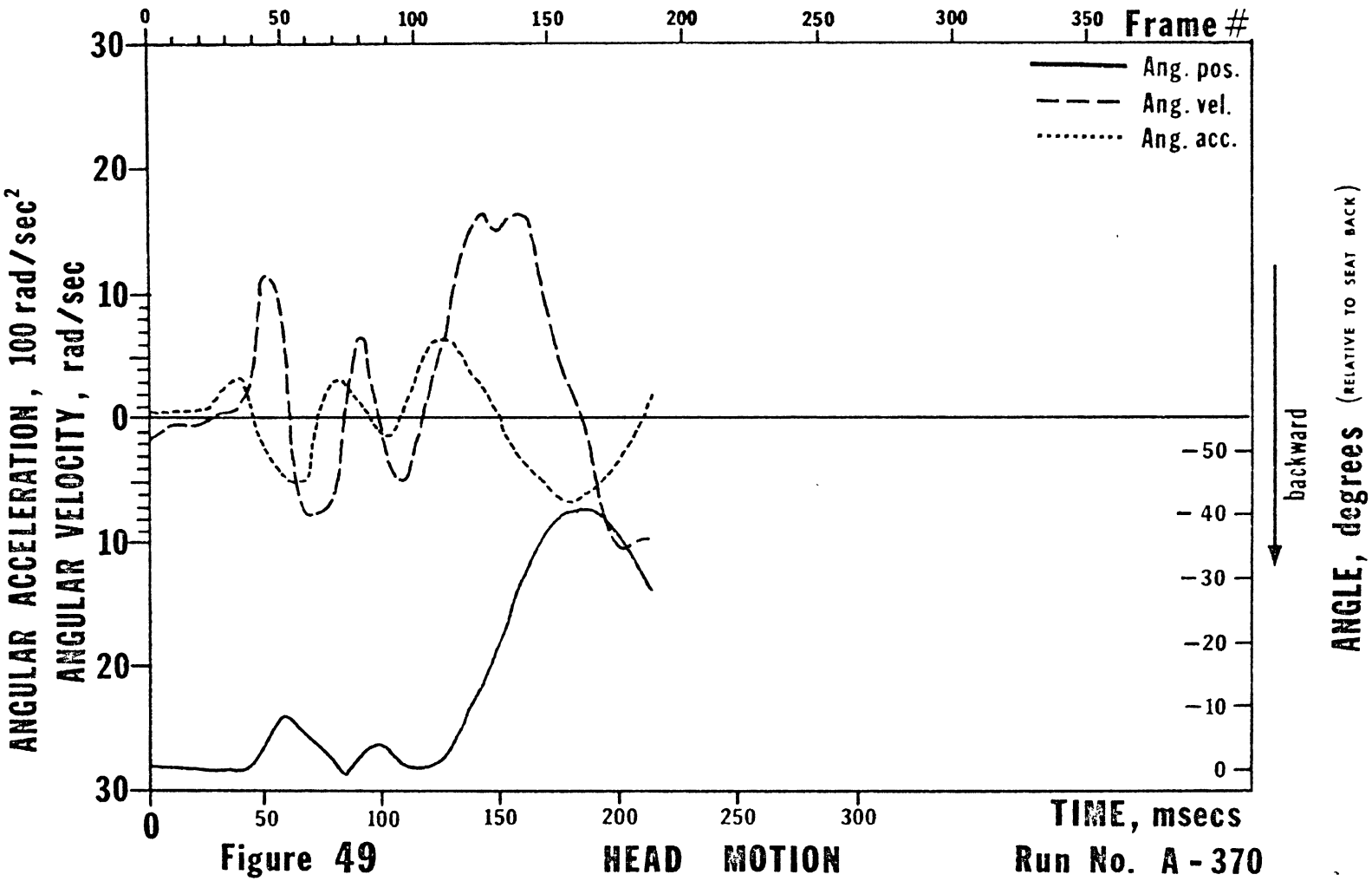

Figure 49 HEAD MOTION Run No. A-370

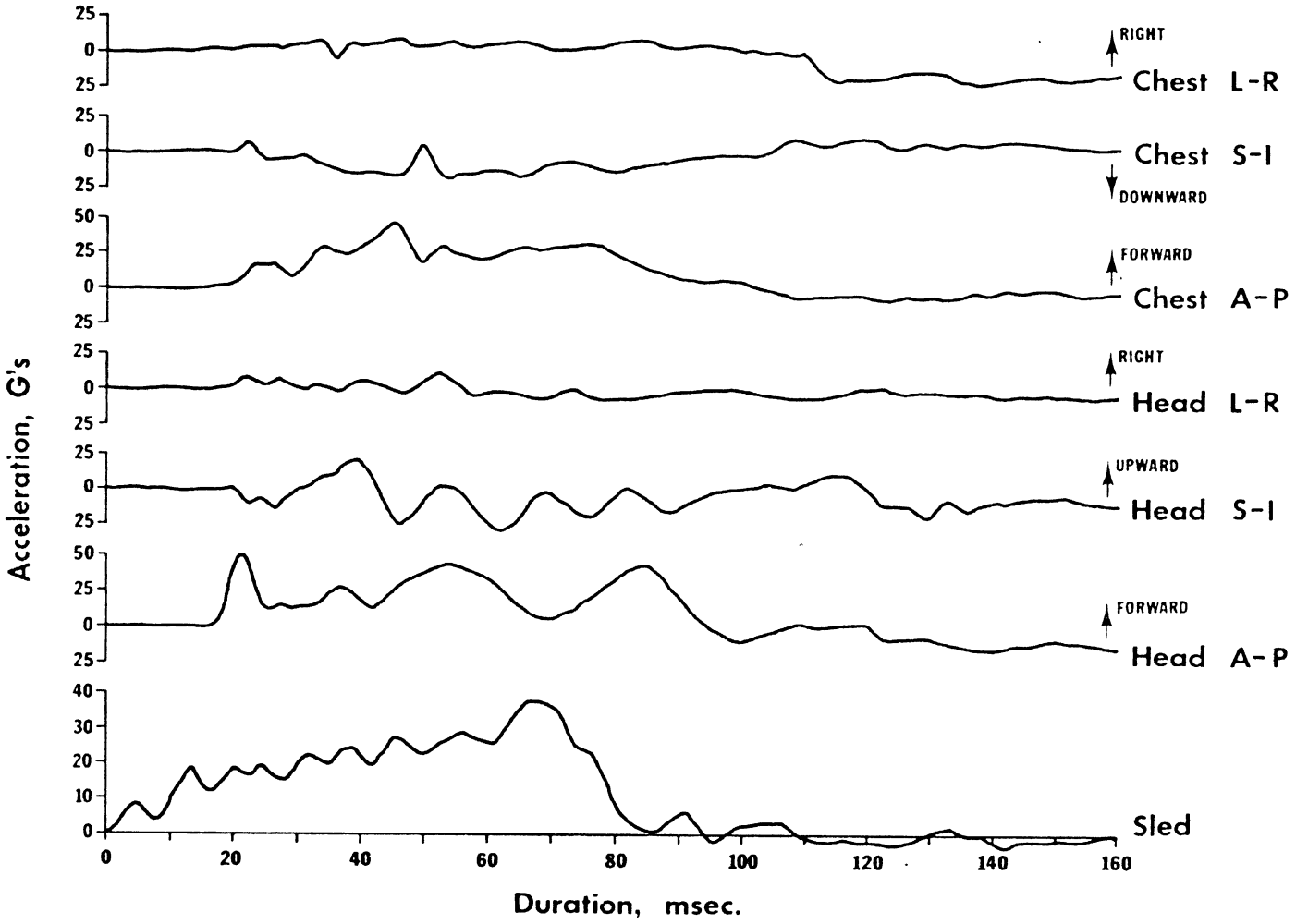

FIGURE 50. VISICORDER TRACES OF SLED TEST A-370

There was very little rotation of the dummy head during these tests and extension did not occur at all as shown by the head angle plots in Figures 46 and 49.

The results of tests A-372 and A-373 using the 95th percentile male dummy are presented in Figures 51, 52, 53, 54, 55 and 56. Bag slap against the dummy was much less pronounced than with the female dummy and bag shape oscillations did not produce significant motions of the dummy head. In the 40 mph test (A-373) the bag caused a slight forward rotation of the head prior to the normal rearward rotation. In these two tests the peak head angular accelerations were in the forward direction corresponding to the maximum rearward rotation of the head. The values of the peaks were 711 rad/sec^2 for test A-372 and 916 rad/sec^2 for test A-373. As in the tests with the female dummy no extension occurred. The peak head A-P accelerations were 32 G for the 30 mph test and 42 G for the 40 mph test. In these tests with the male dummy the height of the dummy was such that its head loaded the restraint bag in a manner very similar to the headform loading in the Instron test. Because of this it was possible to use photometric analysis to get the deflection of the dummy head into the bag and use the maximum deflection to estimate the peak load on the dummy head at that deflection from the load-deflection relation of Figure 39 using the 10 psi curve. The values of maximum load on the head were converted to equivalent head A-P accelerations with the results being 34.6 G for test A-372 and 45.8 G for test A-373. These estimated values of head acceleration agree quite well with the dummy head accelerometer readings thus indicating that the restraint bag is supporting the dummy head in such a manner that the forces at the neck are minimized. The rebounds of the dummy from the seat were more severe than with the female dummy but they were still quite acceptable, the forward velocity of the dummy shoulders being 4.4 mph in test A-372 and 5.3 mph in test A-373. Similarly, the ramping was slightly greater, 2.75 inches and 3.9 inches for tests A-372 and A-373 respectively.

A useful measure for evaluating the degree of optimization of the head restraint design from the standpoint of head acceleration is to consider the ratio of peak head acceleration to peak sled acceleration. The resulting number is an amplification factor which ideally should be unity for a system which also minimizes occupant motion. Calculation of this factor for the

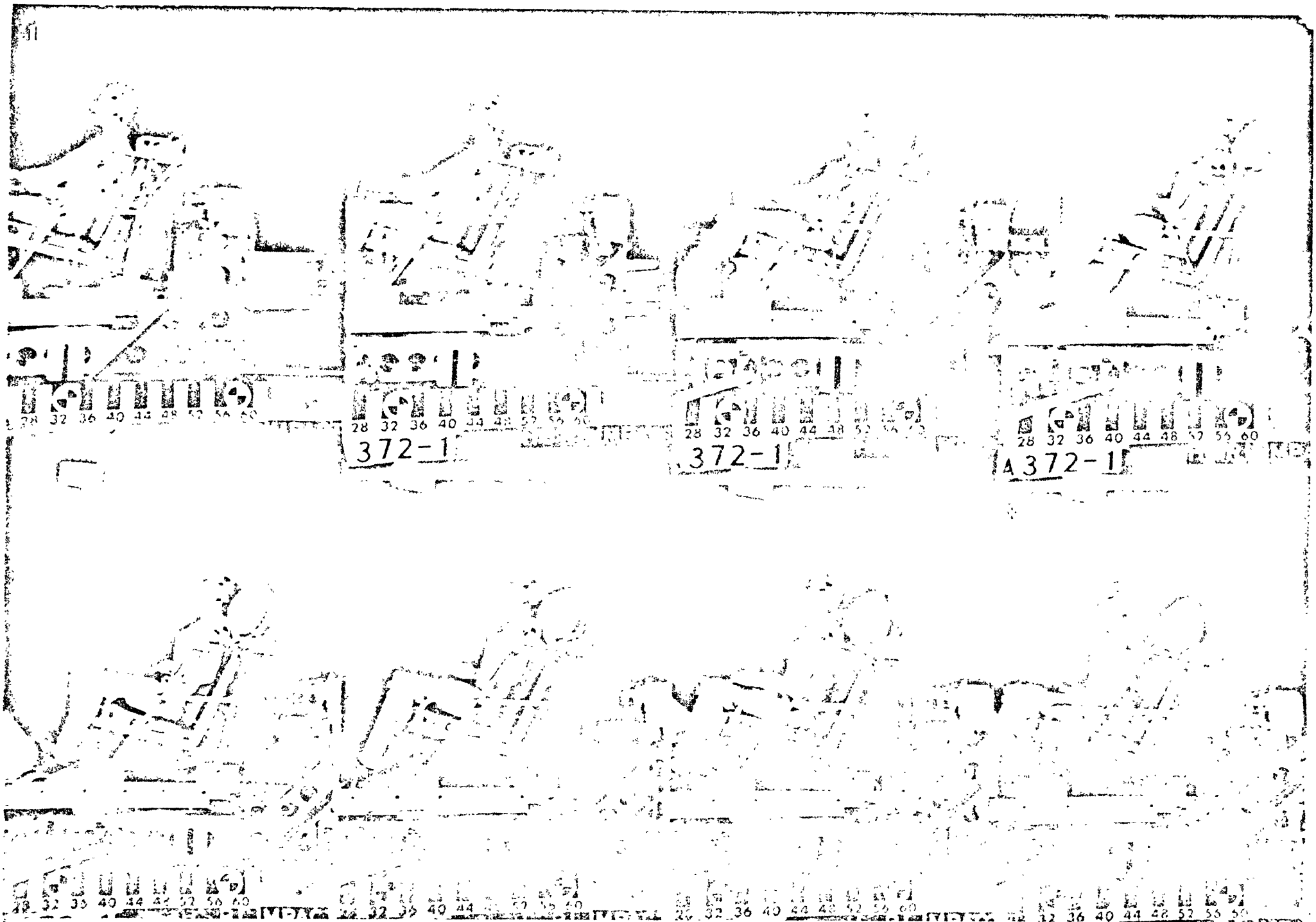

Figure 51. Sequence Photographs of Test A-372 (~25 msec between pictures)

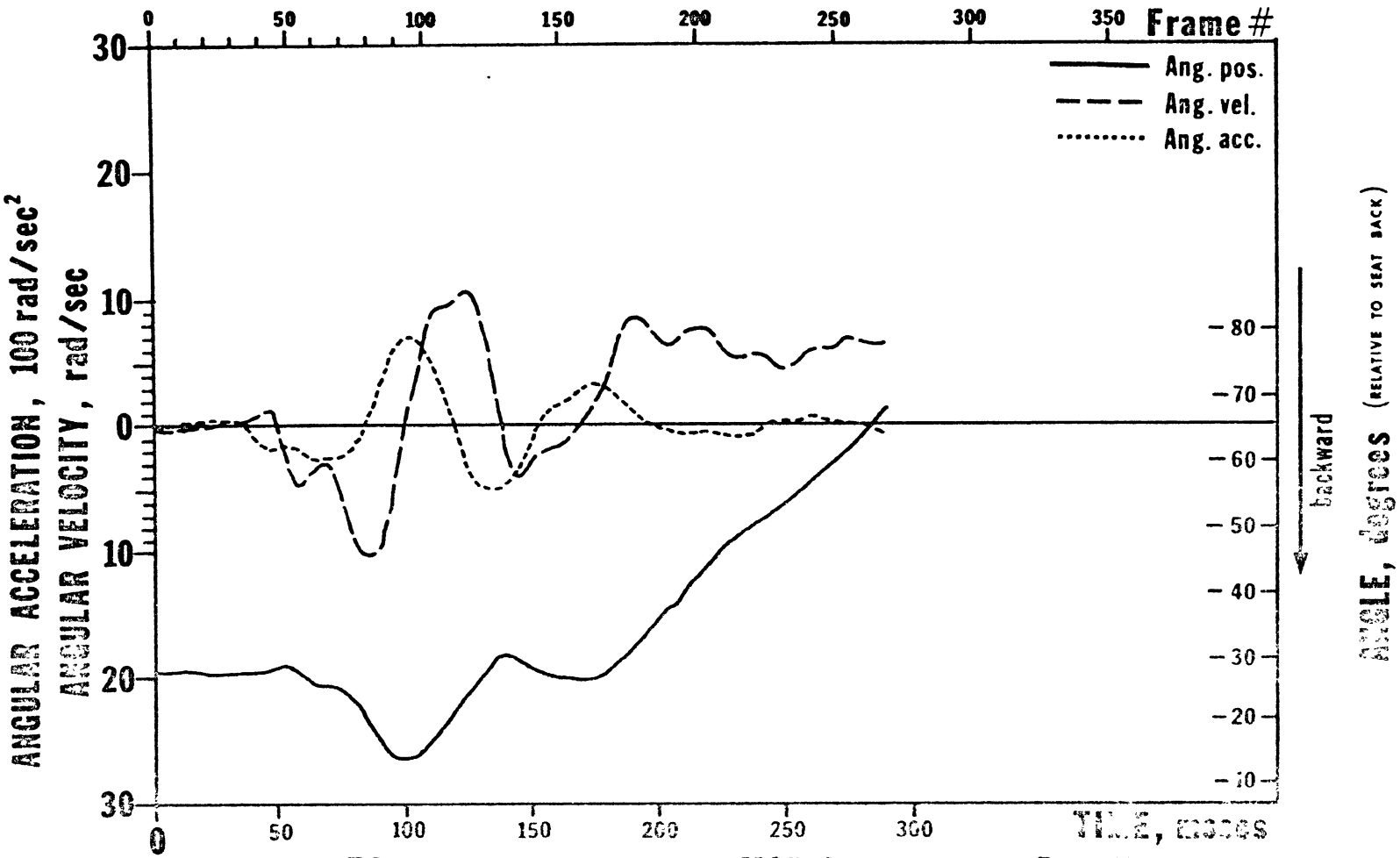

Figure 52 HEAD MOTION Run No. A-372

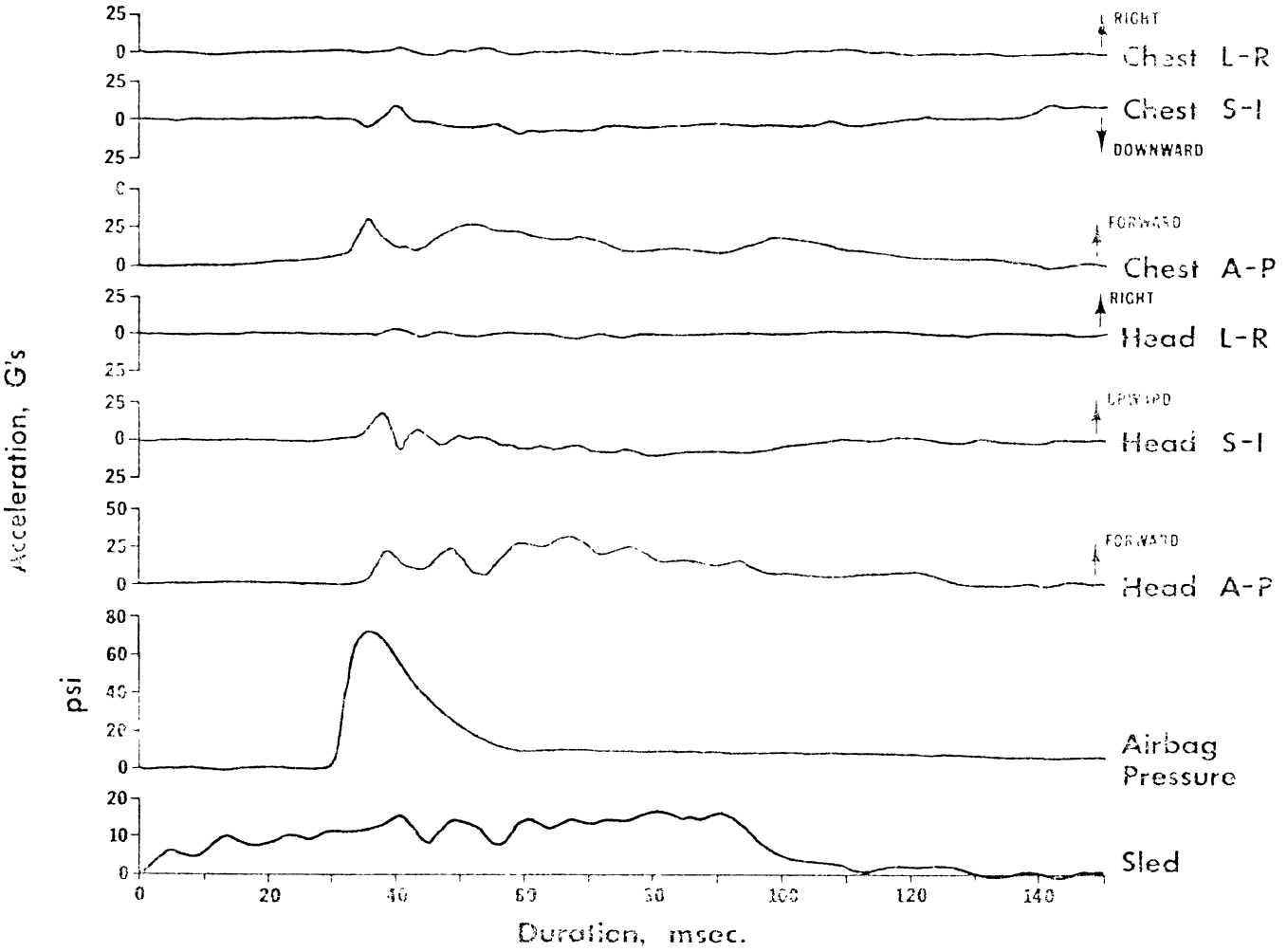

FIGURE 53. VISICORDER TRACES OF SLED TEST A-372

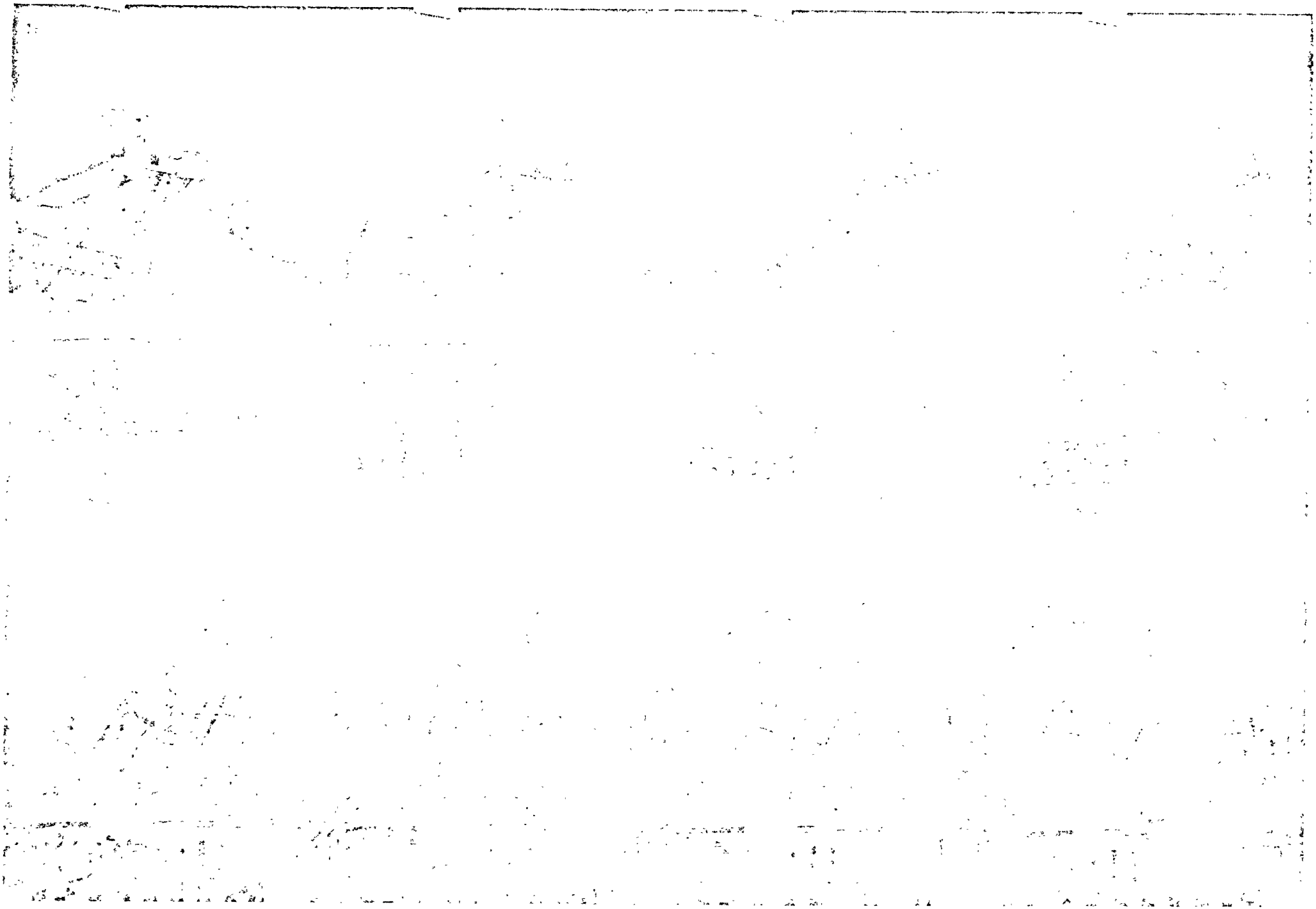

Figure 54. Sequence Photographs of Test A-373 (~25 msec. between pictures)

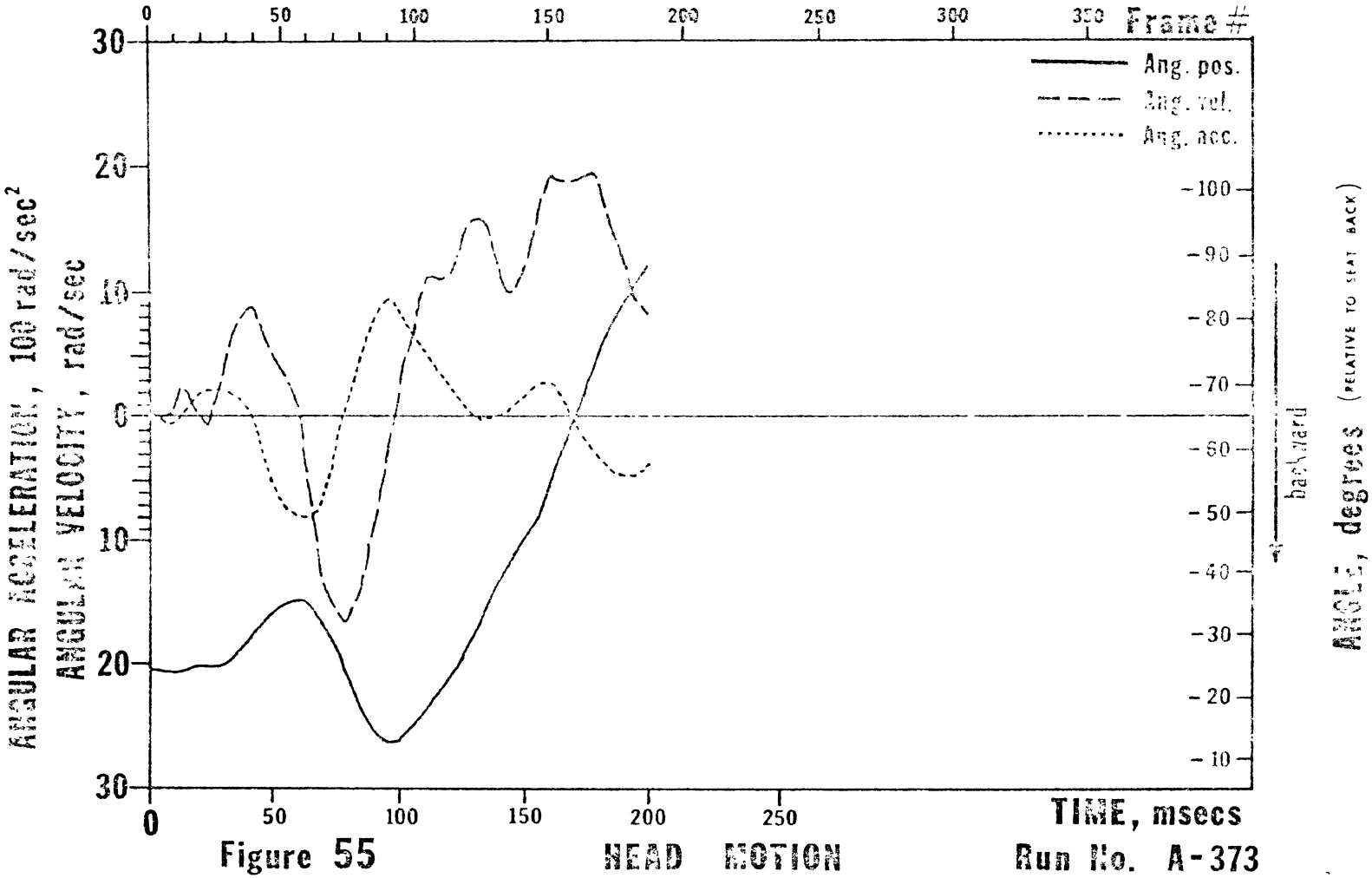

Figure 55 HEAD MOTION Run No. A-373

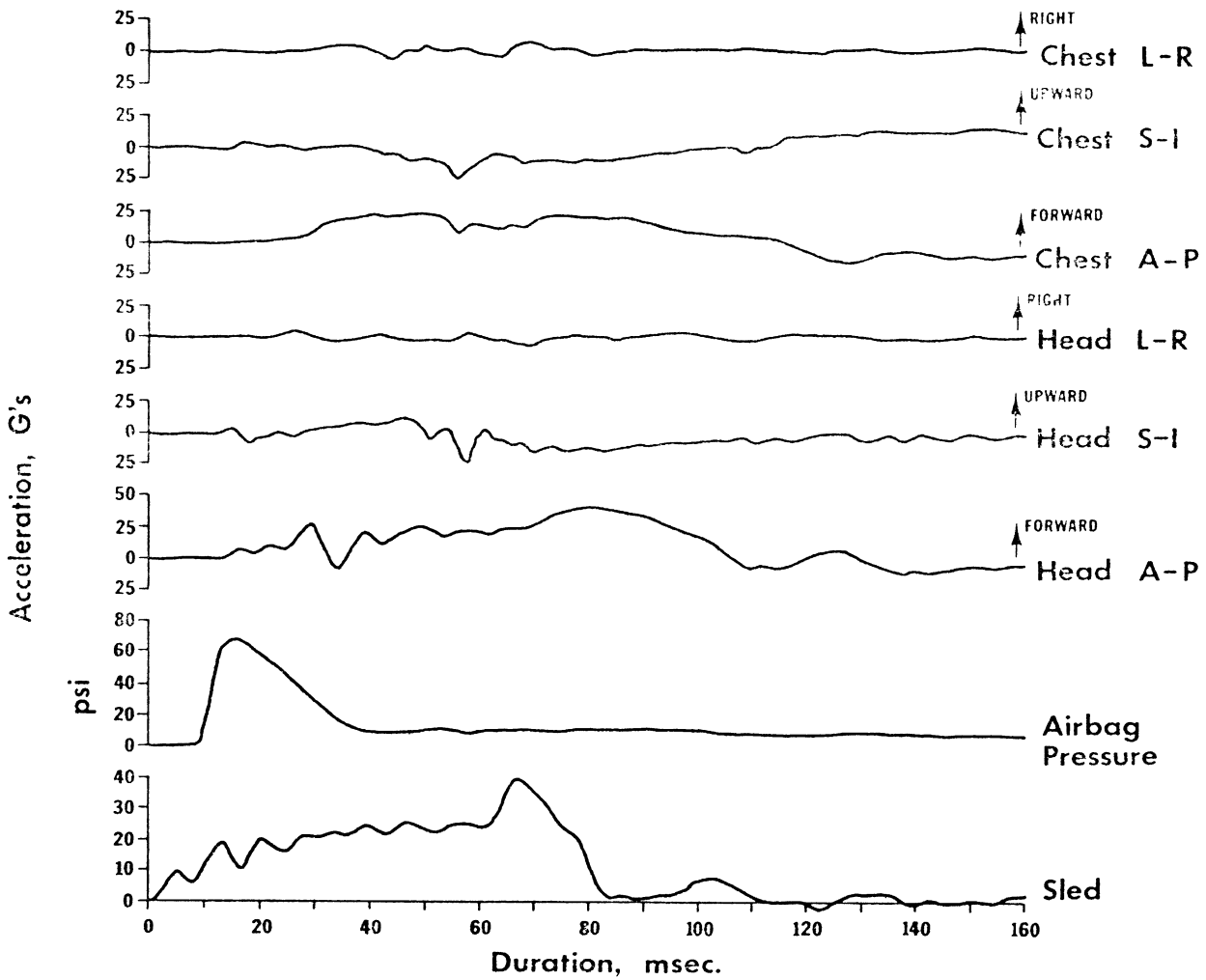

FIGURE 56. VISICORDER TRACES OF SLED TEST A-373

case of the 5th percentile female dummy shows the system to be quite good at both the 30 mph test level (the ratio being 1.05) and the 40 mph test level (the ratio being 1.13), whereas for the taller 95th percentile male dummy the system optimizes at the 40 mph level (the ratio being 1.05) while at 30 mph the ratio is up at 1.78.

It is evident from the above test results that the inflatable head restraints used in this study proved to be remarkably effective in preventing whiplash, and in addition their combination with the seat structure produced a highly effective means for general severe rear-end crash survival.

Additional tests performed to evaluate the Olin system performance in crash situations other than direct rear-end crashes were 22.5° oblique rear-end crash simulations and rebound of the dummy from a lap belt-shoulder harness combination during a frontal crash.

The results of the 22.5° oblique rear-end crash simulation are shown in Figures 57 and 58 of test A-376. The bag was somewhat effective in preventing sidewards motion of the head and shoulders although it did allow slight extension to occur. The head A-P acceleration was noticeably lower in this test than in the direct rearward crash simulations.

The results of the frontal crash rebound test are shown in Figure 59. The head restraint did arrest the motion of the dummy head; however, the dummy had achieved an extension angle of +30° prior to its contact with the bag.

8.3 AIR MAT INFLATABLE HEAD RESTRAINT

The most successful test of the Air Mat head restraint was A-349. In comparison with the performance of the bag type head restraints with stabilizing flaps, this system, as tested, was not very effective. However, judged on the basis that this system was the only one tested that offered the possibility of producing adequate fore and aft stiffness without the need for additional rigid stabilizing structures the results must be judged encouraging.

There are several factors which must be taken into consideration when evaluating the performance of this particular system. Due to limited supply of the dropweave material and the fact that it could only be obtained in a planar form the shape of the head restraint was less than ideal. The effect of the flat surface geometry was magnified by the necessity of mounting the restraint somewhat back from the plane of the seat back. These factors of

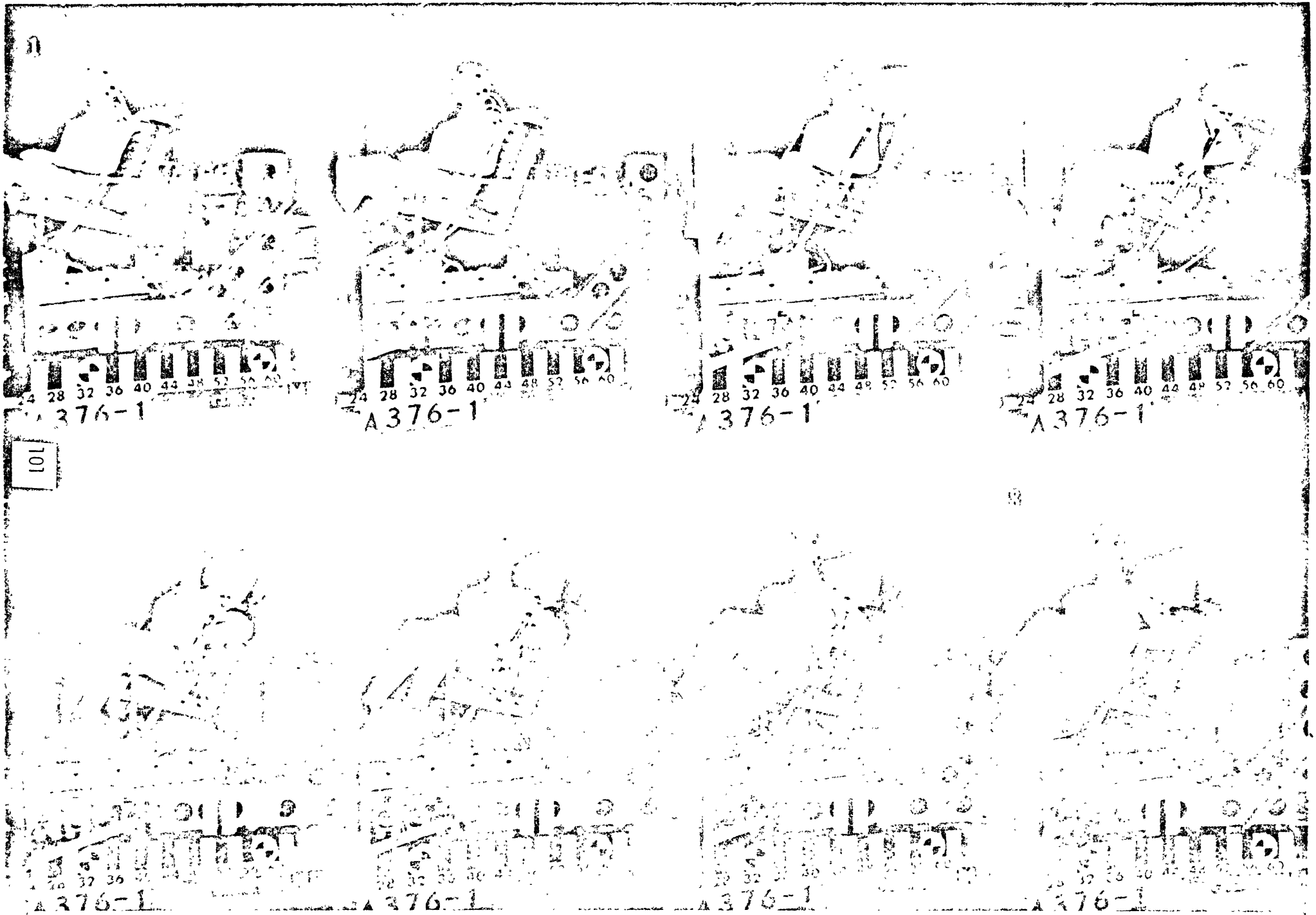

Fiaure 57. Sequence Photographs of Test A-376 (~25 msec. between pictures)

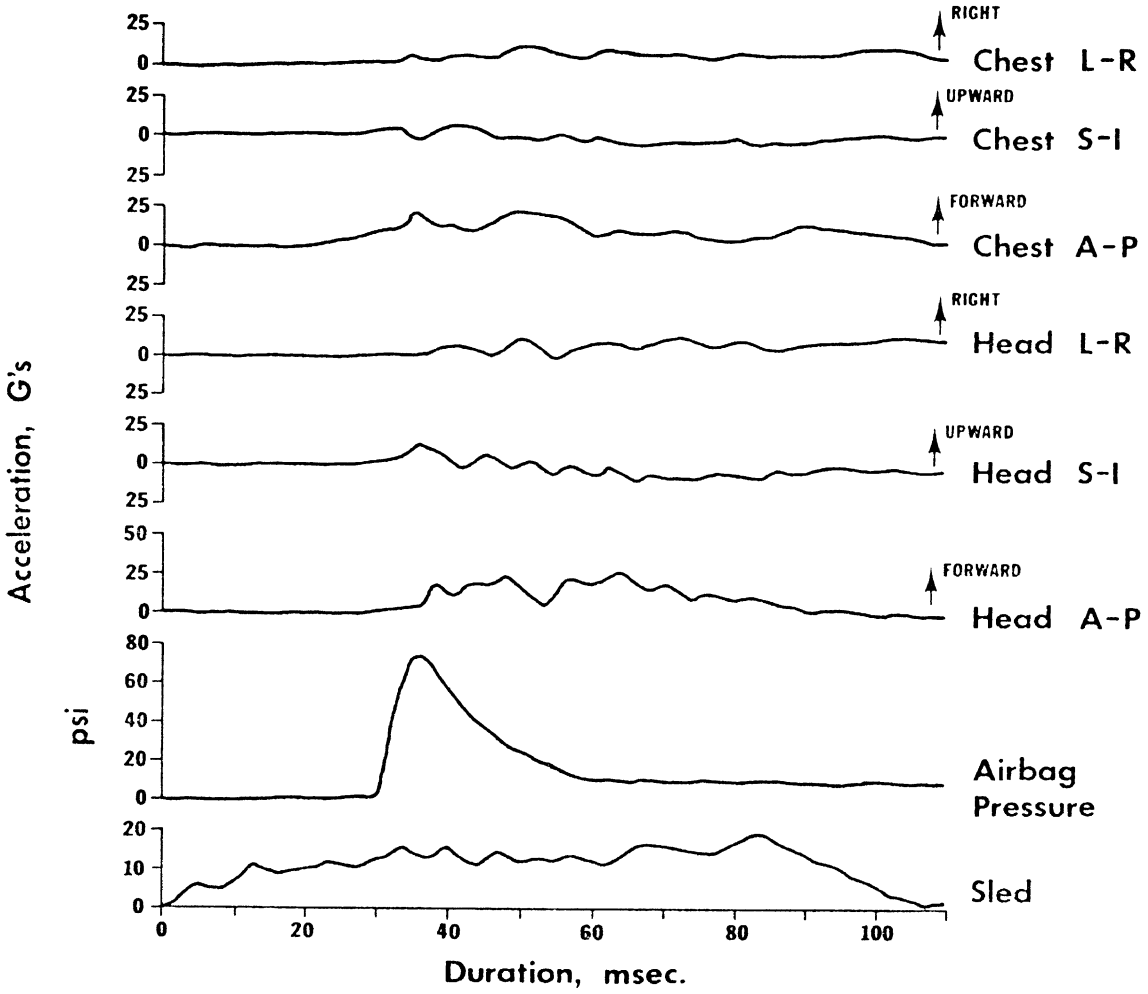

FIGURE 58. VISICORDER TRACES OF SLED TEST A-376

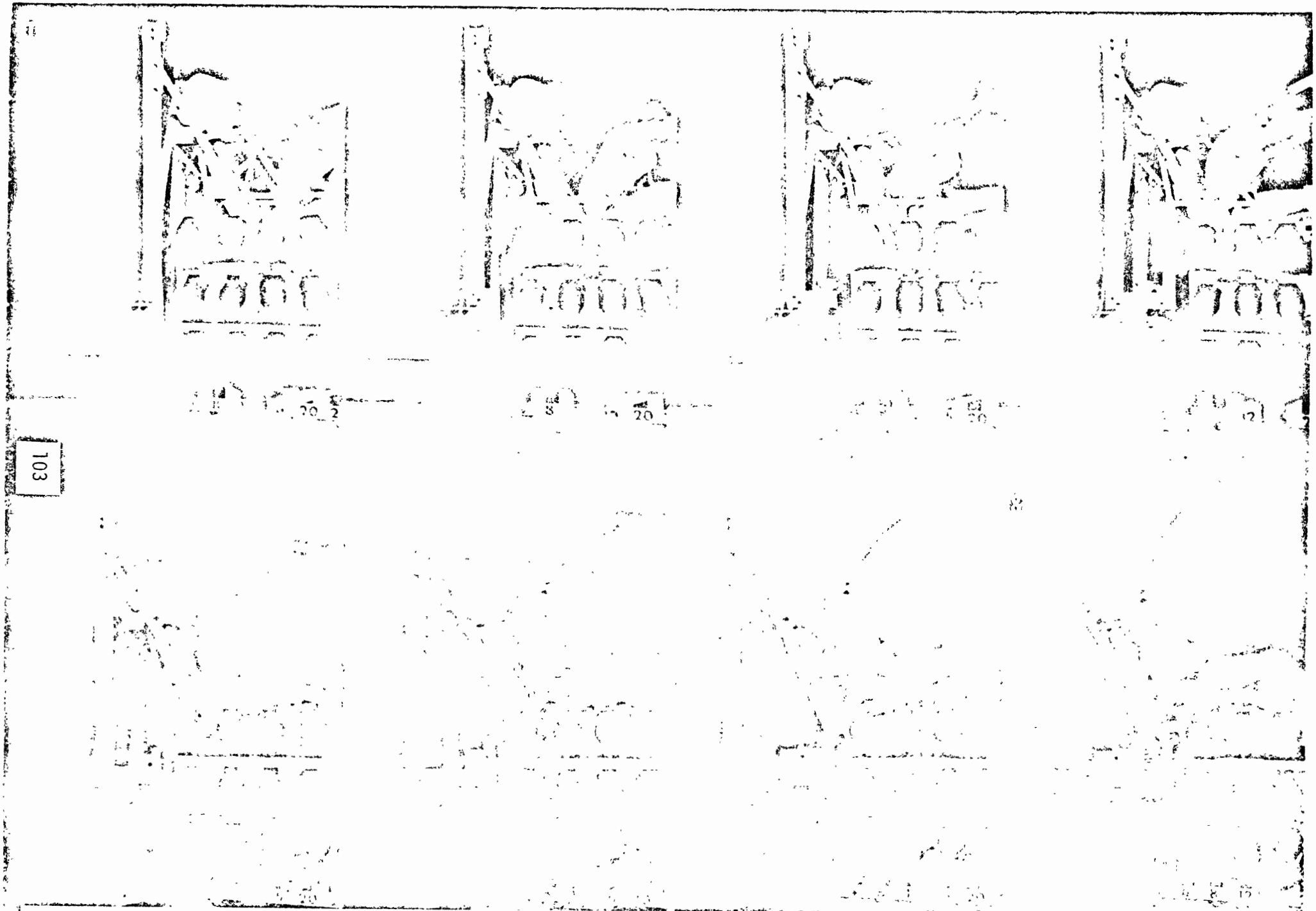

Figure 59. Sequence Photographs of Test A-379 (~25 msec. between pictures)

poor shape and rearward offset of the restraint combined to limit its performance by allowing significant rearward head motion prior to contact with the head restraint. As shown in Figure 60 the restraint did not pocket the shoulders. Although head-neck extension occurred (Figure 61) the restraint did limit it to the +30° level. The extension was accompanied by a 1500 rad/sec^2 angular acceleration peak in the forward mode and, as shown in Figure 62, a head A-P acceleration peak of 33 G's. The head restraint partially buckled at that time allowing the rearward motion to become even more excessive. The high value of angular acceleration demonstrates clearly the necessity to avoid large elastic deformations in restraint systems.

8.4 RIGID DEPLOYABLE HEAD RESTRAINT

The dynamic deployment test of the rigid sliding restraint system was performed in Test A-371. The results of the analysis of this test are shown in Figures 63, 64 and 65. The drogue chute thruster was ignited at t=27 msec and the system was fully deployed in 9 msec. The forces generated by the arrest of the upward motion of the head restraint manifested themselves in a variety of ways. The cushioning material on the front face of the head restraint tore loose and continued to fly upward until it was trapped by the dummy head coming back on it. The arresting forces caused the entire seat structure to rise upward in an elastic manner approximately one-half inch at about t=42 msec resulting in the disturbance of the sled accelerometer pulse shown in Figure 65. Finally, the transverse square steel tube structure of the head restraint was severely bent due to the inertial forces due to arresting the restraint upward motion as shown in Figure 66.

The basic sled pulse was more severe than the pulse of the comparable predeployed test A-362, but the general response of the system was similar to the predeployed test. The peak angular acceleration was 911 rad/sec^2 in the forward direction and extension did not occur. The peak head A-P acceleration was 50 G or about a factor of two higher than the sled peak acceleration. This amplification factor was true for the predeployed test also; adjustment of the head restraint cushion properties could diminish the amplification. The restraint offered no significant pocketing effect and the resulting ramping was 4.5 inches. Upon rebound, the dummy tended to slide forward along the seat in a slouching manner resulting in virtually no forward motion of the shoulders.

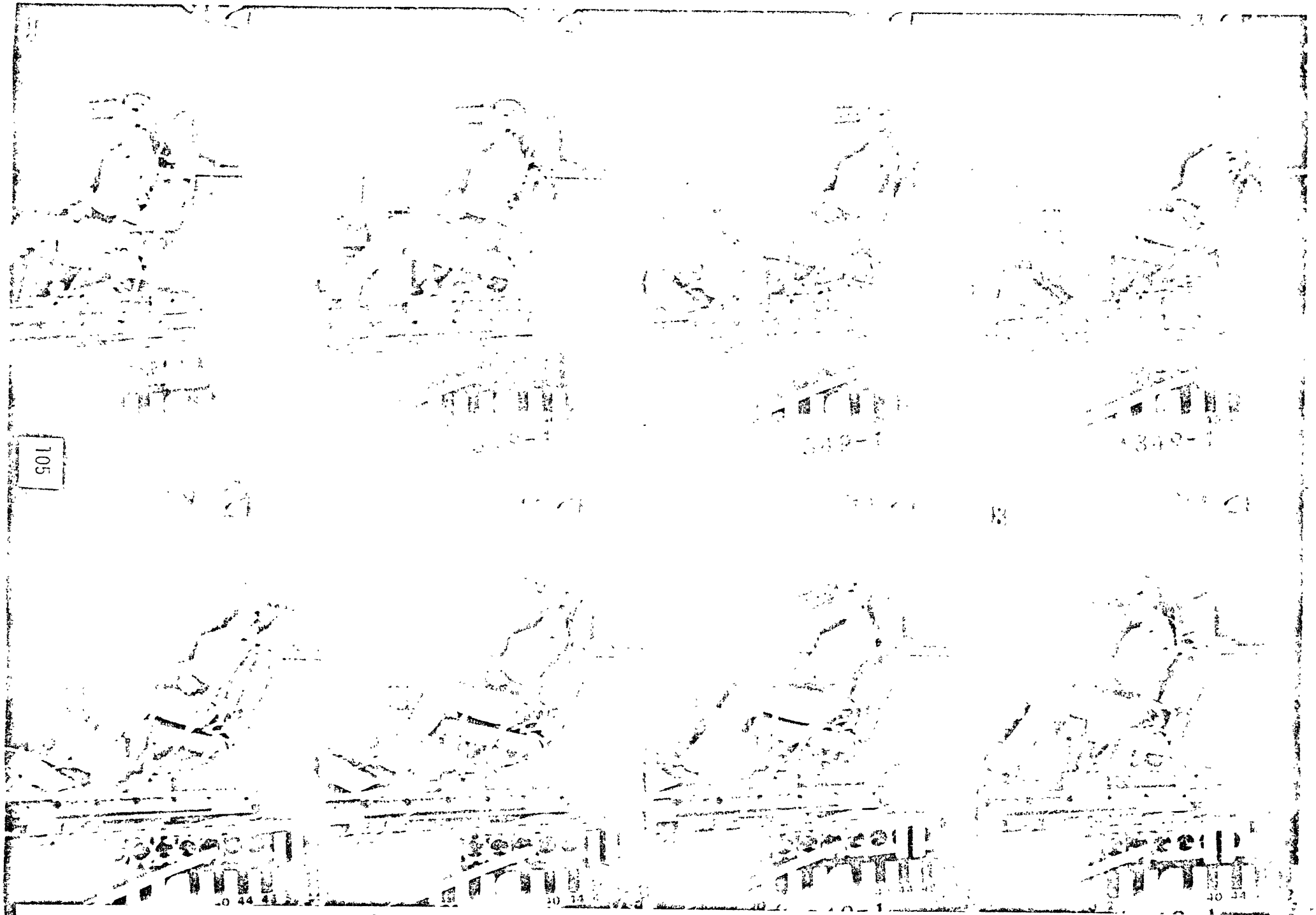

Figure 60. Sequence Photographs of Test A-349 (~25 msec. between pictures)

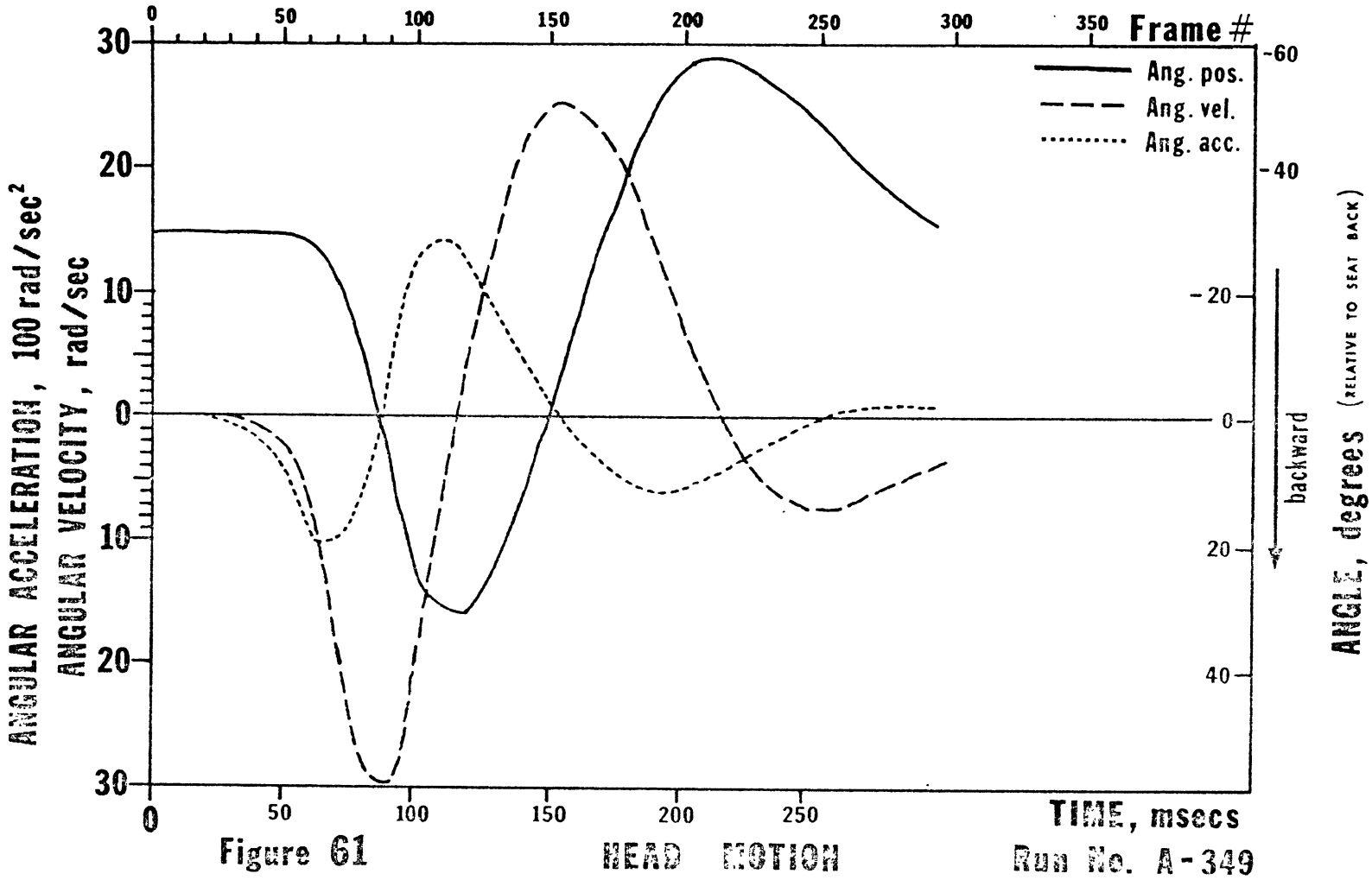

Figure 61 HEAD MOTION Run No. A-349

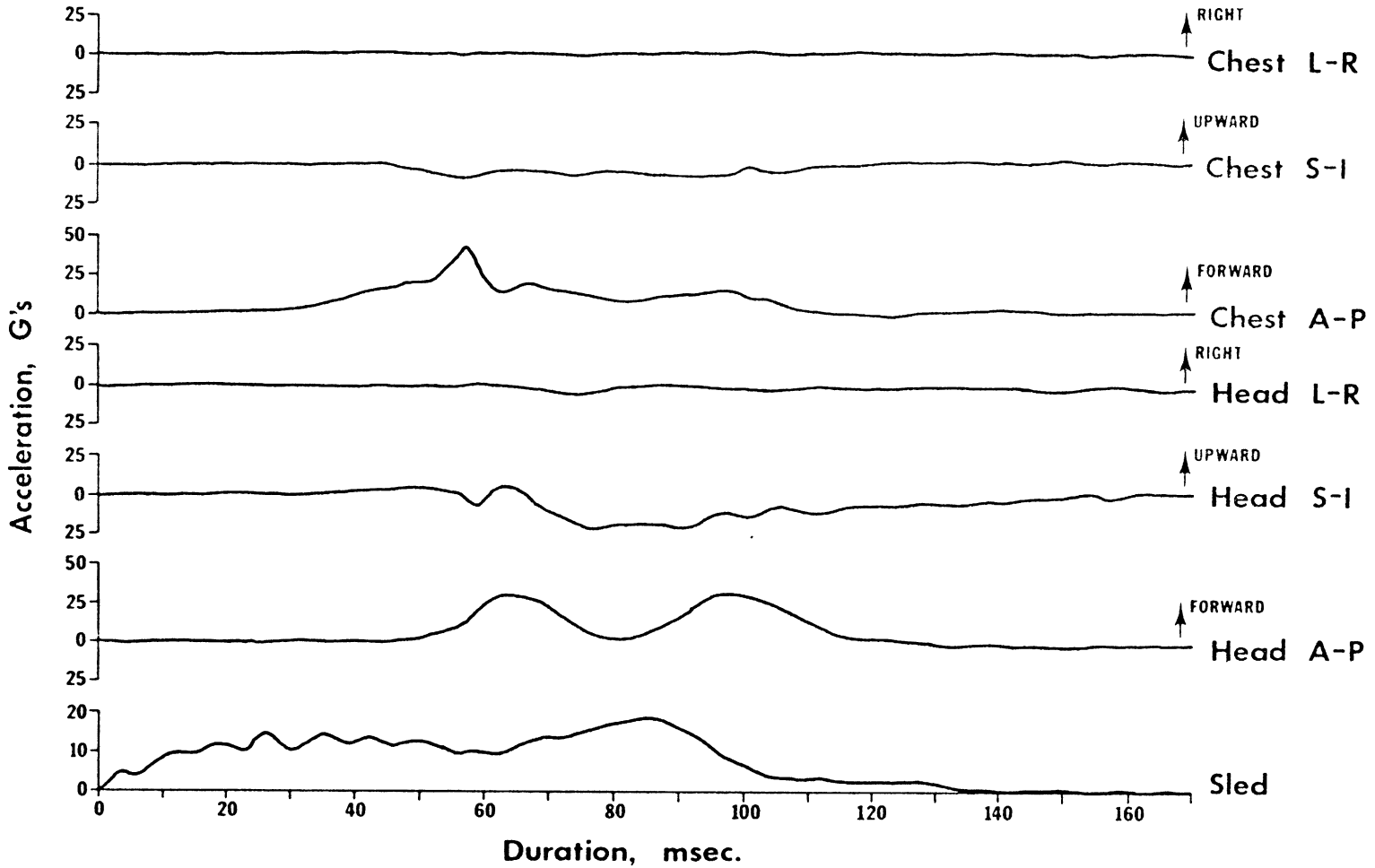

FIGURE 62. VISICORDER TRACES OF SLED TEST A-349

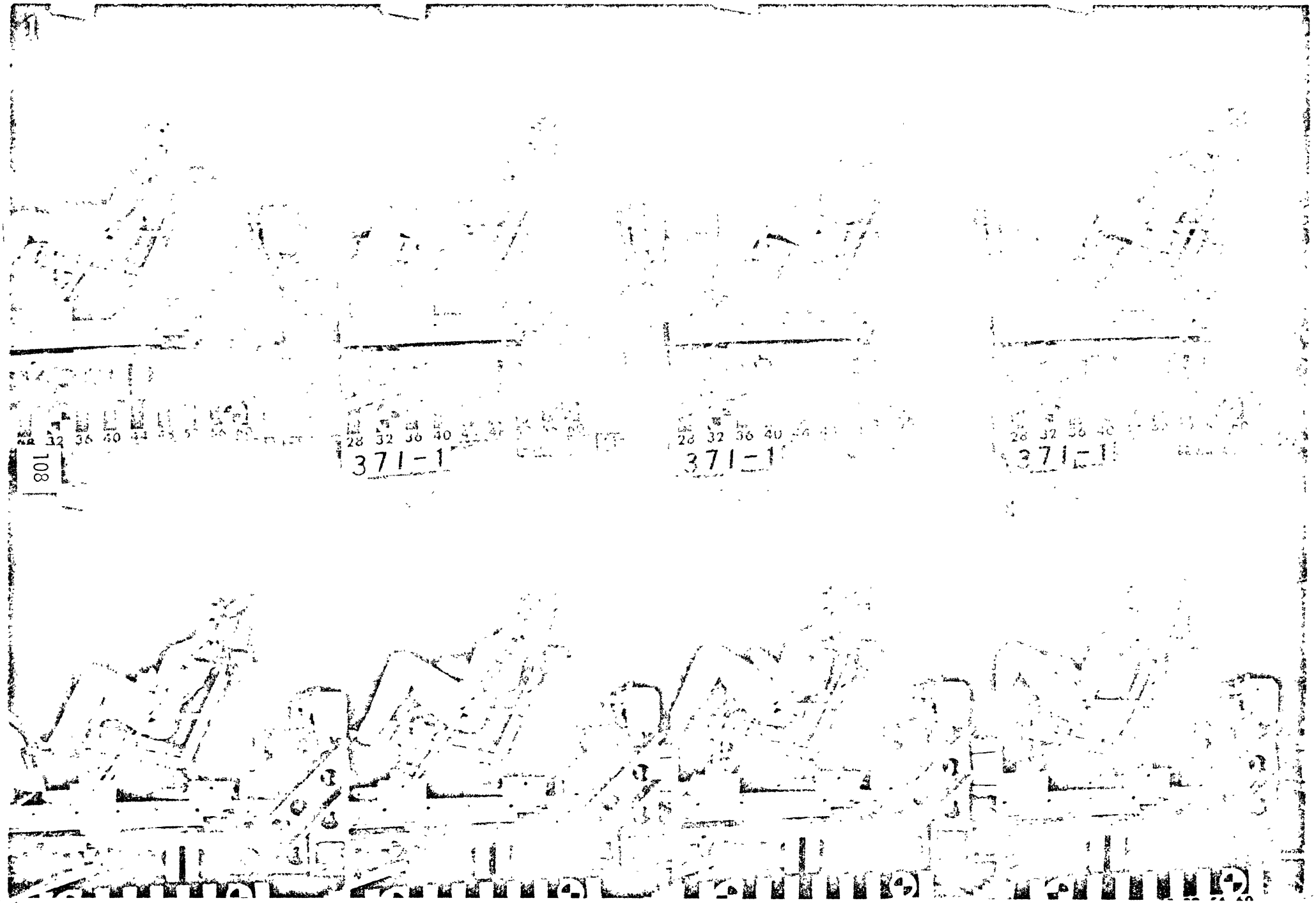

Figure 63. Sequence Photographs of Test A-371 (~25 msec. between pictures)

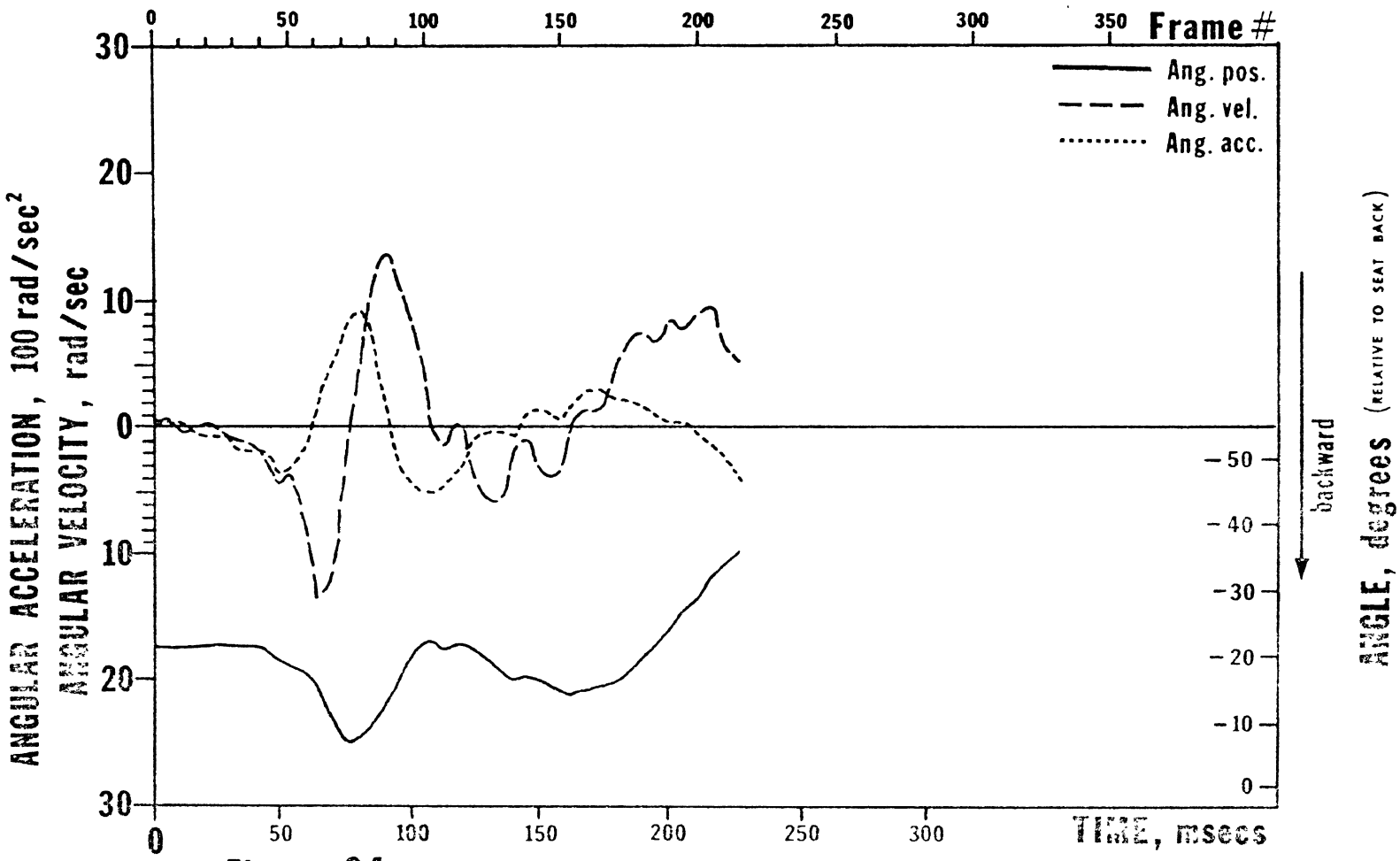

Figure 64 HEAD MOTION Run No. A-371

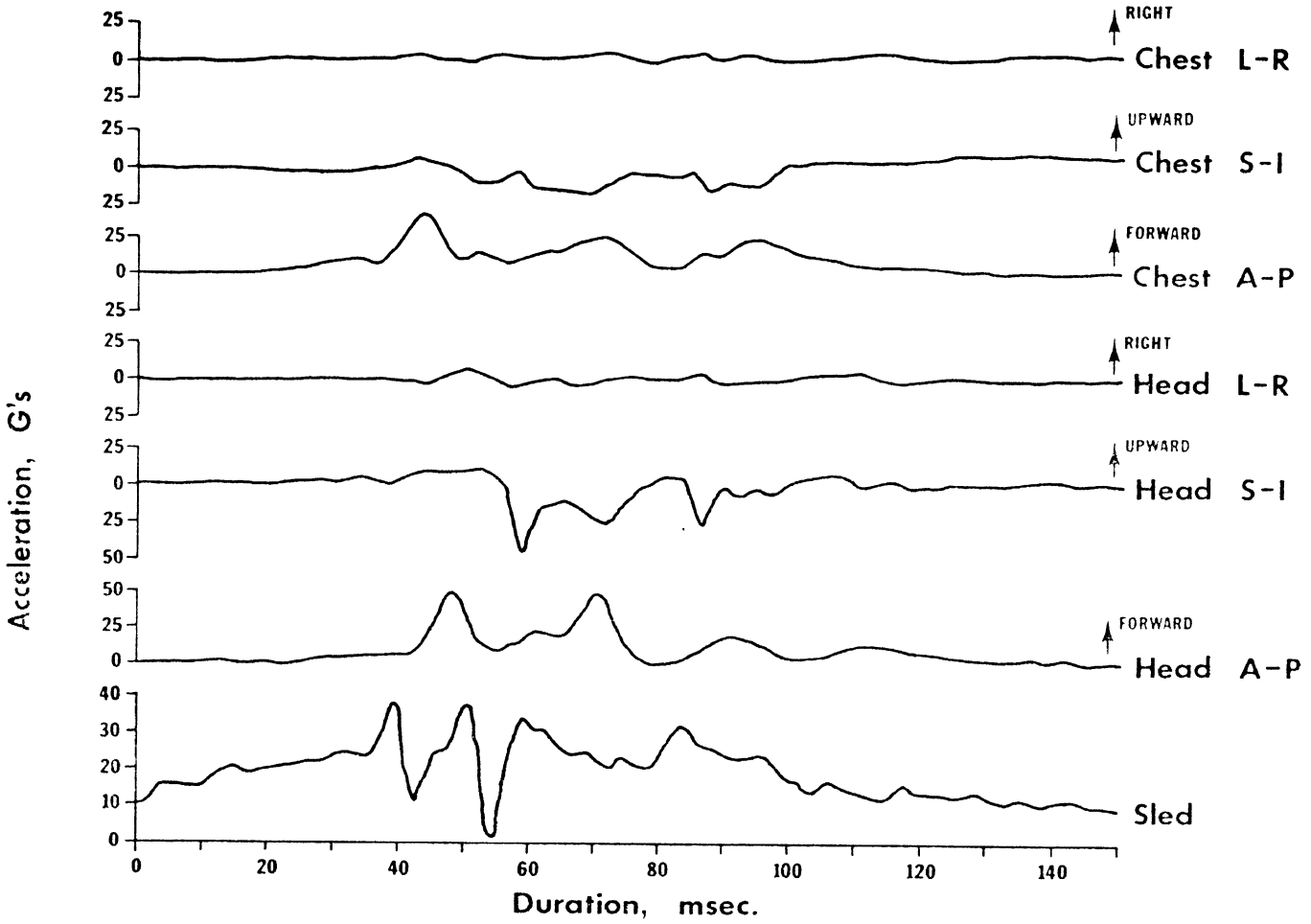

FIGURE 65. VISICORDER TRACES OF SLED TEST A-371

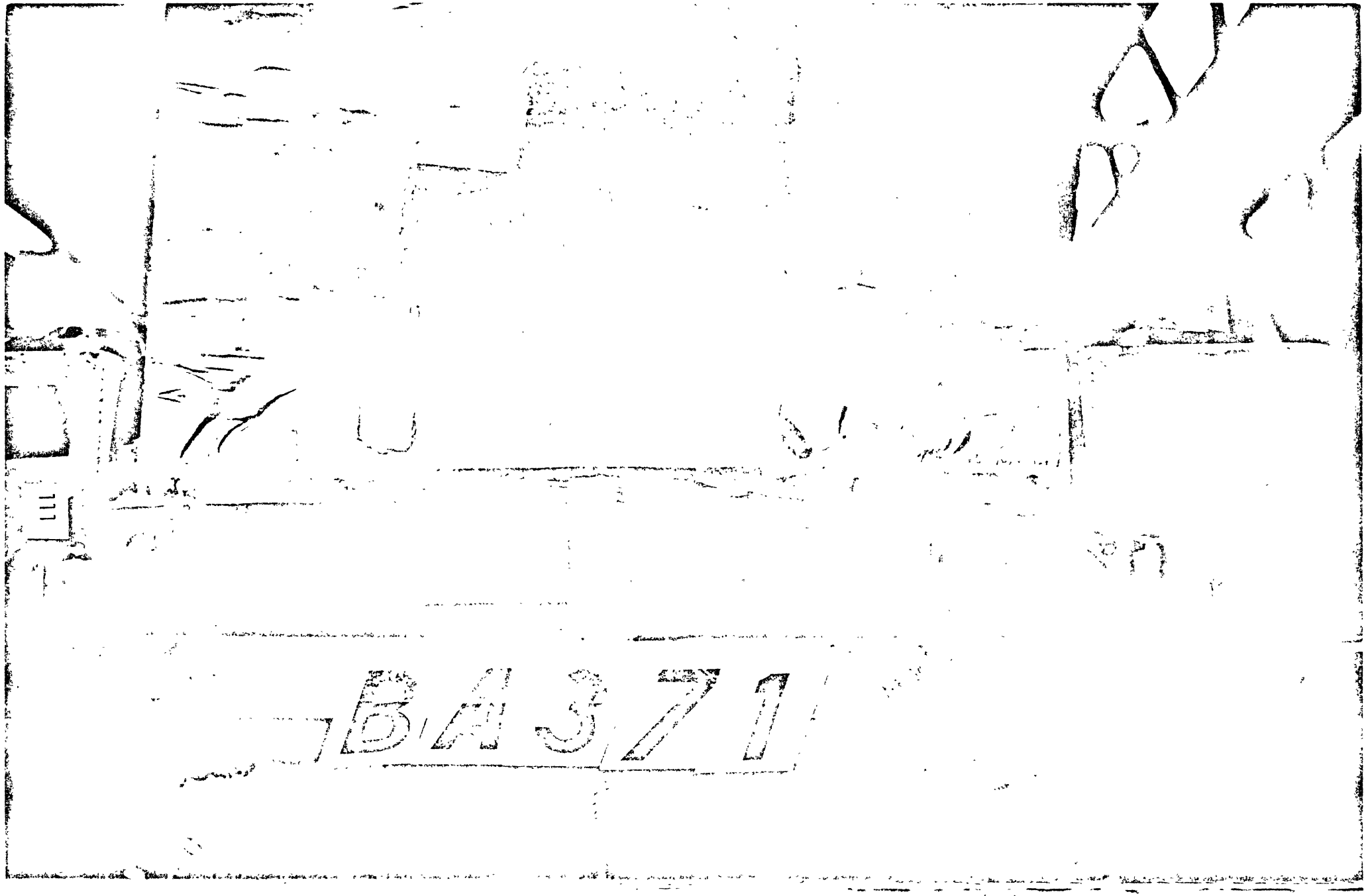

Figure 66. Deformations of the Rigid Sliding Head Restraint Due to Deployment

9. PERFORMANCE REQUIREMENT RECOMMENDATIONS AND COMPLIANCE TEST PROCEDURES

The basic nature of this research program has been that of a feasibility study of deployable head restraints. The results of this study do permit some general observations on the performance requirements and compliance test procedures suitable for deployable head restraint design evaluation. However, as pointed out in preceeding sections of this report, the head restraint characteristics and therefore its performance must always be considered in relation to the characteristics and performance of the associated seat back.

The results of this research program indicate that an effective deployable head restraint-seat combination should satisfy the following criteria:

1. Rearward linear and rotational displacement of the head should be minimized.
2. Linear and angular accelerations of the head should be minimized.
3. Differential motions of the head relative to the neck and torso should be minimized.
4. Ramping of the occupant up the seat back should be minimized.
5. Rebound of the occupant should be minimized.

The first three of these criteria are interdependent and the magnitude of the quantities involved are dependent on the mechanical characteristics of the system being evaluated (for example, a seat back with deep soft cushioning and a correspondingly matched head restraint stiffness would allow larger absolute rearward linear displacements of the occupant than a stiffer system but the matching would still minimize head rotations and differential motions). Control of occupant ramping is basically a problem of proper shape of the front of the head restraint for adequate pocketing of the shoulders. Prevention of ramping is more critical for taller occupants.

Additional requirements for proper deployable head restraint performance are that the restraint remain in place for a sufficient time to protect against multiple collisions, and that it not interfere with driver control of the vehicle.

The dynamic nature of deployable head restraints demands that tests performed to assess the compliance of a system with the above criteria must be dynamic sled tests with realistic simulations of rear-end crash acceleration environments. These tests should be carried out using anthropometric dummies

covering the range of seated heights expected for automobile drivers (5th percentile female to 95th percentile male).

Instrumentation for these tests should include both transducers for measurement of acceleration loads applied to the head and chest of the dummy and high speed photographic devices for recording the dummy motions.

REFERENCES

Adams, T.: Research in Progress. Michigan State University, 1968.

Berton, R.: Whiplash: Tests of the Influential Variables. SAE Paper No. 280080, January 1968.

Ewing, C. L., et al.: Dynamic Response of the Head and Neck of the Living Human to $-G_X$ Impact Acceleration. Proc. Twelfth Stapp Car Crash Conference, pp. 424-439, 1968.

Ewing, C. L., et al.: Living Human Dynamic Response to $-G_X$ Impact Acceleration. II-Accelerations Measured on the Head and Neck. Proc. Thirteenth Stapp Car Crash Conference, pp. 400-415, 1969.

Fabricius, B.: Abrupt Acceleration of Auto Occupants as a Result of Rear-End Collision. (In German), Dissertation for Doktor-Ingenieur, Technischen Universität Berlin, 1969.

Furusho, H., et al.: Analysis of Occupant Movements in Rear-End Collisions. Parts I and II. Paper Nos. 13-14 of JSAE Safety Research Tour, 1969.

Gay, J. R. and Abbott, K. H.: Common Whiplash Injuries to the Neck. J. Am. Med. Assoc. 152:1968 (1953).

Gurdjian, E. S.: Neckache and Backache Due to Degenerative and/or Traumatic Musculoskeletal Processes. A By-Product of Modern Culture. Neckache and Backache, Springfield, Thomas, pp. 3-23, 1970.

Haley, J. L. and Turnlow, J. W.: Impact Test Methods and Retention Hardness Criteria for U.S. Army Aircrewmen Protective Head Gear. USA AV LABS Tech. Report 66-29, 1966.

Lombard, C. F., et al.: Some Factors Contributing to Head and Neck Injuries During Whole Body Impact Using Guinea Pig Subjects in $\pm G_X$ Orientations. Proc. Twelfth Stapp Car Crash Conference, pp. 338-351, 1968.

Martinez, J. L.: Headrest and Seat Back Design Proposals. Proc. Twelfth Stapp Car Crash Conference, pp. 164-171, 1968.

Martinez, J. L. and Garcia, D. J.: A Model for Whiplash: J. Biomechanics 1: 22-32 (1968).

Martinez, J. L., Wickstrom, J. and Barcelo, B. T.: Tulane University Studies of Acceleration Injuries in Animals. 9th Stapp Car Crash Conference, Oct. 1965.

Meldrum, J.: Automotive Driver Eye Position. SAE Paper No. 660804, 1965.

Mertz, H. J. and Patrick, L. M.: Investigation of the Kinematics and Kinetics of Whiplash. SAE Paper No. 670919, 1967.

Nakalsuka, T., et al.: Dynamical Considerations on Whiplash Motion of an Occupant Caused by Rear-End Collision. Report from Vehicle Dynamics and Safety Lab, Isuzu Motors, Ltd., 1969.

Ommaya, A. K.: The Role of Whiplash in Cerebral Concussion. Proc.Tenth Stapp Car Crash Conference, 197-203, 1966.

Ommaya, A. K., et al.: Scaling of Experimental Data on Cerebral Concussion in Sub-Human Primates to Concussion Threshold for Man. Proc. Eleventh Stapp Car Crash Conference, pp. 47-52, 1967.

Ommaya, A. K., Hirsch, A. and Martinez, J. L.: The Role of Whiplash in Cerebral Concussion. SAE Paper No. 660804, 1967.

Ommaya, A. K., et al.: Comparative Tolerances for Cerebral Concussion by Head Impact and Whiplash Injury in Primates. 1970 International Automobile Safety Conference Compendium, pp. 808-817, SAE, 1970.

Portnoy, H. D., et al.: Intracranial Pressure and Head Acceleration During Whiplash. Proc. 14th Stapp Car Crash Conference, pp. 152-168, 1970.

Severy, D. M., et al.: Preliminary Findings of Head Support Designs. Proc. Eleventh Stapp Car Crash Conference, pp. 220-270, 1967.

Severy, D. M., et al.: Safer Seat Designs. Proc. Thirteenth Stapp Car Crash Conference, pp. 314-335, 1969.

Severy, D. M., et al.: Vehicle Design for Passenger Protection from High-Speed Rear-End Collisions. Proc. Twelfth Stapp Car Crash Conference, pp. 94-163, 1968.

Severy, D. M., Brunk, J. M. and Baird, J. D.: Backrest and Head Restraint Design for Rear-End Collision Protection. SAE Paper No. 680079, 1968.

Severy, D. M., Mathewson, J. H. and Bechtol, C. O.: Controlled Automobile Rear-End Collisions. Can. Ser. Med. J., 727-759, N-1955.

Snyder, R. G.: Occupant Restraint Systems. Crash Protection Symposium, Wayne State University, Detroit, May 1968.

U.S. Bureau of Public Roads Motor Vehicle Accident Data, Ford Motor Company Automotive Safety Research Office Report No. S-70-1, May 1970.

Wickstrom, J., et al.: Cervical Sprain Syndrome Experimental Acceleration Injuries of the Head and Neck. The Prevention of Highway Injury, Published by HSRI, Ann Arbor, pp. 182-186, 1967.

Young, J. W. and Snyder, R. G.: Unpublished test data, Ford Motor Company, 1968.

APPENDIX A

A CRASH POWER LEVEL SENSOR FOR PASSIVE RESTRAINT SYSTEMS

A Master's Degree Project
by George H. Person
Department of Mechanical Engineering
The University of Michigan

April 26, 1971

Low acceleration levels are characteristically associated with rear-end collisions involving front engine cars. An acceleration coupled crash sensor cannot discriminate between such a crash and normal road noise. It is therefore necessary to develop a crash sensor which monitors some parameter unique only to a crash situation.

THE THERMODYNAMICS OF A CRASH

If the car is considered as a system as in Figure 67, and the crash process occurs on a level surface, changes in internal and potential energy may be neglected and the first law equation governing the adiabatic process may be written as

$$_1KE_2 = -_1W_2$$

or the change in kinetic energy of the system is equal to the work done on the system by its surroundings. It also governs a process in which the car would be towed or pushed by another vehicle since it does not relate properties which are unique to a crash situation. The rate of change in kinetic energy is the factor which distinguishes a crash from any other process.

$$\frac{\Delta KE}{\Delta t} = -\frac{\Delta W}{\Delta t}$$

For example, for a crash of a 3000 lb. vehicle with an initial velocity of 30 mph occuring in 100 msec:

$$\frac{\Delta KE}{\Delta t} = 900{,}000 \text{ ft-lb/sec} = 1600 \text{ HP}$$

The same car braking at a constant 1 G. would stop in 1.38 sec. and

$$\frac{\Delta KE}{\Delta t} = 66{,}200 \text{ ft-lb/sec} = 120 \text{ HP}$$

A POWER LEVEL CRASH SENSOR

Since mechanical power level is the unique property in a crash, a sensor should measure mechanical power to determine the existence of a crash. Such a sensor is shown schematically in Figure 68. It would be mounted on the vehicle with appropriate load distributing structures so that it would directly receive the force of impact. For example, it could be part of the supporting structure of a rigid bumper.

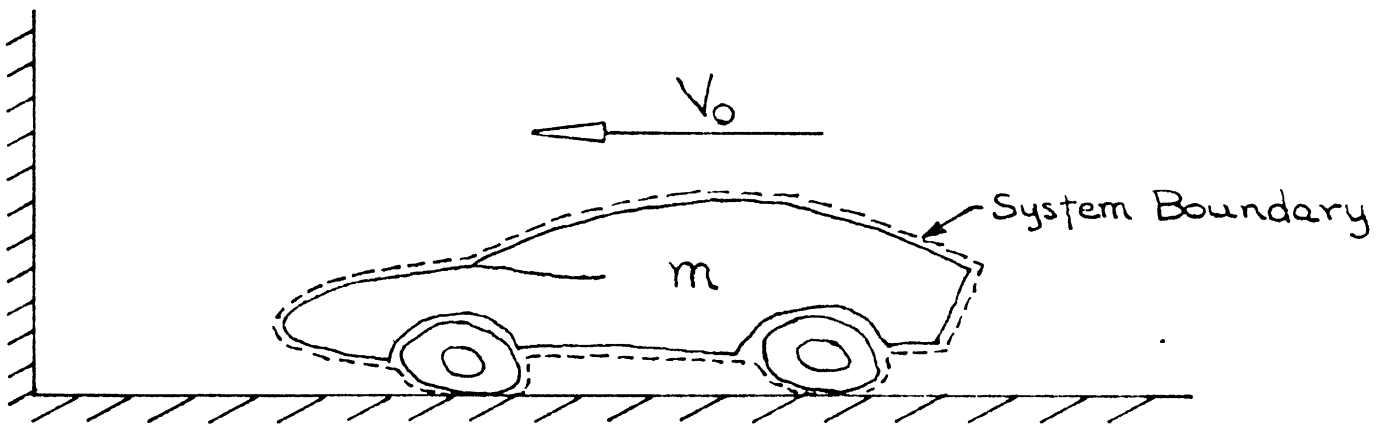

FIGURE 67. THE VEHICLE AS A SYSTEM

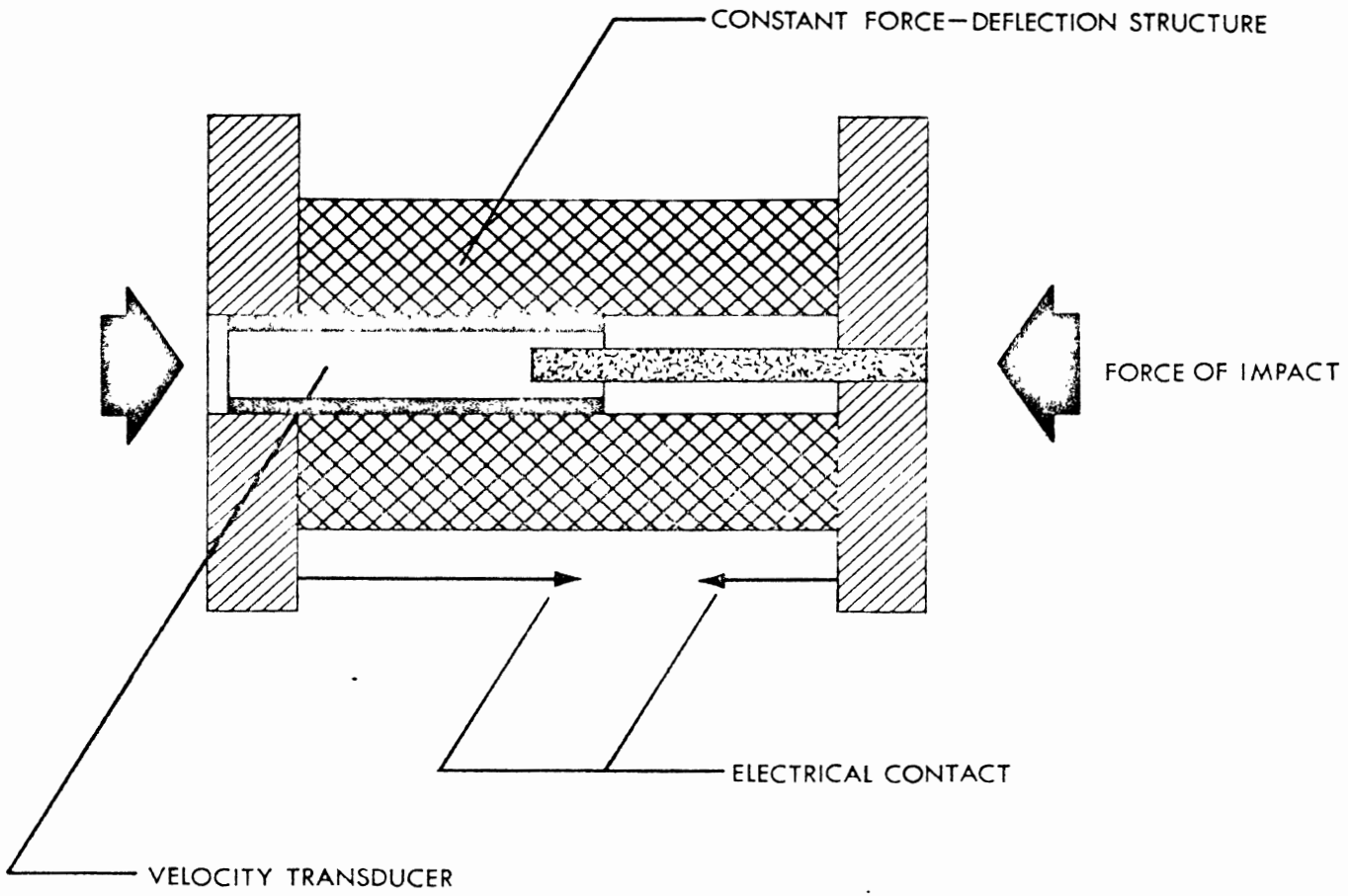

FIGURE 68. CRASH POWER LEVEL SENSOR CONCEPT

The electrical contacts shown in Figure 68 would close after a finite amount of deformation of the constant force-deflection structure. At this time, the rate of deformation as measured by the velocity transducer, if sufficiently high, would cause a restraint system to be deployed. Since the deflection of the structure occurs at a finite force level, the criteria for deployment is power level.

Power = Force x Velocity

The force level could be set sufficiently high to insure that the object hit by the vehicle would be capable of exerting a damaging force on the vehicle. This would exclude objects with low inertia and safety designed objects such as break-away roadside posts. The minimum velocity would be that determined for restraint deployment. The initial finite deflection serves the dual purpose of allowing time for the initial transients of elastic collision to decay and insuring that the object struck is capable of doing work on the vehicle.

Solid state integrated circuits containing Schmidt triggers and operational amplifiers are available at low cost and could be used with the sensor to properly operate restraint deployment devices.

PROTOTYPE TESTING

A prototype sensor was constructed following the drawing shown in Figure 69. Styrofoam was selected to model the square wave energy absorbing structure. The velocity transducer was a coil of four layers of laminar wrapped, fine gauge magnet wire, on a paper core enclosed in a steel tube. When a permanent magnet is passed through the coil axially, a voltage is induced in the coil proportional to the relative velocity of the magnet. The voltage versus velocity calibration data is shown in Figure 71. The electrical contacts were two brass rods inserted in the sensor as shown. When the piston touched the ends of the rods, current would pass between them.

The results of two tests in the Plastechon high speed testing machine at 5 and 10 mph are shown in Figures 71and 72 . It may be observed that the force level was nearly constant up to the point that the brass contacts were struck, and that the velocity transducer output had become stable at that point. Pertinent information from the tests is tabulated in Table 4 .

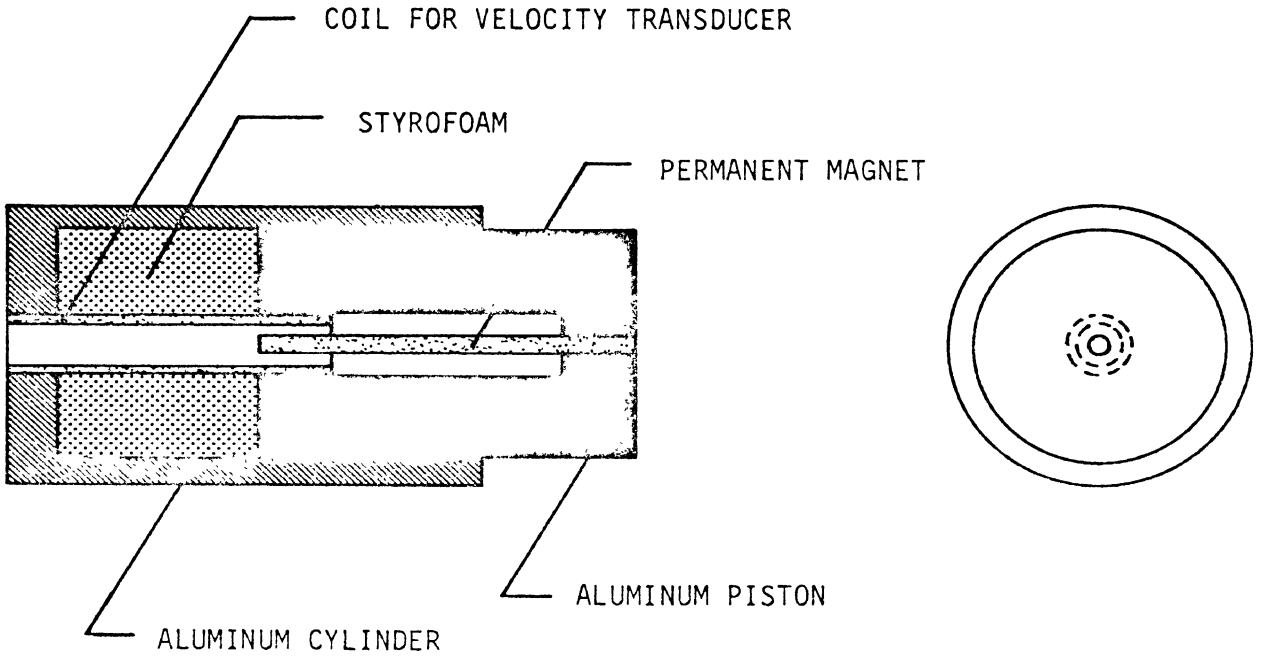

FIGURE 69. PROTOTYPE SENSOR DIAGRAM

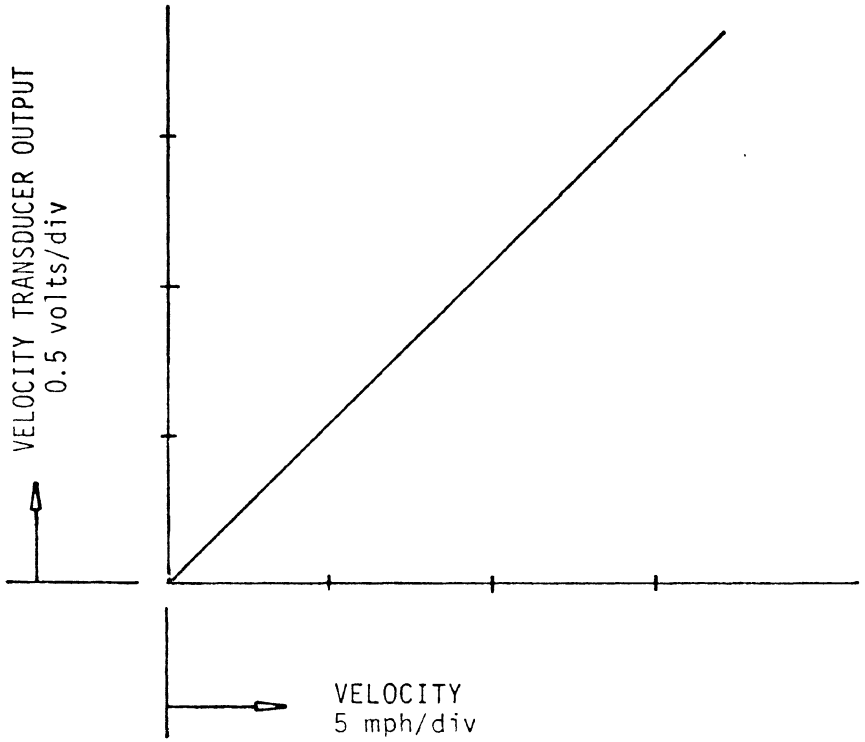

FIGURE 70. VELOCITY TRANSDUCER CALIBRATION DATA

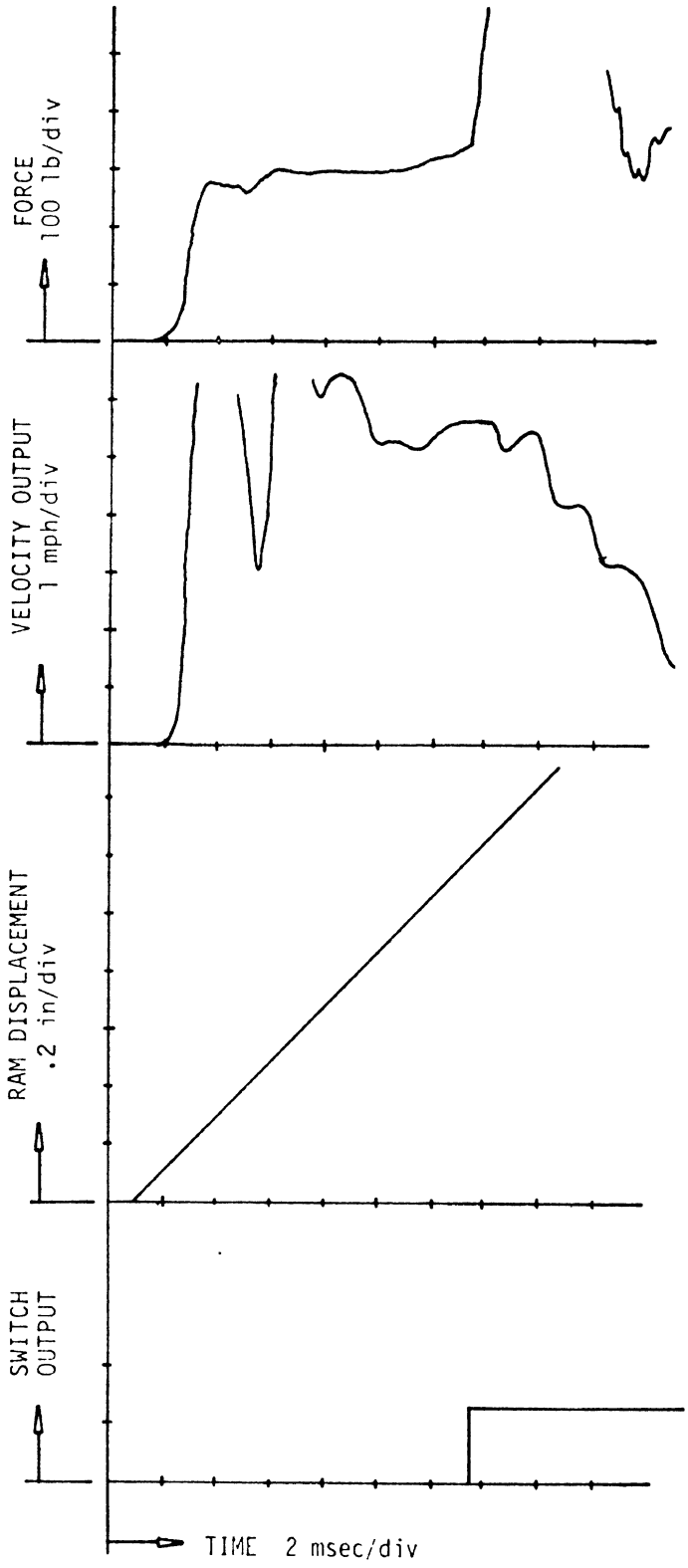

FIGURE 71. PROTOTYPE IMPACT TEST AT 5 mph

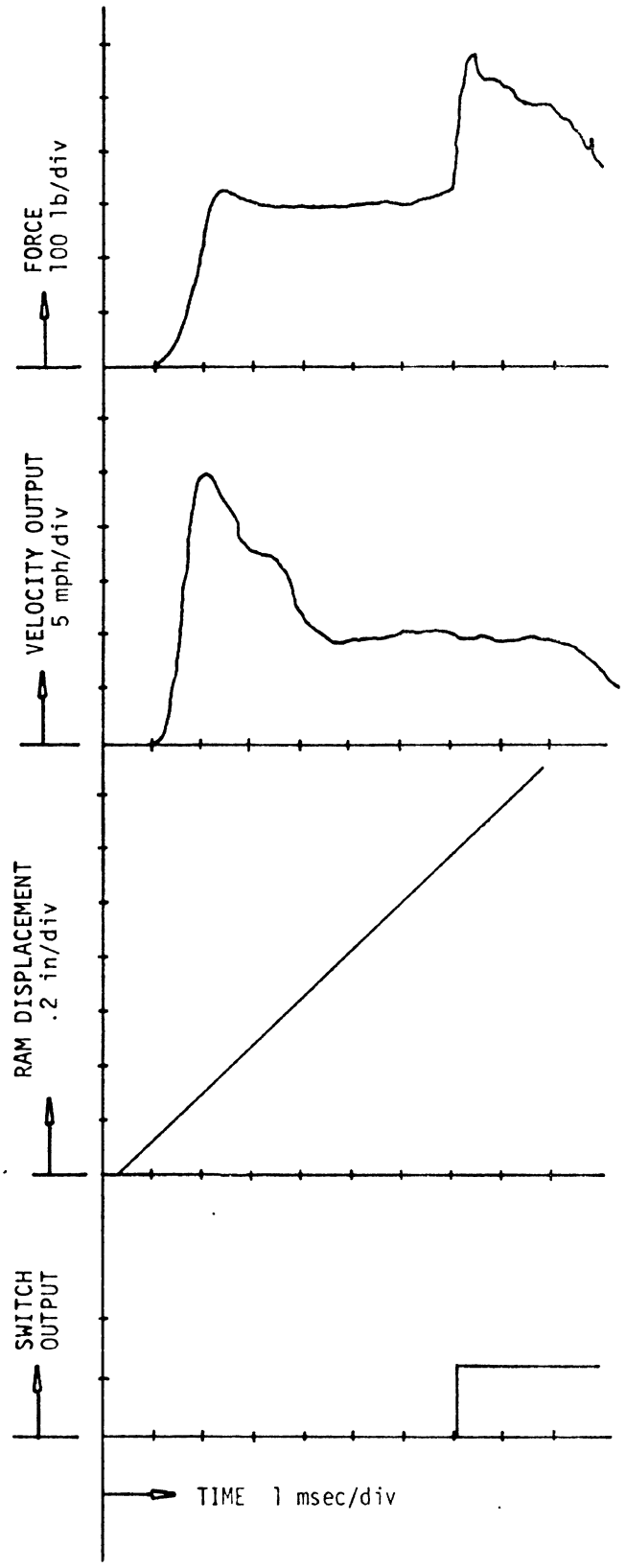

FIGURE 72. PROTOTYPE IMPACT TEST AT 10 mph

DISCUSSION

The concept of a contact power level crash sensor provides a straightforward method for establishing the criteria for restraint deployment. It is necessary only to determine the highest force which could be exerted on the vehicle, after the prescribed amount of initial work has been done by a struck object in the worst case which should not cause restraint deployment, and the minimum relative speed at which deployment should occur. The sensor would then be constructed so that it would be slightly stronger than that force and the electronics would be set to trigger at the voltage representing that speed.

The concept is very compatible with square-wave energy-absorbing bumpers for both front and rear impacts. For example, a bumper which would dissipate all of the energy of a 3000 lb. car in 3 in. of travel in a 5 mph collision would require 10,000 lb. for deflection and would create less than 4 G average acceleration. A force level of 10,000 lb. could be sufficient to fracture a break-away pole with less than 2,500 ft-lb of work. This collision would not trigger the restraint system at any velocity. If the car equipped with this bumper struck another similar vehicle, the impact velocity must be greater than the minimum for deployment.

The operation of a power level sensor is independent of the transmissibility of the vehicle structure. It is not affected by road noise and cannot be actuated in critical vehicle maneuvers. It would operate very early in the crash time budget allowing greater time for restraint deployment before critical acceleration levels could occur. It is a simple, implementable solution to the problem of crash sensing.

TABLE 4. PROTOTYPE TEST SUMMARY

NOMINAL TEST SPEED	5 mph	10 mph
AVERAGE FORCE	300 lb	300 lb
VELOCITY OUTPUT AT SWITCH CLOSING	5.8 mph	10 mph
WORK DONE ON SENSOR TO FIRE	375 lb-in	375 lb-in
POWER LEVEL AT SWITCH CLOSING	4 HP	8 HP
TIME TO FIRE	13.5 msec	7 msec

APPENDIX B

TEST EQUIPMENT SPECIFICATIONS AND CALIBRATION PROCEDURES

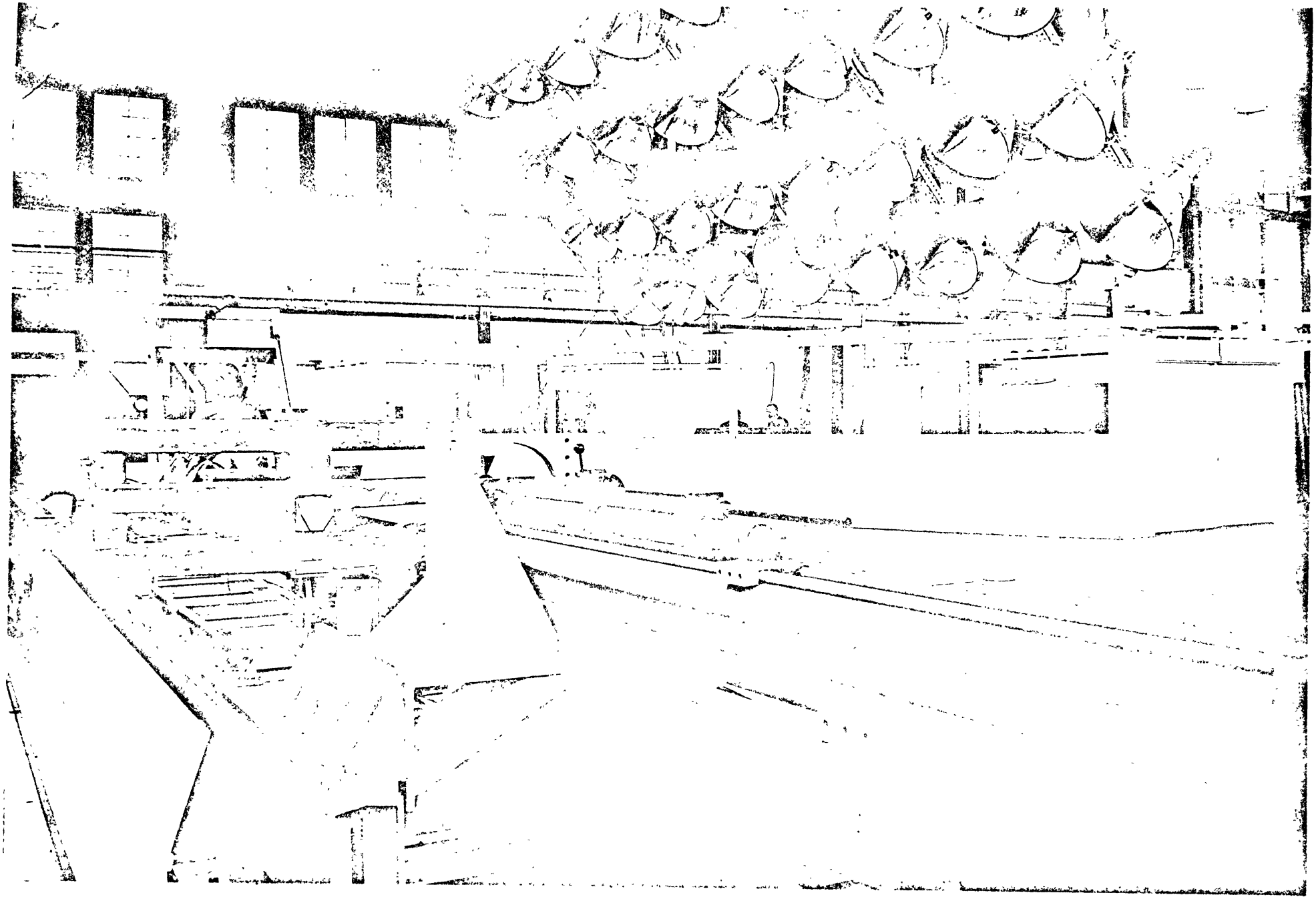

Figure 73. HSRI Impact Sled Facility

A. Equipment Specifications

Transducers

1. Kistler Piezotron Model 818 Accelerometer (Dummy)
   Type: Piezoelectric with integral impedance converter
   Range: ±250 G
   Sensitivity: 10 mv/G
   Freq. Response: 2 to 5000 Hz (±5%)
   Resonant Freq.: 3000 Hz

2. Statham Model A69TC-100-350 Accelerometer (Sled)
   Type: Temperature compensated, unbounded strain gage
   Range: ±100 G
   Natural Freq.: 1800 Hz
   Damping: 0.7 (±0.1) of critical at room temp.

3. Lebow Model 3371 Belt Load Cell
   Type: Strain gage
   Range: 3500 pounds, with 50% overload capacity
   Sensitivity: 2.2906 mv/V/3500 pounds

Signal Conditioners

1. Honeywell Model 120 D.C. Amplifier
   Type: Solid state, direct coupled, wideband differential
   Gain: 10 - 1000
   D.C. Gain linearity: better than ±0.2% of full scale
   D.C. Gain accuracy, calibrated gain ranges: better than ±0.5%
   Freq. Response: ±2% D.C. to 10 KHz

2. Honeywell Model 105 Bridge Balance (Gage Control) Unit
   Freq. Response: ±DC to 10 KHz within ±0.5%

Recorders

1. Honeywell Model 1612 Visicorder Light-Beam Oscillograph
   Galvanometer response:

M-3300 (15 channels): ±5%, 0 to 2000 Hz
M-1650 (4 channels): ±5%, 0 to 1000 Hz
M-1000 (1 channel): ±5%, 0 to 600 Hz

2. Honeywell Model 7600 F.M Tape Recorder/Reproducer
   Tape speeds: 1 7/8 to 120 ips
   Freq. response: ±1.0 db 0 - 10000 Hz (at recording speed used - 30 ips)
   Harmonic distortion: 1.2%

3. CEC Model VR-3300 F.M. Tape Recorder
   Tape speeds: 1 7/8 to 60 ips
   Freq. response: ±0.5 db 0 - 10000 Hz (at recording speed used - 30 ips)
   Harmonic distortion: 1.5%

B. Calibration Procedures

Transducers: The calibration senstitivities of the transducers are checked to insure that there has been no appreciable deviation from manufacturer's specified sensitivity.

1. Kistler Piezotron Model 818 Accelerometers.
   The sensitivities of these piezoelectric accelerometers, which are used in the crash test dummies, are checked with a Kistler Model 894L Shock Calibration System. This system compares, on peak-reading voltometers, the output of the test accelerometer and an NBS-traceable load cell onto which the accelerometer is dropped. Accuracy of the load cell and associated peak meters is checked against a NBS-traceable standard accelerometer prior to calibration of the test accelerometers.
2. Statham Model A69TC Accelerometer
   This strain-gage accelerometer, used to monitor sled deceleration, is calibrated by comparing its output with that of an NBS-traceable standard accelerometer. The two accelerometers are mounted piggy-back on a common carrier block and impacted. Their outputs are displayed, via the sled umbilical and the signal conditioning system, on the oscillograph. The excitation voltage of the Statham is adjusted until its output agrees with the standard accelerometer. This excitation voltage becomes the standard for subsequent use of the accelerometer.

3. Lebow Seat-Belt Load Cells

Calibration sensitivity of these load cells is checked by applying a known load to a length of seat-belt material on which the cell is mounted. The output signal is compared with that obtained when a shunt resistor is paralleled with one leg of the transducer's bridge. The resistor value is that which has been specified by the manufacturer to produce a transducer output equal to the output produced by a known load.

Signal Conditioning/Recording Systems (Electronics)

1. Kistler Accelerometer Channels

A calibrated voltage, equal to the output at a given G-level (10 G's) of the Kistler 818 accelerometer used, is applied and the input attenuator is adjusted to achieve an output voltage from the Honeywell Model No. 120 amplifier which will drive the associated oscograph galvanometer to the desired deflection (1" = 50 G's).
The tape recorder is calibrated, by adjusting its input attenuator, so that the voltage producing the specified 1" galvanometer deflection will also cause 13 1/3% (4" = 150 G = 40%) deviation in frequency of the F.M. carrier of the tape recorder.

2. Strain-Gage Transducer Channels

Calibration of strain-gage channels is accomplished by introducing shunt resistors across one leg of the bridge of the transducers in question, and checking the excitation required to produce the galvanometer deflection desired. A significant change in the required excitiation for any transducer would indicate the need to check the calibration sensitivity of the transducer, or otherwise determine the cause of the change. For the Statham accelerometer channel, the calibration resistors are the internal "Cal I" and "Cal II" calibration resistors of the Honeywell 105 gage unit, and their corresponding G-value and galvanometer deflection were determined at the time of calibration of the transducer itself. In the case of the Lebow belt load cells, a 60 K-ohm resistor is introduced in the transducer cable parallel to one leg of the transducer bridge, and whose corresponding belt load value was specified by the manufacturer.

Calibration of the tape recorder is accomplished by adjusting its input attenuators to obtain a 40% carrier frequency deviation when the voltage necessary to cause 3" deflections of the oscillograph galvanometers is impressed on the tape inputs.

3. Calibration Frequency

Calibration of the signal conditioning equipment, oscillograph, and top units is done routinely for each sled test.